UNIVERSIDADE DE SÃO PAULO
INSTITUTO DE FÍSICA DE SÃO CARLOS

Caio Botelho Naves

Studies on the generalized elephant quantum walk

São Carlos

2022

Caio Botelho Naves

Studies on the generalized elephant quantum walk

Dissertation presented to the Graduate Program in Physics at the Instituto de Física de São Carlos da Universidade de São Paulo, to obtain the degree of Master in Science.

Concentration area: Theoretical and Experimental Physics

Advisor: Prof. Dr. Diogo de Oliveira Soares Pinto

Corrected version

(Original version available on the Program Unit)

São Carlos

2022

Naves, Caio Botelho
Studies on the generalized elephant quantum walk / Caio Botelho Naves; advisor Diogo de Oliveira Soares Pinto - corrected version -- São Carlos 2022.
107 p.

Dissertation (Master's degree - Graduate Program in Theoretical and Experimental Physics) -- Instituto de Física de São Carlos, Universidade de São Paulo - Brasil , 2022.

1. Quantum walks. 2. Generalized elephant quantum walk. 3. Entanglement. I. Soares Pinto, Diogo de Oliveira, advisor. II. Title.

ACKNOWLEDGEMENTS

Um certo cientista uma vez disse:“se eu vi mais longe, foi por estar sobre ombros de gigantes”. Seria impossível não agradecer ao meu “gigante” que não só tornou possível este trabalho mas que também sempre se dispôs a me levar a olhar mais longe. Obrigado Diogo, pela sua orientação e me ensinar física, pela sua amizade e gentileza desde os meus tempos de graduação. Obrigado por constantemente me motivar, mesmo em tempos difíceis. Obrigado pelas infinitas recomendações. Espero, um dia, ser capaz de reproduzir os seus ensinamentos com a mesma leveza e humanidade que você carrega. A todos outros professores que fizeram parte da minha educação, minha eterna gratidão.

Este trabalho certamente também não seria possível sem a inestimável colaboração de Marcelo e Sílvio, que com suas gentilezas e experiências aceitaram fazer parte do desenvolvimento dos resultados obtidos. Agradeço pelas longas discussões, sugestões e correções. À ambos, minha gratidão.

Agradeço aos meus amigos que durante os tempos de isolamento me fizeram companhia e trouxeram diversão. Em especial, agradeço ao Lucas e Estevão, pelas longas e divertidas conversas.

Serei eternamente grato ao Instituto de Física de São Carlos que em um momento de grandes incertezas e cortes no financiamento da ciência brasileira se manteve firme na crença em seus alunos e optou por tornar possível o meu ingresso no seu programa de pós-graduação. Agradeço também à Coordenação de Aperfeiçoamento de Pessoal de Nível Superior (CAPES) pela continuação do financiamento da minha pesquisa. À ciência brasileira, todas as honras.

Obrigado Marcella, por ser minha fonte de alegria e esperança de que um futuro melhor está por vir. Agradeço a toda minha família, pelo suporte incondicional e motivação para seguir meus sonhos. É por vocês.

This study was financed in part by the Coordenação de Aperfeiçoamento de Pessoal de Nível Superior – Brasil (CAPES) – Finance Code 001.

"O andar é lento porque é lento
desde lentos tempos de antanho.

Se alguém corre, fica marcado
infrator da medida justa.

É o lento passo dos enterros,
como é o passo dos casamentos.

O pausado som das palavras.
O tranquilo abrir de uma carta.

Há lentidão em dar o leite
da lenta mama a um sem pressa

neném que mama lentamente,
na lenta espera de um destino.

Não é lenta a vida. A vida é ritmo
assim de bois e de pessoas,

no andar que convém andar
como sugere a eternidade."

Carlos Drummond de Andrade

ABSTRACT

NAVES, C. B. **Studies on the generalized elephant quantum walk**. 2022. 107p. Dissertation (Master of Science) - Instituto de Física de São Carlos, Universidade de São Paulo, São Carlos, 2022.

Quantum walks have been a platform for the study and modeling of many processes and physical systems, going from its application on the development of quantum algorithms to the study of energy transport in biological molecules. In the same way that in general aspects of quantum theory, it also aroused the necessity of studying the introduction of noise in the evolution of quantum walks, given that it is a major factor in experimental applications. In this context, in 2018 G. D. Molfetta *et al.* presented a quantum model of the classical elephant random walk, the elephant quantum walk, that analyzes a noisy unitary evolution. Posteriorly, M. A. Pires *et al.* generalized this walk into the generalized elephant quantum walk, showing to have an interesting property of controlling the diffusive behavior of the walker while maintaining the maximum generation of entanglement between its degrees of freedom, something unknown until then. In this work we proposed ourselves to study, through numerical experiments, the generation of entanglement in the generalized elephant quantum walk in general initial settings and evolutions. For such, first we introduce classical random walks, reviewing the necessary probability concepts. After, we approach quantum walks and restrict the description to coined discrete time quantum walks, the type of quantum walk to be studied. Our results indicate that this type of quantum walk potentially generates maximally entangled states for almost all initial states and evolutions, even with a low degree of noise. These results indicate that a dynamically random evolution, being it either in the coin operator, as previously studied for other authors, or in the shift operator as in this walk, generates maximally correlated states.

Keywords: Quantum walks. Generalized elephant quantum walk. Entanglement.

RESUMO

NAVES, C. B. **Estudos sobre o passeio quântico de elefante generalizado**. 2022. 107p. Dissertação (Mestrado em Ciências) - Instituto de Física de São Carlos, Universidade de São Paulo, São Carlos, 2022.

Passeios quânticos têm sido uma plataforma para o estudo e modelagem de vários processos e sistemas físicos, variando entre a sua aplicação no desenvolvimento de algoritmos quânticos e o estudo de transporte de energia em moléculas biológicas. Assim como em aspectos mais gerais da teoria quântica, também surgiu a necessidade de se estudar os efeitos da introdução de ruído na evolução dos passeios quânticos, visto que trata-se de um fator importante em aplicações experimentais. Nesse contexto, G. D. Molfetta *et al.* em 2018 apresentou um modelo quântico do passeio de elefante, denominado passeio quântico de elefante, que analisa uma evolução unitária ruidosa. Posteriormente, tal passeio foi generalizado por M. A. Pires *et al.* no passeio generalizado de elefante, demonstrando possuir a interessante propriedade de controle sobre a difusividade do caminhante enquanto possivelmente gerando emaranhamento máximo entre seus graus de liberdade, algo desconhecido até então. Neste trabalho nos propomos a estudar, através de experimentos numéricos, a geração de emaranhamento no passeio de quântico elefante generalizado em configurações iniciais e de evolução diversas. Para tal, primeiramente introduzimos passeios aleatórios clássicos, revisando os conceitos de probabilidade necessários para o seu entendimento. Posteriormente, abordamos passeios quânticos e afunilamos a descrição para passeios quânticos de tempo discreto com moeda, o tipo de passeio principal a ser estudado. Nossos resultados indicam que este passeio potencialmente gera estados maximamente emaranhados para a maioria dos estados iniciais e evoluções, mesmo com uma baixa taxa de ruído. Estes resultados indicam que uma evolução dinamicamente aleatória, seja ela introduzida no operador moeda, como previamente estudada por outros autores, ou no operador deslocamento como no caso deste passeio, gera estados completamente correlacionados.

Palavras-chave: Passeios quânticos. Passeio quântico de elefante generalizado. Emaranhamento.

LIST OF FIGURES

LIST OF TABLES

CONTENTS

1 INTRODUCTION

Quantum walks has been a quite active field of research since it first appeared in the literature. In their seminal article, Y. Aharonov *et al.*[1] introduced the concept of *quantum random walks*, a quantum version of the classical random walk where they consider measurements in the internal degree of freedom of the walker, the *quantum coin*. The title of their work indicates that the evolution of the quantum walk is random, in the same sense that in the classical random walk, nonetheless, the version of quantum walks that performs only a unitary evolution has shown to be very useful in a variety of problems.

Since then, several authors have been researching the effects and applicabilities of introducing noise in the evolution of quantum walks, going from an open evolution to a random unitary noisy one. Within the last case, many focused on random operations on the quantum coin but only a few studies on the use of random shift operators were made. In this context, G. D. Molfetta *et al.*[2] devised the *elephant quantum walk* later extended to the *generalized elephant quantum walk*,[3] a model where the random step sizes furnishes rich phenomenology yet not seen in the other versions of random unitary quantum walks.

This dissertation thesis intends to provide a full understanding on the generalized elephant quantum walk and its features, central in the development of the results obtained during the MSc studies. With the view to do so, chapter 2 first briefly introduces the essential concepts of probability theory necessary to understand stochastic and Markovian processes. Then, we provide a description of classical random walks, focusing on the discrete time one-dimensional version, with some important properties and its long-time probability distribution.

In chapter 3 initially is provided an introduction in quantum theory in two formalisms, the vector state and density operator formalism, describing important concepts to one fully understand quantum walks and the properties related with our results, such as separability, entanglement entropy, etc. After, it is studied coined discrete-time quantum walks, giving its motivation, evolution, time asymptotic probability distribution and properties. The reduced dynamics of the quantum coin is also included as another interesting perspective that one can take in quantum walks. Finally the generalized elephant quantum walk is introduced.

Chapter 4 describes the results obtained in the study of the generalized elephant quantum walk, an analysis of the entanglement entropy generation in various settings, including localized and delocalized initial states and the relation with the amount of disorder used. We also address an analysis of the quasi-stationary regime.

The conclusion is made in chapter 5, summarizing our results, highlighting some important points and giving some perspectives on possible future lines of research.

Fig. 1 shows a map of the dissertation, intended to give another perspective on the subjects approached by this document. One can use it as a map to navigate between the topics according to its previous knowledge, with some suggestions of paths to follow. In it is also given possible comparisons between the properties of classical random walks and coined discrete-time quantum walks as a way to ease the understanding and resume the possible relations between the two.

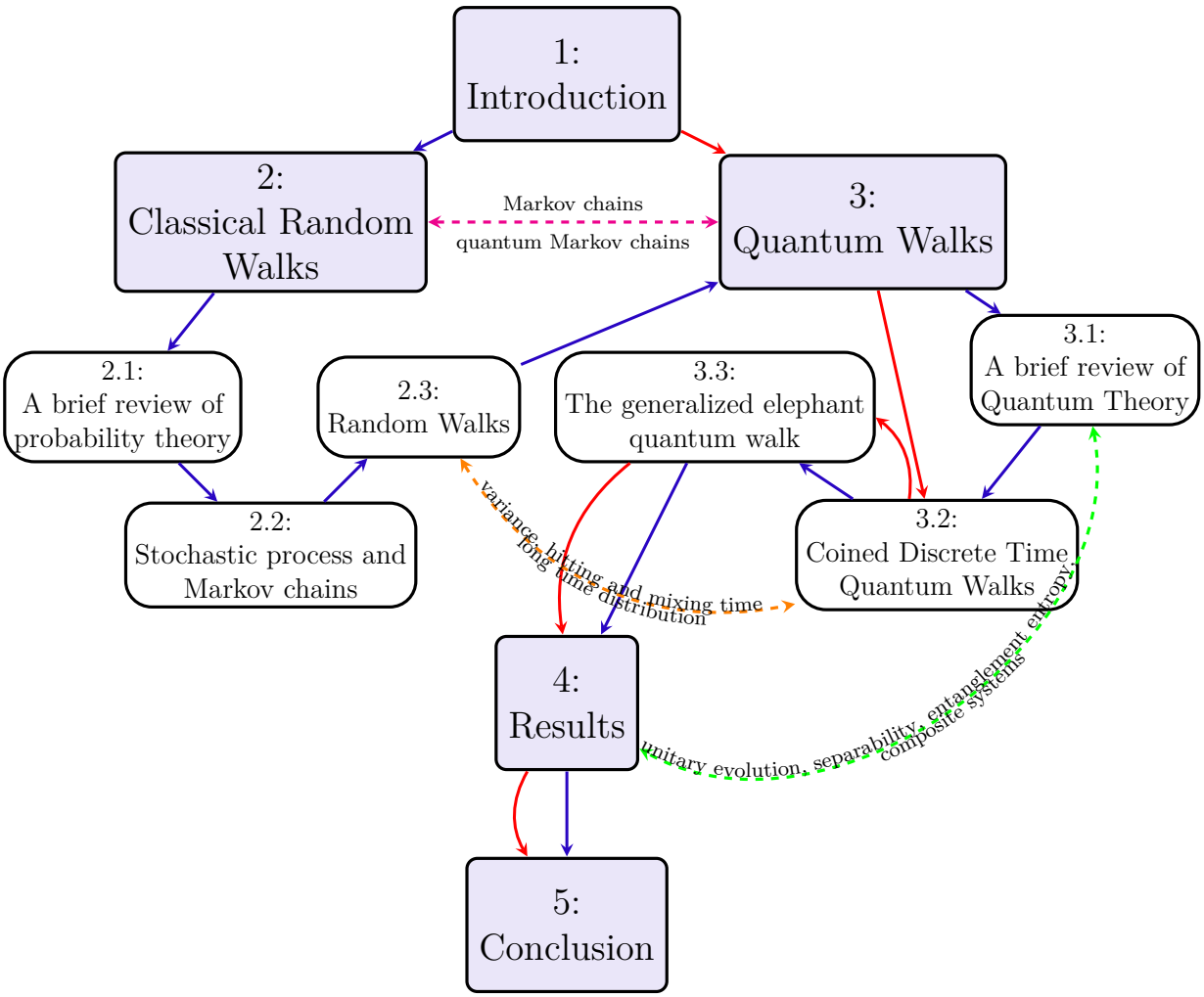

Figure 1 – (Color online) Map of the topics addressed in this thesis. The blue arrows indicate the natural path to read the document and it is recommended to one that was not introduced to any of the essential concepts of classical random walks and quantum walks. The red ones are recommended to the person that already had been presented to classical random walks and quantum theory, yet a fast reading of Sec. 3.2.3 might sum. The dashed double arrowed lines indicate possible comparisons and relations between the topics.

Source: By the author.

2 CLASSICAL RANDOM WALKS

Usually, when one introduces classical random walks to someone we start up by giving the example of a sizeless drunk who lives in a one-dimensional universe and that wants to get home after drinking so much that he can not remember in which direction his house is. Without considering that he might realize that staying in the middle of the way is an option, the drunk is said to have equal probabilities of taking a step to the right or to the left. Given that this is a random process, after some steps the only information that we are going to have is the position probability distribution of the drunken point. This type of random walk is called *unbiased one-dimensional random walk*, or *random walk on a line*. However, the motivation behind the study of random walks does not come only from this fanciful example.

The first time that the term *random walks* appeared in the literature was in the seminal paper by K. Pearson.[4] But before that, some authors already had studied a related problem, the famous Brownian motion,[5] a description of the motion of a particle in a solvent, later studied by A. Einstein[6] where he utilized the kinetic theory of gases to describe the motion of the particle as a result of infinite collisions with the small particles of the solvent. L. Bachelier[7] studied and formalized the same problem in the context of stock market prices. This shows us that, despite the apparent simplicity of the problem, random walks can serve as a toy model for various problems in all fields of science. Other applications of random walks are in the field of computation, where they can be used to develop stochastic algorithms to solve search problems, like the blind search algorithm, to solve satisfiability problems and where it is an essential idea in the Simulated Annealing algorithm, that searches for the ground state of a system through a random search in its sample space. [i]

In this chapter we first briefly have a look at probability theory, following the chapter on the matter in the book from H.-P. Breuer and F. Petruccione,[10] introducing the concept of random variables and some important statistical quantities. After it, we study the definition of stochastic process and what is a Markov process, preparing the way to fully understand classical random walks that are introduced in the next section. We discuss the discrete one-dimensional random walk on the line, as it is the simplest model of random walks and nonetheless show us all the interesting properties of standard random walks, also analyzing its long time limiting behavior.

[i] For a review of some random walk based algorithms look.[8,9]

2.1 A brief review of probability theory

In our daily life, there are events, or happenings, that happen randomly. For example, imagine that you are blindly shooting arrows into a target. The location of where the arrows hit are random, in the sense that the result is not certain given the initial conditions, like the force applied. We can only guess where the arrows will land, and the way we do this is through the assignment of probabilities for the events. Another example of a random event is the tossing of a coin. The individual results, heads or tails, are what we call *elementary events*. We can also note composition of elementary events, like the result of n coin tosses. The set of elementary events is denominated *sample space*, or *space of events*,[10] represented mathematically by the symbol Ω. So, the sample space is a set in which the random events are subsets of it, with the elementary events being the subsets with only one element.

Another important concept in probability theory is the concept of σ-algebra. A σ-algebra $\mathcal{A}$ is a system of subsets of the sample space Ω that specifies which kind of events we want to include in our theory. For that, this system must suit a set of requirements, that are

1. The sample space and the empty space belongs to the σ-algebra, $\Omega \in \mathcal{A}$, $\varnothing \in \mathcal{A}$;

2. Given that A_1 and A_2 are two events from the σ-algebra, $A_1 \cup A_2$, $A_1 \cap A_2$ and $A_1/A_2 \in \mathcal{A}$;

3. If $\{A_i, i = 1 \dots n, n \in N\} \in \mathcal{A}$, then $\cup_{i=1}^{n} A_i \in \mathcal{A}$.

These requirements are important for they allow us to perform logical operations with the events of the sample space. The first requirement say to us that all events is a possible event of our algebra and this includes nothing, the second one means that logical compositions of events are also possible and the final one assures that any countable union of events stills is an event of the σ-algebra.

Next we introduce the notion of a *probability measure* on the σ-algebra. A probability measure $\mu : \mathcal{A} \to \mathbb{R}$ is a map between the set of allowed events and the real numbers, interpreted as the probability of these events. As we want to give it a probability characteristic, the probability measure must satisfy a certain set of axioms, the *Kolmogorov axioms*

1. For all events $A \in \mathcal{A}$

$$0 \leq \mu(A) \leq 1$$

2. The probability measure over the sample space is normalized

$$\mu(\Omega) = 1$$

3. Considering a countable union of disjoint events, the probability measure over it is given by

$$\mu(\cup_{i=1}^{n} A_i) = \sum_{i=1}^{n} \mu(A_i)$$

The sample space together with the σ-algebra and the probability measure μ consists in what we call a *probability space*.

An important concept in probability theory, special to understand Markovian processes, is the notion of conditional probability. The conditional probability of an event A_1 conditioned on the event A_2 is given by

$$\mu(A_1|A_2) = \frac{\mu(A_1 \cap A_2)}{\mu(A_2)} \ . \tag{2.1}$$

The conditional probability also defines the notion of *statistical independence*. From the equation above we find that an event is independent of another if and only if

$$\mu(A_1|A_2) = \mu(A_1) \leftrightarrow \mu(A_1 \cap A_2) = \mu(A_1).\mu(A_2) \ , \tag{2.2}$$

which means that the probability of the events A_1 AND A_2 occur is simply given by the product of the individual probabilities.

In order to one describe mathematically elementary events of any random process the concept of *random variables* must be brought on. A random variable is a map between the elementary events of the sample space and the set of real numbers,

$$X : \Omega \to \mathbb{R} \ , \tag{2.3}$$

where

$$X(\omega) = x \ , \tag{2.4}$$

with $\omega \in \Omega$ being an elementary event and x, called a *realization* of the random variable, $x \in \mathbb{R}$.

However, for a random variable to be well defined it must satisfy the requirement of being a measurable function. To be a measurable function, the pre-image of a random

variable $X^{-1}(B) = A$ over any Borel set B [ii] must belong to the σ-algebra, i.e. $A \in \mathcal{A}$.[10] This ensures that the probability of any pre-image A is also well defined.

With the random variable it is possible to define a *probability distribution*

$$\Pr_X(x) = \mu(X^{-1}(x)) \ ,$$

where $\Pr_X$ denotes the probability distribution associated with the random variable X.

Another mathematical structure that appears frequently in probability theory and especially in physics, associated with the probability distribution, is the *probability density*. But before we introduce the notion of probability density, it is worth to show the requirement for a random variable to have a probability density.

The *cumulative distribution* function of a random variable X is given by

$$F_X(x) \equiv \mu(\{\omega \in \Omega | X(\omega) \leq x\}) \ . \tag{2.5}$$

A random variable has a probability density if its cumulative distribution can be represented as

$$F_X(x) = \int_{-\infty}^{x} dy \ \rho_X(y) \ , \tag{2.6}$$

with ρ_X being the probability density of the random variable X.

The connection between the probability density and the probability distribution is given by

$$\Pr_X(B) = \int_B dx \ \rho_X(x) \ , \tag{2.7}$$

where B is the Borel set of the σ-algebra. We can use the probability distribution and the probability density interchangeably by noting that we can construct a probability density from the probability distribution through the use of Dirac delta functions

$$\rho_X(x) = \sum_y \delta(x - y) \Pr_X(y) \ . \tag{2.8}$$

One of the important quantities to characterize a probability distribution associated with a random variable is the *expectation value* or *mean* of a random variable. Given that

[ii] A Borel set B is an element of the σ-algebra of the Borel sets of $\mathbb{R}$, $\mathcal{B}$. The σ-algebra of the Borel sets of the real numbers, in turn, is the smallest σ-algebra which contains all the subsets of the form $(-\infty, x)$, $x \in \mathbb{R}$.[10]

$\rho_X(x)$ is the probability density associated with a continuous random variable X, the expectation value of it is defined as[10]

$$E(X) = \int_{-\infty}^{\infty} dx\ x\ \rho_X(x)\ . \tag{2.9}$$

If the random variable is over a discrete sample space, using Eq. (2.8) we find

$$E(X) = \int_{-\infty}^{\infty} dx'\ x'\ \sum_x \delta(x' - x)\mathrm{Pr}_X(x) = \sum_x x\ \mathrm{Pr}_X(x)\ . \tag{2.10}$$

Another notation for the expected value of X is $\langle X \rangle$, that for now on we choose to use. We can also calculate the expectation value of transformations of a random variable. The *n-th moment* of a continuous random variable is defined as

$$\langle X^n \rangle = \int_{-\infty}^{\infty} dx\ x^n\ \rho_X(x)\ , \tag{2.11}$$

and discrete version

$$\langle X^n \rangle = \sum_x x^n \mathrm{Pr}_X(x)\ . \tag{2.12}$$

With the first and second moments the *variance*, or square of the standard deviation, of a random variable is defined

$$\mathrm{Var}(X) = \sigma^2(X) = \langle (X^2 - \langle X \rangle)^2 \rangle = \langle X^2 \rangle - \langle X \rangle^2\ . \tag{2.13}$$

This quantity is a measure of the square of the width of the probability distribution around its mean. It will be important for our future characterization of the walks.

In the next section we are going to approach two important concepts in understanding random walks, the ones of stochastic processes and Markov chains.

2.2 Stochastic processes and Markov chains

A stochastic process is a set of random variables $\{X_t\}$, indexed by a time index, on a common sample space Ω.[10] We can think of a stochastic process as a set of observations of the result of a random variable over time, where we see them in discrete time intervals or continuously. Considering our "blindly shooting at a target" example, the stochastic process would be the observations of where the arrows land on the target after subsequent shots. In this case, the observations are done in discrete time intervals and therefore the associated random variables are indexed by a discrete set of time steps (if we are considering a normal archer, he probably can not shoot faster than a normal human can see the arrows hitting the target). More formally, a stochastic process associated with a sample space is

$$X : \Omega \times T \to \mathbb{R}\ , \tag{2.14}$$

with T being the index set.

Given that a stochastic process has length n, i.e $\{X_{t_1}, \ldots, X_{t_n}\}$, the family of joint probability densities of n observations, with $n \in \mathbb{Z}$

$$\rho_n(x_n, t_n; x_{n-1}, t_{n-1}; \ldots; x_1, t_1) \ ,$$

completely determines the correlations between the random variables in different time instants. This joint probability density gives us the probability that the random variable X assumes the results $\{x_1, x_2, \ldots, x_n\}$ in the time instants $\{t_1, t_2, \ldots, t_n\}$.

There is a class of stochastic processes which we call *Markovian processes*. These types of processes are characterized by the fact that the result obtained in a given instant of time depends only on the result obtained on the previous one. We study them because, besides their simplicity, often we can assume that the source of noise in a system acts independently through time.

Putting more formally the definition of a Markovian process, given a set of random variables $\{X_{t_1}, \ldots, X_{t_n}\}$, the one point probability density of the random variable X_n can be written as

$$\rho_1(x_n, t_n) = \int \ldots \int dx_{n-1} dx_{n-2} \ldots dx_1 \ \rho_n(x_n, t_n; \ldots; x_1, t_1) \ .$$

Using the conditional probability definition Eq.(2.1), we can write ρ_n as

$$\rho_n(x_n, t_n; \ldots; x_1, t_1) = \rho_{1|n-1}(x_n, t_n | x_{n-1}, t_{n-1}; \ldots; x_1, t_1) \rho_{n-1}(x_{n-1}, t_{n-1}; \ldots; x_1, t_1) \ .$$

Repeating this procedure, we get

$$\rho_1(x_n, t_n) = \int \ldots \int dx_{n-1} dx_{n-2} \ldots dx_1 \ \rho_{1|n-1} \rho_{1|n-2} \ldots \rho_{1|1}(x_2, t_2 | x_1, t_1) \rho_1(x_1, t_1) \ . \quad (2.15)$$

The Markovian condition is that the conditional probabilities obeys

$$\rho_{1|l-1}(x_l, t_l | x_{l-1}, t_{l-1}; \ldots) = \rho_{1|1}(x_l, t_l | x_{l-1}, t_{l-1}), \ \forall l \in \{1, \ldots, n\} \ , \quad (2.16)$$

that is, the probability of a random variable, in a given time instant, to assume a given result depends only on the immediate past result. This condition is what characterizes a "memoryless" process.

It is worth to mention the Chapman-Kolmogorov equation[10]

$$\rho_{1|1}(x_3, t_3 | x_1, t_1) = \int dx_2 \ \rho_{1|1}(x_3, t_3 | x_2, t_2) \rho_{1|1}(x_2, t_2 | x_1, t_1) \ . \quad (2.17)$$

We can see that every Markovian process satisfies the Chapman-Kolmogorov equation, because

$$\begin{aligned}\rho_2(x_3,t_3;x_1,t_1) &= \int dx_2\ \rho_3(x_3,t_3;x_2,t_2;x_1,t_1)\\ &= \int dx_2\ \rho_{1|2}(x_3,t_3|x_2,t_2;x_1,t_1)\rho_2(x_2,t_2;x_1,t_1)\\ &= \int dx_2\ \rho_{1|1}(x_3,t_3|x_2,t_2)\rho_{1|1}(x_2,t_2|x_1,t_1)\rho_1(x_1,t_1)\ ,\end{aligned}$$

where in the last line we used the Markovian condition. By rewriting the left-hand side of the equation in terms of the conditional probability of X_{t_3} on X_{t_1} we get to the Chapman-Kolmogorov equation

$$\begin{aligned}\rho_{1|1}(x_3,t_3|x_1,t_1)\rho_1(x_1,t_1) &= \int dx_2\ \rho_{1|1}(x_3,t_3|x_2,t_2)\rho_{1|1}(x_2,t_2|x_1,t_1)\rho_1(x_1,t_1)\\ \rho_{1|1}(x_3,t_3|x_1,t_1) &= \int dx_2\ \rho_{1|1}(x_3,t_3|x_2,t_2)\rho_{1|1}(x_2,t_2|x_1,t_1)\ .\end{aligned}$$

Note that every stochastic process that satisfies the Markovian condition satisfies the Chapman-Kolmogorov equation, but the converse is not true. Using the Chapman-Kolmogorov equation it is possible to reconstruct all higher-order probability densities if we have an initial probability density

$$\rho_m(x_m,t_m;x_{m-1},t_{m-1};\ldots;x_1,t_1) = \prod_{n=1}^{m}\rho_{1|1}(x_n,t_n|x_{n-1},t_{n-1})\rho_1(x_0,t_0)\ . \tag{2.18}$$

Is this aspect that makes Markovian processes much simpler to be studied.

The one to one conditional probabilities are called *conditional transition probabilities*, or *propagators*. The reason for this nomenclature is made clearer when we look to the connection between the probability densities

$$\rho_1(x,t) = \int dx'\ T(x,t|x',t')\rho_1(x',t'), \tag{2.19}$$

where $T(x,t|x',t') = \rho_{1|1}(x,t|x',t')$ is the propagator between the states x' at time t' and x at time t.

Markovian stochastic processes in which the sample space is discrete are classified in two categories, in Discrete-Time Markov Chains (DTMC) and in Continuous-Time Markov Chains (CTMC). In the next section we introduce DTMC's since it is an essential topic to one understand the standard random walk. We suggest to the reader the following reference[10] regarding continuous-time Markov chains that here we are not going to address.

2.2.1 Discrete-time Markov chains

Given an initial probability distribution, describing the initial state of the chain, it is possible to construct a matrix equation that describes the probability distribution evolution accordingly with the Markov chain. In the case of the DTMC's over a sample space $\Omega = \{1, 2, \ldots, m\}$, we have a probability vector

$$\vec{p}(t) = \begin{pmatrix} p_1(t) \\ p_2(t) \\ \vdots \end{pmatrix} \tag{2.20}$$

where $p_1(t), p_2(t), \ldots$ are the probabilities of X_t to realize the states $1, 2$, and so on. For the $\vec{p}$ vector to describe a probability vector we have to ensure that $\sum_{i=1}^{m} p_i = 1$ for all times.

The matrix that connects the probability vectors at different times is called *stochastic matrix*. By using the definition of conditional probabilities we can find a relation between the probabilities at different time steps

$$\begin{aligned} p_i(t) &= \sum_j \Pr(X_t = i, X_{t'} = j) \\ &= \sum_j \Pr(X_t = i | X_{t'} = j) p_j(t') \ , \end{aligned} \tag{2.21}$$

and therefore, a relation between the probabilities vectors

$$\vec{p}(t) = T^{(t,t')} \vec{p}(t'), \tag{2.22}$$

where $T^{(t,t')}$ is the stochastic matrix for the transition from the time step $t' < t$ to t and whose elements are the transition probabilities $T_{i,j}^{(t,t')} = \Pr(X_t = i | X_{t'} = j)$.

One property of the stochastic matrix is that, by conservation of the probability, the sum of every element in a given column must be equal to one.

$$\sum_i p_i(t) = \sum_{i,j} T_{i,j}^{(t,t')} p_j(t) \leftrightarrow \sum_j (\sum_i T_{i,j}^{(t,t')}) p_j(t) = 1 \leftrightarrow \sum_i T_{i,j}^{(t,t')} = 1 \ . \tag{2.23}$$

By using the Markovian condition it is possible to rewrite the evolution matrix equation from the initial time step t_0 to t as a successive application of the transition matrix between each time step in this time interval. Following

$$\begin{aligned}\Pr(x_t) &= \sum_{x_{t-1},\ldots,x_0} \Pr(x_t|x_{t-1},\ldots,x_0)\Pr(x_{t-1},\ldots,x_{t_0}) \\ &= \sum_{x_{t-1},\ldots,x_{t_0}} \Pr(x_t|x_{t-1})\Pr(x_{t-1},\ldots,x_{t_0}) \\ &= \sum_{x_{t-1},\ldots,x_{t_0}} \Pr(x_t|x_{t-1})\Pr(x_{t-1}|x_{t-2},\ldots,x_{t_0}))\Pr(x_{t-1},\ldots,x_{t_0}) \ ,\end{aligned}$$

where in the second line we utilized the Markovian condition and in the third the definition of conditional probability. Noting that $\Pr(x_t|x_{t-1})$ are the elements of the transition matrix from $t-1$ to t, by induction we find that

$$\vec{p}(t) = \prod_{j=t_0}^{t-1} T^{(t+t_0-j,t+t_0-j-1)}\vec{p}(t_0) \ . \tag{2.24}$$

If the stochastic process is homogeneous in time, i.e. $T^{(t,t')} = T^{t-t'}$, then

$$\vec{p}(t) = T^{t-t_0}\vec{p}(t_0) \ . \tag{2.25}$$

We are now ready to study classical random walks and its properties. In the following section we are going to define random walks and derive the limiting distribution of a random walk on a line, as well obtain its variance as a function of time and other quantities that give us a complete picture of this kind of stochastic process.

2.3 Random Walks

A random walk is a stochastic process in which random transitions are made through the possible states of a sample space, Ω. More formally, let $G = \{V, E\}$ be a connected and undirected graph where $V = \{v = 1, \ldots, n\}$ is the set of *nodes*, or *vertices*, and $E = \{(i,j) : i,j \in V,\ i \neq j\}$ the set of edges, where (i,j) represents the edge from i directed to j. A graph is connected if there exists a path that leads to every vertex from any starting point. The undirected property means that if $(i,j) \in E$ then $(j,i) \in E$ also. Let T be the stochastic matrix of a random walk over a sample space Ω. We can interpret V as the set of vertices representing the accessible states of the sample space in the random walk, while E is the set of edges representing the possible transitions between them,[9] such that

$$T^{(t,t-1)}_{v_1,v_2} = \begin{cases} \Pr(X_t = v_1 | X_{t-1} = v_2), \text{ if } v_1, v_2 \in V \text{ and } (v_2, v_1) \in E \\ 0 \ , \text{ otherwise.} \end{cases} \tag{2.26}$$

Conversely, a graph can represent a random walk if it encodes in its structure the information about the possible transitions between the states.[9] For example, let G be an

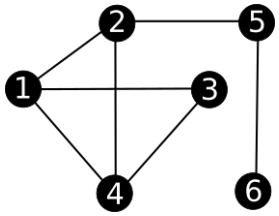

Figure 2 – Six node undirected random graph.

Source: By the author.

undirected and connected graph in which the degree of the vertices are $\deg(v)$. If T is the stochastic matrix of a random walk in G, we may assume that the transition probabilities are

$$T_{i,j} = \begin{cases} \frac{1}{\deg(j)}, \text{ if } (i,j) \in V \\ 0 \text{ , otherwise.} \end{cases} \tag{2.27}$$

In the case of a graph in which $\deg(v) = 2\ \forall v \in V$ and where the possible transitions are made only to two different states and none of them have more than one in common, with no loops, the graph is a line and it characterizes an *unbiased one-dimensional random walk*.

The standard one-dimensional random walk on a infinite line is a Markovian random walk where we assume that the random walk is homogeneous in time and space, i.e. the same stochastic matrix T is used in every time step and the transition probabilities are equal for every position, $T_{i+1,i} = p$ and $T_{i-1,i} = 1 - p$. Thereby, using Eq.(2.21) and the fact that the walker only take unit step sizes, the equation that relates the probabilities in subsequent steps is given by

$$p_x(t) = T_{x,x-1}p_{x-1}(t-1) + T_{x,x+1}p_{x+1}(t-1) \ , \tag{2.28}$$

with $T_{x,x\pm1} = \Pr(X_t = x | X_{t-1} = x \pm 1)$. This tell us that the elements of the infinite transition matrix is simply given by the relation

$$T_{i,j} = p\delta_{j,i-1} + (1-p)\delta_{j,i+1} \ . \tag{2.29}$$

A random walk does not have to be a Markovian process. It is possible to define a random walk in which the transition matrix from a time step t_0 to t cannot be broken into the application of $t - t_0$ transition matrices, meaning that the conditional probabilities depend on distant previous steps. For instance, we have the elephant random walk,[11] a random walk in which the results of the coin depend on its previous results giving the random walk different diffusive behaviors according to the degree of dependence of the present probabilities on the past. This type of random walk can also be interpreted as a

random walk where the one-step transition probabilities are position and time dependent, meaning that random walks are not limited to the time-space homogeneous cases.[iii]

Next we derive the position probability distribution of the random walk on a line and with it some statistical properties, including quantities necessary to quantify the usefulness of a given random walk to computation, and finally derive the time asymptotic limiting probability distribution.

2.3.1 Properties of the one-dimensional random walk

Given that the walker starts at position 0, what is the probability that we will find him in the starting position at time t? The walker could start by taking $t/2$ steps to the right and then take $t/2$ steps to the left. But it is also possible that the walker does the other way around. Or even that it takes one step to the right, then one step to the left and so on. The important fact that we have to note is that it does not matter in what order or how many steps to the left and right the walker takes, provided that the resulting displacement is zero and the number of steps is t. Generalizing this reasoning for any position, that is making the resulting displacement x, the probability of finding the walker at position x at time step t is[13]

$$\Pr(x,t) = \frac{t!}{n_+!n_-!}(1-p)^{n_-}p^{n_+} \ , \tag{2.30}$$

where $n_+ = (t+x)/2$ is the number of steps to the right and $n_- = (t-x)/2$ the number of steps to the left. The multiplying factor $t!/(n_+!n_-!)$ accounts for all possible permutations of the steps that results in the x displacement. We have to introduce another factor into Eq. (2.30) that accounts for the modularity property of the random walk. This property means that if the time step is an even (odd) number, the probability of the walker being in an odd (even) position is zero. Therefore, we have the following equation

$$\Pr(x,t) = \frac{1+(-1)^{t-x}}{2}\frac{t!}{n_+!n_-!}(1-p)^{n_-}p^{n_+}. \tag{2.31}$$

The Eq. (2.30) is called *binomial distribution*. The reason is that this equation represents a term in the binomial formula,

$$(p+q)^t = \sum_{i=0}^{t}\frac{t!}{(t-i)!i!}p^i q^{t-i}, \tag{2.32}$$

as we can see by substituting q by $1-p$ and noting that $n_+ + n_- = t$. In Fig. 3 we have the binomial distribution for a random walk on a line with $p = 1/2$ and at time step $t = 100$.

[iii] For an extensive study and an interesting extension of the elephant random walk we suggest to the reader the thesis of V. M. Monteiro.[12]

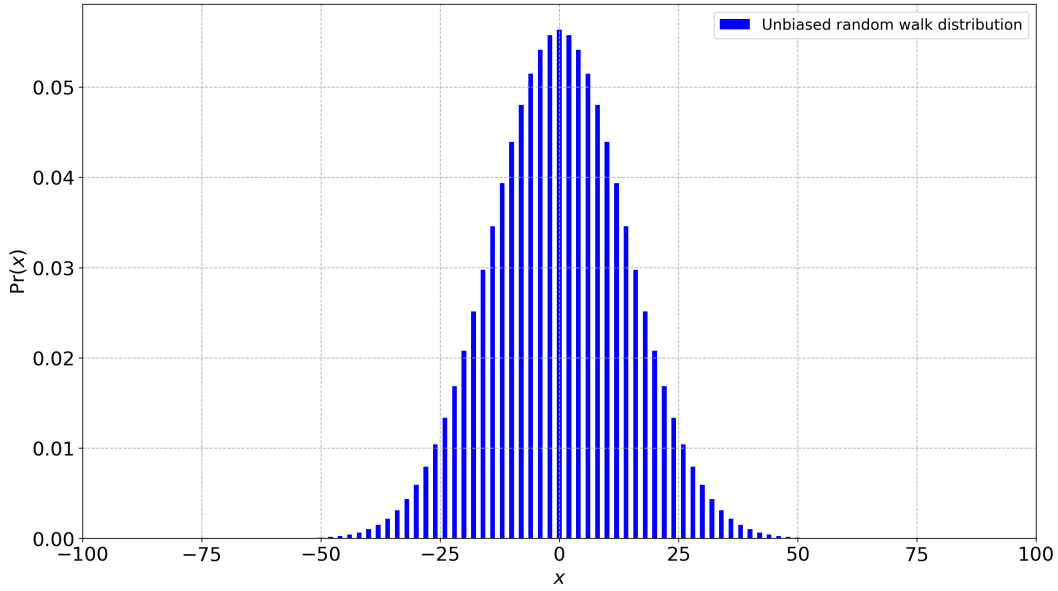

Figure 3 – Classical unbiased random walk binomial distribution at time $t = 100$.

Source: By the author.

With the equation of the probability of the walker being at position x at time t we can derive some statistical properties of the random walk. Initially, let us derive the average, or the first moment, of the walker's position when starting at the origin. Using the discrete random variable first moment definition Eq. (2.10), we get

$$\langle X_t \rangle = \sum_{x=-t}^{t} \frac{t!}{((t-x)/2)!((t+x)/2)!}(1-p)^{(t-x)/2}p^{(t+x)/2}\, x. \tag{2.33}$$

To find the position average we are going to calculate the mean of N_+, the random variable associated with the right displacements n_+, making use of the binomial equation Eq. (2.32). First we have to substitute $(1-p)$ by an independent variable that in the end we are going to set as $(1-p)$. Now, note that

$$p\frac{\partial}{\partial p}(p^{n_+}) = n_+ p^{n_+}, \tag{2.34}$$

consequently we can manipulate Eq. (2.33) first by substituting in such a way that[13]

$$\begin{aligned}\langle N_+\rangle &= \sum_{n_+=0}^{t} \frac{t!}{(t-n_+)!n_+!} q^{t-n_+} \left(p\frac{\partial}{\partial p}(p^{n_+}) \right) \\ &= p\frac{\partial}{\partial p}\left(\sum_{n_+=0}^{t} \frac{t!}{(t-n_+)!n_+!} q^{t-n_+} p^{n_+} \right) \\ &= p\frac{\partial}{\partial p}(p+q)^t \\ &= p\ t\ (p+q)^{t-1}\ ,\end{aligned}$$

where in the second line we used the fact that the sum of the derivative is the derivative of the sum. Setting the particular case where $q = 1 - p$, we find the mean displacement to the right and the mean position using $X_t = 2N_+ - t$

$$\langle N_+\rangle = pt \tag{2.35}$$

$$\langle X_t\rangle = (2p-1)t \tag{2.36}$$

These results are according to our intuition that says that, for example, if $p = 1/2$, i.e. we have equal probabilities of moving to the right or to the left, the average displacement will be zero. Also, the average displacement to the right is simply the probability of moving to the right times the number of steps.

One easier way to calculate the position mean is to use the definition of the position random variable. The position random variable of a random walk on the line can be interpreted as a sum of independent and equally distributed random variables, the coin results. Independency between the coin random variables results is another manifestation that this type of random walk is Markovian. These random variables are modified versions of the Bernoulli distributed random variable

$$\mathrm{Be}(p) = \begin{cases} 1, \text{ with prob. } p \\ 0, \text{ with prob. } (1-p)\ , \end{cases} \tag{2.37}$$

where the results are changed to ± 1. In such a way, X_t will be

$$X_t = \sum_{i=1}^{t} \sigma_i + x_0\ , \tag{2.38}$$

with x_0 being the initial position and

$$\sigma_i = \begin{cases} +1, \text{ with prob. } p \\ -1, \text{ with prob. } (1-p)\ . \end{cases} \tag{2.39}$$

Following Eq. (2.38)

$$\langle X_t \rangle = \sum_{i=1}^{t} \langle \sigma_i \rangle + x_0 \ ,$$

where in the second line we used the fact that the average of the sum is the sum of the averages. By the definition of average, the average value of σ_i is $\langle \sigma_i \rangle = p \cdot (1) + (1-p) \cdot (-1) = 2p - 1$, therefore

$$\langle X_t \rangle = (2p-1)t + x_0 \ . \tag{2.40}$$

Setting $x_0 = 0$ we retrieve the result found on Eq. (2.36).

Given the position mean, we need only to calculate the average position-squared to find the position variance. Taking Eq. (2.11) with $n = 2$, and considering the n_+ random variable

$$\langle N_+^2 \rangle = \sum_{n_+=0}^{t} \frac{t!}{(t-n_+)!n_+!} q^{t-n_+} p^{n_+} n_+^2 \ . \tag{2.41}$$

We employ the derivative trick used earlier, now taking two derivatives with respect to p

$$\begin{aligned}
\langle N_+^2 \rangle &= \sum_{n_+=0}^{t} \frac{t!}{(t-n_+)!n_+!} q^{t-n_+} \left(p \frac{\partial}{\partial p} (p \frac{\partial}{\partial p} p^{n_+}) \right) . \\
&= p \frac{\partial}{\partial p} \left(p \frac{\partial}{\partial p} (\sum_{n_+=0}^{t} \frac{t!}{(t-n_+)!n_+!} q^{t-n_+} p^{n_+}) \right) \\
&= p \frac{\partial}{\partial p} \left(p \frac{\partial}{\partial p} ((p+q)^t) \right) \\
&= p \frac{\partial}{\partial p} \left(pt(p+q)^{t-1} \right) = p \left(t(p+q)^{t-1} + pt(t-1)(p+q)^{t-2} \right) \ .
\end{aligned} \tag{2.42}$$

Setting $q = 1 - p$, we get

$$\langle N_+^2 \rangle = pt + p^2 t(t-1) = \langle N_+ \rangle^2 + tp(1-p) \tag{2.43}$$

$$\langle X_t^2 \rangle = 4\langle N_+^2 \rangle - t^2 - 2t\langle X_t \rangle = t^2(1 - 4p(1-p)) + 4tp(1-p) \tag{2.44}$$

Therefore, using Eq. (2.13), the position variance of the classical one-dimensional random walk is[13]

$$\mathrm{Var}_{X_t}(t) = \langle X_t^2 \rangle - \langle X_t \rangle^2 = 4tp(1-p) \ , \tag{2.45}$$

with the special case $p = 1/2$ resulting in

$$\mathrm{Var}_{X_t}(t) = t \ . \tag{2.46}$$

For completeness, we show the method used to calculate the mean position-squared using the position random variable definition Eq. (2.38). The square of the position random variable will be

$$X_t^2 = \left(\sum_{i=1}^{t} \sigma_i + x_0\right)^2 = \sum_{i,j} \sigma_i \sigma_j + 2x_0 \sum_i \sigma_i + x_0^2 \ . \tag{2.47}$$

The average is

$$\langle X_t^2 \rangle = \sum_{i,j} \langle \sigma_i \sigma_j \rangle + 2x_0 \sum_i \langle \sigma_i \rangle + x_0^2 \ . \tag{2.48}$$

From here we have to note that the average of the product $\langle \sigma_i \sigma_j \rangle$ is divided into two sets, when $i \neq j$ and when $i = j$. In the former case $\langle \sigma_i^2 \rangle = 1$, as $\sigma_i^2 = 1$ always, and in the last case as σ are equally and independently distributed random variables through time the average $\langle \sigma_i \sigma_j \rangle = \langle \sigma_i \rangle \langle \sigma_j \rangle = (2p-1)^2$. Thereby

$$\begin{aligned} \langle X_t^2 \rangle &= \sum_{i=1}^{t} \langle \sigma_i^2 \rangle + \sum_{i,j,i \neq j} \langle \sigma_i \sigma_j \rangle + 2x_0(2p-1)t + x_0^2 \\ &= t + (2p-1)^2(t^2 - t) + 2x_0(2p-1)t + x_0^2 \ , \end{aligned} \tag{2.49}$$

and the position variance is

$$\begin{aligned} \mathrm{Var}_{X_t}(t) &= \langle X_t^2 \rangle - \langle X_t \rangle^2 \\ &= t + (2p-1)^2(t^2 - t) + 2x_0(2p-1)t + x_0^2 - (2p-1)^2 t^2 - x_0^2 - 2x_0(2p-1)t \\ &= \left(-4p^2 + 4p - 1 + 1\right) t = 4tp(1-p) \ , \end{aligned} \tag{2.50}$$

obtaining the previous result Eq. (2.45).

With the above equation we have an important fact that is that the random walk variance does not depend on the initial position as we did not assume any value for x_0. It also tells us that the standard deviation of the position probability distribution grows proportionally with the square-root of the time, a central feature in the use of random walks in the study in many areas.

Other two important quantities in the characterization of random walks – especially in their use to develop stochastic algorithms – are the *hitting time* and the *mixing time*.

But before stating the definition of hitting and mixing time we have to define what is the stationary distribution of a stochastic process. Given that a stochastic process $\{X_t\}$ over the sample space $\Omega = \{x_1, x_2, \ldots\}$ has a probability distribution $\rho_X(x,t)$, the stationary distribution, if it exists, is defined as

$$\lim_{t\to\infty} \rho_X(x,t) = \pi_X(x) \ . \tag{2.51}$$

In the case of a general graph in which the degree of each vertex gives us the transition probabilities of the random walk like in Eq. (2.27), the limiting probability distribution will be[9,14]

$$\pi(x) = \frac{\deg(x)}{2m} \ , \tag{2.52}$$

where $|E| = m$, i.e. the number of edges in the graph.

Definition 2.3.1. (*Hitting time*): The hitting time is the average number of time steps that is needed to a given node j being visited from a starting node i[9,14]

$$h(i,j) = \sum_{m=0}^{\infty} m\Pr(j,m) \ . \tag{2.53}$$

Definition 2.3.2. (*Mixing time*): The e-mixing time is defined as the minimum time in which the random walk probability distribution is e-close to the stationary distribution

$$\mathcal{M}_e = \min\{T : \forall t \geq T,\ |p(.,t) - \pi(.)|_{\text{tvd}} \leq e\} \ , \tag{2.54}$$

where $|.|_{\text{tvd}}$ stands for the total variation distance between the two probability distributions

$$|p(.,t) - \pi(.)|_{\text{tvd}} = \sum_x |p(x,t) - \pi(x)| \ . \tag{2.55}$$

The definition of hitting time accounts for the average time needed to a given vertex being hit by the walker after starting from another vertex. When thinking in devising stochastic algorithms to find a marked vertex, for instance, the hitting time is an important factor that one must consider. With respect to the mixing time, we use it to measure the time needed to get the probability distribution to the limiting probability distribution. For the random walk, its mixing time is upper limited by the square of t, i.e. $\mathcal{M}_e = O(t^2)$.[15]

As an example, we calculate the hitting time of an unbiased one-dimensional random walk. It can be estimated by taking the inverse of position probability distribution.[14] For that, we need to use the Stirling formula that give us an approximation of factorials of big numbers[16]

$$n! \approx \sqrt{2\pi n}\left(\frac{n}{e}\right)^n \ , \tag{2.56}$$

considering long time steps

$$\begin{aligned}\Pr(x,t) &= \frac{t!}{(\frac{t+x}{2})!(\frac{t-x}{2})!}(1-p)^{(t-x)/2}p^{(t+x)/2} \\ &\approx \sqrt{\frac{2t}{\pi(t^2-x^2)}}\frac{(2t)^t}{(t-x)^{(t-x)/2}(t+x)^{(t+x)/2}}(1-p)^{(t-x)/2}p^{(t+x)/2} \ .\end{aligned} \tag{2.57}$$

For the vertices that are closer to the origin, i.e. $|x| \ll t$, using $(t^2 - x^2) \approx t^2$, $(t \pm x) \approx t$ we find

$$\Pr(x,t) \approx \sqrt{\frac{2}{\pi t}}\frac{2^t}{(1-p)^{-t/2}p^{-t/2}} \ . \tag{2.58}$$

With $p = 1/2$, the hitting time is upper limited by the square-root of the time $h(0,x) = O(\sqrt{t})$.[iv]

Taking the vertices that are closer to the distribution edges $x \approx \pm t$, $t \pm x$ is going to be either approximately $2t$ or a very small number. Then we will have two cases

$$\Pr(x,t) \approx \begin{cases} \sqrt{\frac{2}{\pi t}}p^t, \ x \approx t \\ \sqrt{\frac{2}{\pi t}}(1-p)^t, \ x \approx -t \ . \end{cases} \tag{2.59}$$

For an unbiased walk $p = 1/2$, the hitting time will be $h(0,x) = O(2^t)$. Note that in this case it does not matter if $x \approx t$ or $x \approx -t$. This tells us that for vertices that are far away from the origin the hitting time can be exponentially larger than those that are closer.

Summarizing, for the classical unbiased random walk the hitting time between the origin and the remaining vertices is given by[14]

$$h(0,x) = \begin{cases} O(\sqrt{t}), \ |x| \ll t \\ O(2^t), \ x \approx \pm t \ . \end{cases} \tag{2.60}$$

From now on we look at the long-time behavior of the one-dimensional random walk taking as reference the book of F. Reif.[13]

[iv] The big-O notation describes the limiting behavior of some function $g(x)$. If $g(x) = O(f(x))$, this means that there exists some $M > 0$ and some x_0 such that $g(x > x_0) \leq Mf(x > x_0)$, i.e. $g(x)$ is upper limited by $f(x)$.

2.3.2 Long-time limit of the classical one-dimensional random walk

The binomial probability distribution has an interesting property that when t becomes large enough it starts to have a pronounced peak around a value and rapidly decreases when one moves away from it. This means that, when $t \gg 1$, the variation of the probability distribution around the maximum is small and we can treat it as a continuous distribution.[13] Let us analyze this in more detail.

In order for us find the time asymptotic behavior of the one-dimensional random walk's distribution we are going to first find the maximum value of the logarithm of the right steps distribution, $\tilde{n_+}$. The reason why we are going to use logarithms is because in a Taylor's expansion the sum of the terms can converge more rapidly as logarithms vary more slowly.

Taking the logarithm of Eq. (2.56) we find that $\ln n! \approx n \ln n - n + O(\ln n)$. Applying it on the binomial distribution

$$\begin{aligned} \ln \Pr(n_+, t) &= \ln t! - \ln n_+! - \ln(t - n_+)! + n_+ \ln p + (t - n_+) \ln(1 - p) \\ &\approx t \ln t - n_+ \ln n_+ - (t - n_+) \ln(t - n_+) + n_+ \ln p + (t - n_+) \ln(1 - p) \ . \end{aligned} \tag{2.61}$$

Deriving with respect to n_+ and setting it to zero, we find $\tilde{n_+}$

$$\begin{aligned} \left. \frac{\partial \ln \Pr(n_+, t)}{\partial n_+} \right|_{n_+ = \tilde{n_+}} &\approx \ln\left(\frac{t - \tilde{n_+}}{\tilde{n_+}} \right) + \ln\left(\frac{p}{1 - p} \right) = 0 \\ &\leftrightarrow \tilde{n_+} = tp \ . \end{aligned} \tag{2.62}$$

Realizing another derivative, we can find the second derivative of the distribution on $n_+ = \tilde{n_+}$

$$\left. \frac{\partial^2 \ln \Pr(n_+, t)}{\partial n_+^2} \right|_{n_+ = \tilde{n_+}} \approx \frac{1}{t - \tilde{n_+}} - \frac{1}{\tilde{n_+}} = \frac{-t}{\tilde{n_+}(t - \tilde{n_+})} = \frac{-1}{tp(1 - p)} < 0 \ . \tag{2.63}$$

The above results tell us that, following the second derivative rule for extremal points, the maximum value of the long time limit of the right step sizes happens in the value of n_+ that is equal to the mean right displacement $\langle N_+ \rangle = tp$.

Performing a Taylor's expansion of $\ln \Pr(n_+, t)$ around $\tilde{n_+}$

$$\ln \Pr(n_+, t) = \ln \Pr(\tilde{n_+}, t) + \alpha_1 (n_+ - \tilde{n_+}) + \alpha_2 (n_+ - \tilde{n_+})^2 + O(n_+^3) \ , \tag{2.64}$$

where

$$\alpha_k = \frac{1}{k!}\frac{\partial \ln \Pr(n_+, t)}{\partial n_+}\bigg|_{n_+=\tilde{n_+}} . \tag{2.65}$$

Given that in $\tilde{n_+}$ we have a maximum, $\alpha_1 = 0$ and we can write

$$\Pr(n_+, t) = N e^{(\alpha_2 (n_+ - \tilde{n_+})^2 + \alpha_3 (n_+ - \tilde{n_+})^3 + O(n_+^4))}, \tag{2.66}$$

where N is a normalization factor.

If we neglect higher order terms after the second power, and by substituting α_2, we obtain a gaussian probability distribution

$$\Pr(n_+, t) \approx N e^{\frac{-(n_+ - \tilde{n_+})^2}{2tp(1-p)}} . \tag{2.67}$$

We have now to state the conditions where the above approximations made are valid. First, when we throw off the higher-order terms in the expansion Eq. (2.64) we are saying that the difference between the right displacement and the mean right displacement cannot be greater than some value. Analyzing the higher-order α_k terms, we find that[13]

$$n_+ - \tilde{n_+} \ll tp(1-p) . \tag{2.68}$$

Moreover, we also need to have the probability distribution decaying very quickly when moving away from the maximum value. This means that $|\alpha_2|(n_+ - \tilde{n_+})^2$ must be much greater than one, that is

$$n_+ - \tilde{n_+} \gg \sqrt{tp(1-p)} . \tag{2.69}$$

Joining these two requirements, we find that the major requirement for Eq. (2.67) to be a good approximation of the probability distribution is that $tp(1-p) \gg 1$. This imposes a restriction on the probabilities of moving to the right and to the left: neither p or $1-p$ can be much less than one.[13]

Reminding that $n_+ = (t+x)/2$ we move to the position probability distribution

$$\Pr(x, t) \approx N e^{\frac{-(x - \langle x \rangle)^2}{2\sigma^2}} . \tag{2.70}$$

By imposing the normalization of the probability distribution N is determined. As we are treating the probability distribution as a continuous function the sum is substituted by an integral. The integration limits can be considered as the whole position domain, as

the probability distribution decays very quickly when one gets away from the maximum value. Then

$$\int_{-\infty}^{\infty} \Pr(x,t)\, dx = \int_{-\infty}^{\infty} N e^{\frac{-(x-\langle x\rangle)^2}{2\sigma^2}}\, dx = 1 \leftrightarrow N = \frac{1}{\sqrt{2\pi\sigma^2}}\ , \tag{2.71}$$

leading finally to the well know gaussian distribution of the classical random walk

$$\Pr(x,t) \approx \frac{1}{\sqrt{2\pi\sigma^2}} e^{\frac{-(x-\langle x\rangle)^2}{2\sigma^2}}\ . \tag{2.72}$$

3 QUANTUM WALKS

Both the discrete time quantum walk (DTQW) and continuous time quantum walk (CTQW) were extensively studied and, since its first appearance, have been fruitful in a variety of fields. In the field of quantum computation it was shown that quantum walks can be very useful to develop quantum search algorithms,[17–20] as a way to speedup classical random walk based algorithms. We can mention for example the quantum spatial search,[21] that has an exponential gain over its classical counterpart. Also, A. Childs[22] showed that continuous-time quantum walks can be used as a universal model for quantum computation[22] and after it the same conclusion was found for the discrete-time version.[23,24] More recently, this model was extended to the domain of noisy quantum operations.[25] In physics, for instance, discrete time quantum walks were used to study the thermalization of open qubits,[26–28] neutrino oscillations,[29] photosynthetic energy transfer[30] and in the context of quantum hydrodynamics.[31]

The time-asymptotic properties of the one-dimensional discrete time quantum walk version was first derived in[15,32] and an extension of the one-dimensional model to more general graphs was made.[33] The quantum-classical transition was another subject of study of the community,[34,35] where some noise models were utilized, like the broken-link in a two-dimensional model[36] and a experimental investigation was made.[37] We recommend the following review articles in these subjects with focus on the algorithmic properties of quantum walks,[9,38,39] considering search algorithms,[40] with a brief account of the connection between the discrete and continuous time model and experimental realizations,[14] focusing on the behavior of quantum walks under decoherence[41] and a more systematic review of the field is provided in.[42]

First, in Sec. 3.1 we are going to provide a brief review of the essential concepts in quantum theory in order to one fully understand the underlying mechanisms involved in a quantum walk. Then, in Sec. 3.2 we are going to study a version of discrete-time quantum walks, the coined discrete-time quantum walk. After it we look at its time-asymptotic properties following,[15,32] deriving its long time limit probability distribution, spreading behavior and other features. We also analyze in Sec. 3.2.3 the evolution from the quantum coin perspective, finding a quantum channel for it and showing that it is not Markovian, as in comparison with the classical random walk coin evolution. Then, in Sec. 3.3 we introduce the discrete quantum walk model used in our work, the generalized elephant quantum walk.

3.1 A brief review of quantum theory

In quantum theory, the physical objects fundamental properties are given only a statistical description, as opposed to classical theory where the deterministic nature of the physical objects is the main picture. The quantum objects are described by *quantum states* that encode the probabilities of them having a given state property. Unlike in classical stochastic processes, the evolution of a closed quantum system is governed by a unitary operator – meaning that it is reversible – and the statistical nature of the quantum properties is revealed only when one takes into account measurements. In the following we are going to provide a brief description of the static and dynamical features of quantum theory, first following the vector state formalism and then the density operator formalism, important when talking about open quantum systems. Also, we introduce important concepts and quantifiers such as *entanglement* and *von Neumann entropy*. For a more complete description and deeper discussions on quantum theory we reference the reader to the well known books of M. Nielsen[43] and M. Wilde[44] that give special attention for the computational and informational aspects relevants for the following text.

3.1.1 Vector state formalism

The quantum state of a closed quantum system $|\psi\rangle$ is a vector in a complex vector space with inner product and dimension d, $\mathcal{H}_d$, the Hilbert space and whose matrix representation is set to be a column matrix in $\mathbb{M}_{d\times 1}(\mathbb{C})$. The Hilbert space is generated by a basis, i.e. $\mathcal{H}_d = \text{span}\{|s\rangle\}$, where s indexes a given basis state. In the case of a discrete system, a quantum state can be described as a linear combination or *superposition* of the basis states

$$|\psi\rangle = \sum_s \alpha_s |s\rangle \ , \tag{3.1}$$

where $\alpha_s \in \mathbb{C}$ and the statistical interpretation of quantum theory imposes that the quantum state must be a unit vector, that is $\sum_s |\alpha_s|^2 = 1$.[43] A two-level system is called a *qubit* and it can be represented as $|\psi\rangle = \alpha|\uparrow\rangle + \beta|\downarrow\rangle$, in reference to the quantum spin property, or as $|\psi\rangle = \alpha|0\rangle + \beta|1\rangle$ in the computational basis.

The inner product between two vectors in a Hilbert space $\mathcal{H}$ is set to be $(|\psi\rangle, |\phi\rangle) = \langle\psi|\phi\rangle$, where $\langle\psi|$ is the dual vector of $|\psi\rangle$ obtained through the complex conjugate operation, i.e. $\langle\psi| = (|\psi\rangle)^\dagger$. Let $|\psi\rangle = \sum_i \alpha_i |i\rangle$ and $|\phi\rangle = \sum_j \beta_j |j\rangle$, then in matrix representation their inner product would be

$$\langle\psi|\phi\rangle := \begin{pmatrix}\alpha_1^* & \alpha_2^* & \dots\end{pmatrix} \cdot \begin{pmatrix}\beta_1 \\ \beta_2 \\ \vdots\end{pmatrix} = \sum_i \alpha_i^* \beta_i \ . \tag{3.2}$$

Measurements disturbs the quantum state, breaking the quantum superposition and showing us only a result according to a given basis state. To capture the statistical nature of quantum systems, measurements are described as a collection of operators $\{M_s\}$, where s indexes the possible results with probability given by Born's rule[43]

$$\Pr(s) = \langle\psi| M_s^\dagger M_s |\psi\rangle \ , \tag{3.3}$$

where $M_s^\dagger$ and $\langle\psi|$ are the complex-conjugate transpose of M_s and $|\psi\rangle$, respectively. Given that the probabilities must sum up to one, the measurement operators must satisfy the *completeness relation*

$$\sum_s M_s^\dagger M_s = \mathbb{I} \ , \tag{3.4}$$

with $\mathbb{I}$ being the identity operator on the same space. After the measurement, the final state is given by

$$|\psi_s\rangle = \frac{M_s |\psi\rangle}{\sqrt{\langle\psi| M_s^\dagger M_s |\psi\rangle}} \ . \tag{3.5}$$

As an example of measurement operators we have the projective measurements, that is, measurement operators characterized by the properties $M_s M_{s'} = \delta_{s,s'} M_s$ and $M_s^\dagger = M_s$. For instance, in a two level system we can have the following projective measurements $M_\uparrow = |\uparrow\rangle\langle\uparrow|$, $M_\downarrow = |\downarrow\rangle\langle\downarrow|$ resulting in the state $|\uparrow\rangle$ and $|\downarrow\rangle$, respectively.

In comparison with classical stochastic processes, we see that it is not possible to know the state of a quantum system without disturbing it. This is a major factor that one must bear in mind in devising measures to characterize quantum systems and quantum evolutions, such as the previously mentioned hitting time. Another important feature that arises is the quantum interference. If a system has a state like $|\psi\rangle = \sum_s \alpha_s |s\rangle$ and we consider a set of projective measurements on the same basis, Born's rule Eq. (3.3) tells us that the probability of the property s being measured is equal to $\Pr(s) = |\alpha_s|^2$. The fact that the probabilities are given by the square norm of the state coefficients, and these coefficients are complex numbers, make it possible for interference effects to happen, something that does not appear in classical stochastic processes.

The evolution of a closed quantum system is characterized by a unitary operator U.[43] An operator is said to be unitary if it satisfies $UU^\dagger = U^\dagger U = \mathbb{I}$. In the case of discrete-time evolution, the system evolves by the simple application of the unitary operator

$$|\psi(t+1)\rangle = U |\psi(t)\rangle \ . \tag{3.6}$$

Reversibility is shown if we apply the complex-conjugate of U into the evolved system, leading to $U^\dagger |\psi(t+1)\rangle = U^\dagger U |\psi(t)\rangle = |\psi(t)\rangle$. If the system evolves continuously through

time, the equation that governs the time evolution of the quantum system is the Schrödinger equation[43]

$$i\hbar \frac{d\,|\psi(t)\rangle}{dt} = H\,|\psi(t)\rangle \ , \tag{3.7}$$

where H is the system's Hamiltonian. With $U(t, t_0)$ being the unitary operator that evolves the system from the initial time t_0 to t, i.e. $|\psi(t)\rangle = U(t, t_0)\,|\psi(t_0)\rangle$, the Hamiltonian is related to the unitary operator through, using Eq. (3.7)

$$U(t, t_0) = \exp\left\{\frac{-i}{\hbar}\int_{t_0}^{t} H(t')dt'\right\} . \tag{3.8}$$

The Hilbert space of composite quantum systems, or quantum systems with composite properties, are described by the tensor product of the respective quantum systems.[43] For example, considering n quantum systems the total Hilbert space will be given by $\mathcal{H}_T = \mathcal{H}_1 \otimes \mathcal{H}_2 \otimes \ldots \mathcal{H}_n$. Therefore, vectors on this Hilbert space can be expanded in a superposition of the tensor product of the individual Hilbert space basis states. Given that we have a composition of two qubits, for example, the quantum state would be expanded as $|\psi\rangle = \alpha\,|\uparrow,\uparrow\rangle + \beta\,|\uparrow,\downarrow\rangle + \gamma\,|\downarrow,\uparrow\rangle + \delta\,|\downarrow,\downarrow\rangle$, where $|\uparrow,\uparrow\rangle$ is the short notation for $|\uparrow\rangle \otimes |\uparrow\rangle$.

Some interesting features start to emerge when one considers compositions of quantum systems. One of them is that there are quantum states that are not separable in the tensor product of individual states. This means that the individual quantum systems cannot be characterized. When this happens we say that the quantum system is *entangled* or *non-separable* [i]. For instance we have the Bell basis state $|\uparrow,\uparrow\rangle + |\downarrow,\downarrow\rangle$, up to a normalization factor, that cannot be separable into the tensor product of two individual states. Nonetheless, a more complete description of a quantum system can be provided through the *density operator*, or *density matrix*, that carries all the information about the correlations with other systems.

3.1.2 Density matrix formalism

The density matrix of a quantum system ρ is a positive semi-definite hermitian operator with unit trace that acts on the Hilbert space of the system, i.e. $\rho = \rho^\dagger > 0$ and $\mathrm{tr}(\rho) = 1$[43] given by

$$\rho = \sum_j p_j\,|\psi_j\rangle\langle\psi_j| \ . \tag{3.9}$$

[i] A review on quantum entanglement, its applications, measures and more, is provided in the remarkable review article by Horodecki *et al.*[45]

We can think of the density matrix as representing an ensemble of quantum states $\{p_j, |\psi_j\rangle\}$, where p_j is the probability of preparing the quantum state $|\psi_j\rangle$, explaining the unit trace condition. We say that a quantum state in which $\rho = |\psi\rangle\langle\psi|$, i.e. all but one $p_j = 0$ is a *pure state*, otherwise it is in a *mixed state*.

Measurements are described in the same manner as in the vector state formalism. Here the probability of a given result m associated with a measurement operator M_m is

$$\Pr(m) = \mathrm{tr}(M_m \rho M_m^\dagger) \ , \tag{3.10}$$

with resulting state equal to

$$\rho_m = \frac{M_m \rho M_m^\dagger}{\mathrm{tr}(M_m \rho M_m^\dagger)} \ . \tag{3.11}$$

Compositions of quantum systems with the density operator formalism are made in the same way that in the quantum state formalism, i.e. through the tensor product.[43] For instance, consider a bipartite quantum system with Hilbert space $\mathcal{H} = \mathcal{H}_A \otimes \mathcal{H}_B$. If the state of system A is ρ_A and the state of system B is ρ_B, the total state is described by $\rho_A \otimes \rho_B$. Given a state of composite quantum system ρ_{AB}, the *reduced density matrix* of system A, for instance, is given by the partial trace over B's degrees of freedom $\rho_A = tr_B(\rho_{AB})$.[43] The partial trace operation takes the trace with regard to only one system basis. For example, if $\rho_{AB} = |\uparrow\rangle\langle\uparrow| \otimes (|\uparrow\rangle\langle\uparrow| + |\uparrow\rangle\langle\downarrow|) + |\downarrow\rangle\langle\downarrow| \otimes |\downarrow\rangle\langle\downarrow|$, $\rho_A = |\uparrow\rangle\langle\uparrow| (\langle\uparrow|\uparrow\rangle \langle\uparrow|\uparrow\rangle + \langle\downarrow|\uparrow\rangle \langle\uparrow|\downarrow\rangle + \langle\uparrow|\uparrow\rangle \langle\downarrow|\uparrow\rangle + \langle\downarrow|\uparrow\rangle \langle\downarrow|\downarrow\rangle) + |\downarrow\rangle\langle\downarrow| (\langle\downarrow|\downarrow\rangle^2 + \langle\uparrow|\downarrow\rangle \langle\downarrow|\uparrow\rangle) = |\uparrow\rangle\langle\uparrow| + |\downarrow\rangle\langle\downarrow|$.

With regard to the non-separability of quantum states in the density operator formalism, first we have to state an important theorem that deliver us a method of diagnose entanglement in bipartite quantum states, the *Schmidt decomposition*[43,44,46]

Theorem 3.1.1. ***Schmidt decomposition****: Let $|\psi_{AB}\rangle$ be a pure state of a bipartite system AB. There is an orthonormal set for the Hilbert space $\mathcal{H}_A$, $\{|i_A\rangle\}$, and one for $\mathcal{H}_B$, $\{|i_B\rangle\}$, such that a pure state on $\mathcal{H}_A \otimes \mathcal{H}_B$ can be expand as*

$$|\psi_{AB}\rangle = \sum_i \lambda_i |i_A\rangle \otimes |i_B\rangle \ \ , \tag{3.12}$$

where λ_i are positive real numbers called Schmidt coefficients. The number of non-zero Schmidt coefficients is called the Schmidt number.

A quantum system is a product state, i.e. separable, if and only if it has Schmidt number equal to one. To see this, let $|\alpha_A\rangle$ be a state of the quantum system A and $|\beta_B\rangle$ be a state of B. Then from Schmidt decomposition theorem 3.1.1 we know that $|\alpha_A\rangle$ and $|\beta_B\rangle$ can be expanded in the basis $\{|i_A\rangle\}, \{|i_B\rangle\}$, respectively. Therefore

$$|\psi_{AB}\rangle = |\alpha_A\rangle \otimes |\beta_B\rangle = \left(\sum_i \alpha_i |i_A\rangle\right) \otimes \left(\sum_j \beta_j |j_B\rangle\right) = \sum_{i,j} \alpha_i \beta_j |i_A, j_B\rangle \ , \tag{3.13}$$

using the Schmidt decomposition

$$|\psi_{AB}\rangle = \sum_i \lambda_i |i_A, i_B\rangle = \sum_{i,j} \alpha_i \beta_j |i_A, j_B\rangle \tag{3.14}$$

$$\leftrightarrow \alpha_i \beta_j = \lambda_i \delta_{i,j} \ . \tag{3.15}$$

The only non-trivial solution to the above equation is that we must have only one non-zero Schmidt coefficient λ_k, i.e. $\lambda_i = 0 \ \forall i \neq k$. Consequently, if a quantum system is separable then it has a Schmidt number equal to one. If the quantum system has Schmidt number equal to one, then it is separable as follows trivially from Eq. (3.1.1).

The same reasoning goes for density matrices. The quantum system AB is a product state if and only if the reduced density matrices ρ_A and ρ_B are pure states. This means that all mixed quantum states ρ are entangled with other quantum systems, with $\rho = \mathbb{I}_d/d$ being the maximally mixed state, where d is the dimension of the Hilbert space.

Another extremely important quantity in the field of quantum information, that is related to quantum entanglement and will play an important role in our results, is the *von Neumann* or *entanglement entropy*. Entropy can be regarded as a quantifier of the amount of lack-of-knowledge one has about a system's state prior to measurement. For classical systems we have the Shannon entropy associated with a given probability distribution $\{p_i, i = 1, \ldots, n\}$,[43,44,47]

$$H(p_1, \ldots, p_n) = -\sum_{i=1}^{n} p_i \log p_i \ , \tag{3.16}$$

with the logarithm taken with respect to the base two. Note that if we have a probability distribution where all but one state has probability equal to zero, that is we know with certainty what the state of the system will be, then its Shannon entropy returns the minimum value equal to zero indicating no lack-of-knowledge.

In the quantum scenario, the probability distribution is substituted by the density matrix, resulting in the von Neumann entropy[43–45]

$$S_E(\rho) = -\mathrm{tr}(\rho \log \rho) = -\sum_i \lambda_i \log \lambda_i \ , \tag{3.17}$$

where $\{\lambda_i\}$ is the set of eigenvalues of ρ. Let us now see some features of it.

Given that the density matrix is a positive semi-definite hermitian matrix with unit trace, this means that the entanglement entropy is always positive $S_E(\rho) \geq 0$. The equality

is achieved only when the state is separable, that is ρ has only one non-zero eigenvalue. The upper bound on the entanglement is determined by the dimensionality of the system and it is satisfied when the system is in the maximal mixed state, that is $\rho = \mathbb{I}_d/d$. To see this one must take into account the relative von Neumann entropy between two quantum states,[43,44,48]

$$S_E(\rho||\sigma) = \mathrm{tr}(\rho \log \rho) - \mathrm{tr}(\rho \log \sigma) \ . \tag{3.18}$$

Klein's inequality[45,49] tell us that the relative entanglement entropy is always positive. This means that, the relative entropy between ρ and a maximally entangled state $\mathbb{I}_d/d$ is $-S_E(\rho) + \log d \geq 0$, and consequently $S_E(\rho) \leq \log d$. Therefore, the entanglement entropy is a continuous function of the density matrix eigenvalues and can be used to quantify the degree of entanglement of a system.

Joining with Schmidt's decomposition theorem, another key property of the entanglement entropy arises. Let ρ_{AB} be a pure quantum state of a bipartite system AB. Then, Schmidt decomposition Eq. (3.1.1) say to us that all Schmidt coefficients of the reduced density matrices ρ_A and ρ_B are equal, i.e. $\rho_A = \sum_i \lambda_i^2 \, |i_A\rangle\langle i_A|$, $\rho_B = \sum_i \lambda_i^2 \, |i_B\rangle\langle i_B|$.[43] Therefore, as the eigenvalues of ρ_A and ρ_B are equal, $S_E(\rho_A) = S_E(\rho_B)$, that is, the entanglement entropy of the reduced systems A and B are equal if the joint state is a pure one. We highlight this property because when considering quantum systems with many degrees of freedom, one can take a bipartion of the total system where one have a simpler quantum system in one part and a more complex one in the other, then, by calculating the entanglement of the simpler one, one can access the entanglement entropy of the more complex part.

For completeness, we now introduce the dynamics of density matrices. This will be important when we look at the reduced dynamics of the coin in the coined quantum walk Sec. 3.2.3.

The evolution of density matrices introduces us to another perspective about quantum systems: as ones evolving through open dynamics.[10] While in the vector state formalism only closed unitary dynamics is defined, with density matrices one can think of the evolution of the quantum system interacting with others. In this case, the evolution does not need to be unitary. Nonetheless, some important requirements are necessary to be satisfied. Given that a quantum system has state ρ, it is related to its future state through

$$\rho(t) = \mathcal{E}(t, t_0)(\rho(t_0)) \ , \tag{3.19}$$

where $\mathcal{E}(t, t_0)$ is the *quantum operation* or *quantum map* between the states at time t_0 and

t. If the system is closed, the evolution is given accordingly with an unitary evolution[ii]

$$\rho(t) = U(t, t_0)\rho(t_0)U(t, t_0)^\dagger \ . \tag{3.20}$$

The first obvious requirement is that the quantum operation must map quantum states to quantum states, that is to preserve the hermitian positive semi-definite property and be trace-preserving (TP), $\mathrm{tr}(\rho(t)) = \mathrm{tr}(\mathcal{E}(t, t_0)(\rho(t_0))) = \mathrm{tr}(\rho(t_0))$. One can relax the trace-preserving requirement if we include in the quantum operations set quantum measurements, in which case the resulting state being

$$\rho' = \frac{\mathcal{E}(\rho)}{\mathrm{tr}(\mathcal{E}(\rho))} \ , \tag{3.21}$$

with $\mathrm{tr}(\mathcal{E}(\rho))$ being equal to the probability of the measurement represented by $\mathcal{E}$ happen. In this case the requirement is changed to $0 \leq \mathrm{tr}(\mathcal{E}(\rho)) \leq 1$.[43]

The second requirement is that the quantum map must be convex-linear, i.e. $\mathcal{E}(\sum_i p_i\rho_i) = \sum_i p_i\mathcal{E}(\rho_i)$.[43] This requirement comes from the fact that it is physically impossible to differentiate an evolution that has been carried in a quantum state ρ_i that was selected with probability p_i from one that was carried first on the ensemble of quantum states and then we looked at what quantum state has been evolved.

The last, and less obvious one, is that the quantum map must be completely positive (CP). Complete positivity means that, given a quantum system A and a quantum operation $\mathcal{E}$, if we introduce another quantum system B of any dimensionality, such that the total state is ρ_{AB}, the map $(\mathbb{I}_B \otimes \mathcal{E})(\rho_{AB})$ must be a valid map for any quantum state, i.e. map positive operators on positive operators.[43] This odd requirement arises because of another odd feature in quantum theory, quantum entanglement. When we have a quantum system that is entangled with another one, a map that is positive when taking into account only one system may cease to be when considering the joint evolution with the other quantum system. Therefore, complete positivity ensures that the quantum operation is valid even in presence of quantum correlations.

But how are quantum operations characterized? One useful representation of quantum operations that help us to answer this question is the *Kraus operator* or *operator-sum representation* of quantum maps.[51] Given that the total initial state of the quantum system is $\rho(t_0) = \rho_S \otimes |E_0\rangle\langle E_0|$, where S stands for system and E for environment, and it evolves accordingly with an unitary evolution, the quantum state of the system of interest is given by

[ii] For a connection between the quantum map formalism with the continuous-time evolution we refer the reader to the seminal paper of G. Lindblad[50] and the previously mentioned book of Breuer.[10]

$$\rho_S(t) = \mathrm{tr}_E(U(t,t_0)\rho(t_0)U(t,t_0)^\dagger) = \sum_i \langle i_E| U(t,t_0)\rho(t_0)U(t,t_0)^\dagger) |i_E\rangle =$$
$$= \sum_i E_i(t,t_0)\rho_S(t_0)E_i(t,t_0)^\dagger \ , \tag{3.22}$$

where $\{|i_E\rangle\}$ is a given environment basis and $E_i(t,t_0)$ are the Kraus operators given by

$$E_i(t,t_0) = \langle i_E| U(t,t_0) |E_0\rangle \ , \tag{3.23}$$

satisfying the operator-sum completeness condition $\sum_i E_i(t,t_0)^\dagger E_i(t,t_0) = \mathbb{I}$.

We see through Eq. (3.23) that in one hand we can devise a set of Kraus operators that represents some open system dynamics accordingly with the interaction of the system with its environment, satisfying the completeness condition, and in the other we can find them through the closed unitary dynamics of the total system.

Now that we have presented the main concepts and quantities important to understand quantum walks and its properties, we move to study the central type of quantum walk used in this work, namely coined discrete-time quantum walks.

3.2 Coined discrete-time quantum walks

A possible first idea on devising a quantum walk over a discrete lattice could be a simple quantization of the position state space, where the possible position states are transformed into position quantum states.[9] The Hilbert space of the quantum walk over a line would be $\mathcal{H} = \mathrm{span}\{|x\rangle, x \in \mathbb{Z}\}$. The translational invariant unitary operator, in analogy with the classical random walk stochastic matrix, give us the transition probabilities from one site to another

$$U|x\rangle = p|x-1\rangle + \sqrt{1-p^2}|x+1\rangle \ , \forall x \in \mathbb{Z} \ . \tag{3.24}$$

But this operator cannot be unitary for any value of p, as we can see by applying it onto an orthogonal state to $|x\rangle$ and taking the inner product

$$U|x+2\rangle = p|x+1\rangle + \sqrt{1-p^2}|x+3\rangle$$
$$\rightarrow \langle x+2| U^\dagger U |x\rangle = p\sqrt{1-p^2} = \langle x+2|x\rangle = 0 \leftrightarrow p = 0 \text{ or } p = 1 \ , \tag{3.25}$$

restricting the evolution to a trivial walk.

Coined quantum walks solve this problem by introducing another degree of freedom, the *quantum coin*, or, as sometimes it is called, *chirality*.[15,32] Its role, in analogy with the classical random walk, is to determine the position transitions, associating one state of

the coin with a movement in one direction. Let us now introduce formally the definition of a coined discrete time quantum walk.

Let $G = \{V, E\}$ be a connected d-regular graph, where $V = \{v_i, i = 1, ..., N\}$ is the set of vertices in which $\deg(v_i) = d \; \forall v_i \in V$ and E the set of edges with $|E| = Nd/2$. Let $\mathcal{H}_v = \text{span}(\{|v_i\rangle\})$ be the Hilbert space generated by the graph vertices states and $\mathcal{H}_c = \text{span}(\{|1\rangle, \ldots, |d\rangle\})$ the coin Hilbert space, generated by an auxiliary set of states called colors or coin faces, so that $\mathcal{H} = \mathcal{H}_v \otimes \mathcal{H}_c$. Each undirected edge can be thought of as bidirected edges, in this way, we associate to each outgoing edge from a given vertex a number going from 1 to d, such that it is possible to reach every vertex of the graph through a given color. The operation that updates the edge states of the walker is the quantum version of the coin toss operation, C. To update the position state of the walker we introduce the shift operator S, that acts as $S|v, c\rangle = |v \oplus c, c\rangle$, where $v \oplus c = v'$ if there is an edge c connecting v and v'. Therefore, the unitary operator $U = S(\mathbb{I}_v \otimes C)$ defines a quantum version of the Markov chain over G, the coined discrete time quantum walk.[9,52]

For instance, the total Hilbert space of a coined DTQW on a one-dimensional lattice would be $\mathcal{H} = \mathcal{H}_p \otimes \mathcal{H}_c$, where $\mathcal{H}_p$ is the Hilbert space associated with the position degree of freedom and $\mathcal{H}_c = \text{span}\{|\uparrow\rangle, |\downarrow\rangle\}$ is the coin Hilbert space. In this case, the quantum coin is a simple qubit system.

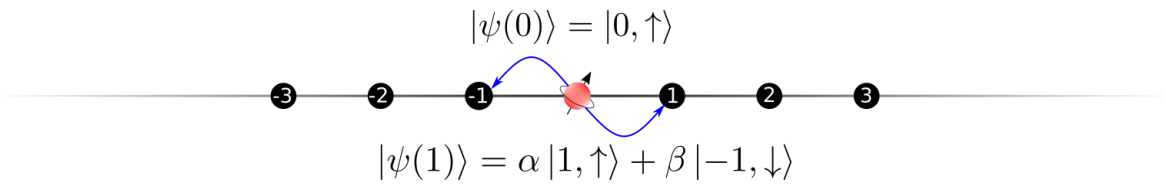

Figure 4 – Representation of one time step evolution of the coined discrete time quantum walk.

Source: By the author.

The coin-toss operators in the one-dimensional case are matrices from the unitary group of degree 2, $U(2)$.

$$C_2 = \begin{pmatrix} \cos\theta & \sin\theta e^{i\beta} \\ \sin\theta e^{i\gamma} & -\cos\theta e^{i(\gamma+\beta)} \end{pmatrix}, \tag{3.26}$$

in a general form. For example, we can use the Hadamard operator ($\theta = \pi/4, \beta = \gamma = 0$)

$$H = \frac{1}{\sqrt{2}} \begin{pmatrix} 1 & 1 \\ 1 & -1 \end{pmatrix}, \tag{3.27}$$

that characterizes a *Hadamard Walk*, or a set of non-Hermitian form of qubit unitary

operators, like the *Kempe coin* ($\beta = \gamma = \pi/2$)

$$C_k(\theta) = \begin{pmatrix} \cos\theta & i\sin\theta \\ i\sin\theta & \cos\theta \end{pmatrix}. \tag{3.28}$$

To complete the description of the unitary evolution of a one-dimensional coined discrete time quantum walk, we introduce the position *shift operator*

$$S = \sum_{x=-\infty}^{\infty} \left(|x+1\rangle\langle x| \otimes |\uparrow\rangle\langle\uparrow| + |x-1\rangle\langle x| \otimes |\downarrow\rangle\langle\downarrow| \right) , \tag{3.29}$$

and the unitary evolution operator is

$$U = S(I_p \otimes C_2). \tag{3.30}$$

From Eq. (3.29) we can clearly see that the up (down) state is associated with a shift to the right (left).

Let us compare the position probability distribution of some steps of the Hadamard Walk with the classical unbiased random walk. In Fig. 5, we have the quantum walk probability distribution at the same time step as the classical random walk distribution in Fig. 3 and consider the equal superposition state as the coin initial state. It is possible to see that the behavior of the quantum walk probability distribution is very different from the classical random walk binomial distribution. Also, we can infer that the spreading rate in the quantum walk can be greater than the classical spreading rate, as in some position interval around the origin the probability distribution is almost uniform.

Furthermore, it is important to say that these mentioned characteristics are coin initial-state dependent and coin operator dependent. This means that if we change the coin initial state, for example, we get a different probability distribution, something that does not happen in classical random walks. In the case of the Hadamard Walk, if we do not use a symmetric coin-initial state we do not get a symmetric position probability distribution, as we can see in Fig. 6.

Considering the initial state $|\psi(0)\rangle = |0,\uparrow\rangle$, the state at $t = 1$ will be

$$|\psi(1)\rangle = U\,|\psi(0)\rangle = \frac{|1,\uparrow\rangle + |-1,\downarrow\rangle}{\sqrt{2}} . \tag{3.31}$$

The probabilities of being in the ± 1 position is $1/2$ each. Applying once more the evolution operator give us

$$|\psi(2)\rangle = U\,|\psi(1)\rangle = \frac{|2,\uparrow\rangle + |0\rangle\left(|\uparrow\rangle + |\downarrow\rangle\right) - |-2,\downarrow\rangle}{2},$$

with probability of $1/4$ of being at ± 2 and $1/2$ at 0, like in the second step of the CRW.

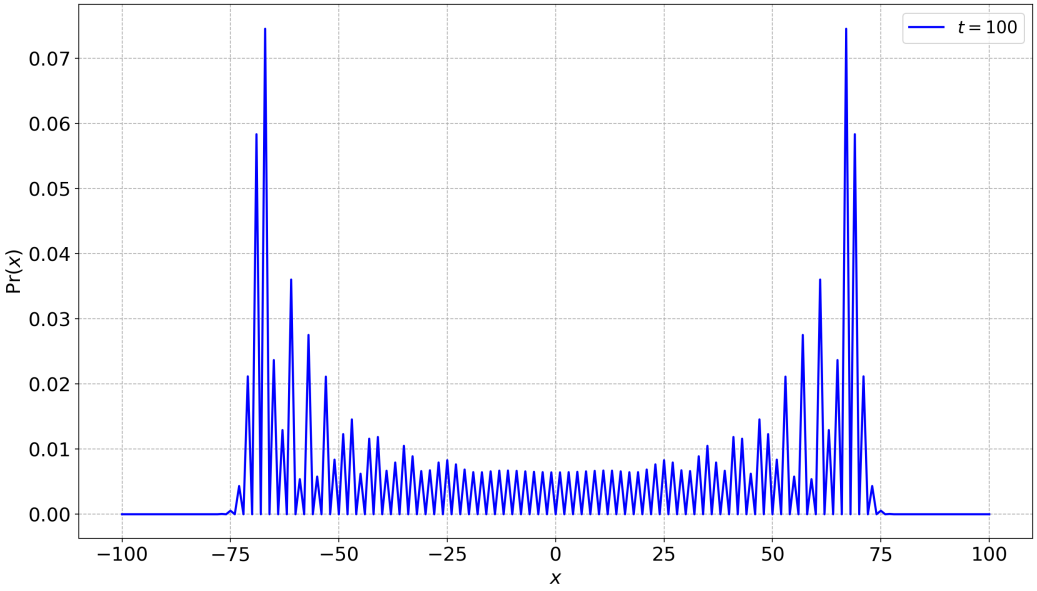

Figure 5 – Position probability distribution for the Hadamard walk. The quantum walker initial state was $|0\rangle \otimes \frac{|\uparrow\rangle+|\downarrow\rangle}{\sqrt{2}}$ and the time step plotted is $t = 100$.

Source: By the author.

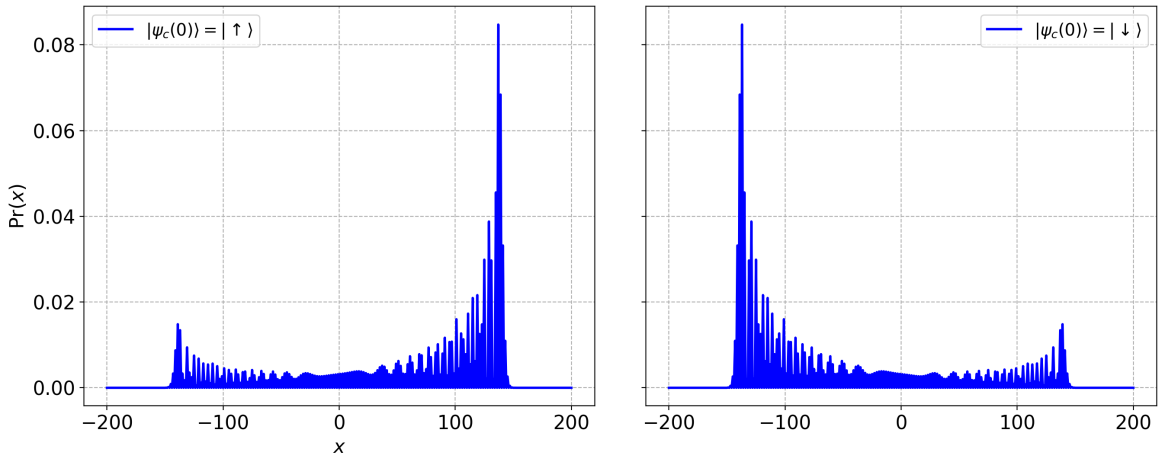

Figure 6 – Position probability distribution of the Hadamard walk with different coin initial states. The time step plotted is $t = 200$.

Source: By the author.

We can see that if we keep measuring (without reading) the position of the walker, the position probability distribution of the Hadamard Walk will become equal to the classical unbiased random walk distribution.[1,9] The previously commented properties of the quantum walks come from interference effects that does not occur on the classical random walk; by continuously measuring the position of the quantum walker, we destroy the quantum coherence and lose them.

Now we look at the evolution of the one-dimensional DTQW, deriving its long term properties and position probability distribution.

3.2.1 Time asymptotic distribution of the DTQW on a infinite line

A general walker state on the one-dimensional DTQW at the t time step can be described as

$$|\psi(t)\rangle = \sum_x \sum_{i=\uparrow,\downarrow} c_i(x,t)\,|x,i\rangle \ . \tag{3.32}$$

With $|\psi(0)\rangle$ being the walker initial state, the walker state at time t is obtained through, following Eq. (3.6)

$$|\psi(t)\rangle = U^t\,|\psi(0)\rangle\,. \tag{3.33}$$

We get the position probability distribution by considering the probability of the walker having its either coin states in a given position. Using projective measurements and Born's rule Eq. (3.3)

$$\Pr(x,t) = \sum_{i=\uparrow,\downarrow} |\,\langle x,i|\psi(t)\rangle\,|^2 = \sum_{i=\uparrow,\downarrow} |\,\langle i|\psi_c^x(t)\rangle\,|^2 = |c_\uparrow(x,t)|^2 + |c_\downarrow(x,t)|^2\ , \tag{3.34}$$

where $|\psi_c^x(t)\rangle$ is the coin state at position x.

In order to obtain an analytical expression for the position probability distribution, we are going to use the *Schrödinger approach* [iii]following.[15,32] This approach consists in analyzing the quantum state coefficients evolution in the momenta space by using a Discrete Time Fourier Transform (DTFT),[16] based on the fact that the DTQW evolution is homogeneous in time and space, making the evolution much simpler in the momenta space. From here and until the end of this section we will consider the Hadamard coin operator Eq. (3.27), i.e. the Hadamard walk. We choose to do so because all essential properties of quantum walks can be derived from such a walk,[15,32] however, a generalization of the following results can be found on.[9]

Initially, we notice that upon the action of the unitary operator Eq. (3.30) the coin states changes to

$$\begin{aligned} U\,|\psi(t)\rangle &= S\left(\sum_x \frac{(c_\uparrow(x,t)+c_\downarrow(x,t))}{\sqrt{2}}\,|x,\uparrow\rangle + \frac{(c_\uparrow(x,t)-c_\downarrow(x,t))}{\sqrt{2}}\,|x,\downarrow\rangle\right) \\ &= \sum_x \frac{(c_\uparrow(x,t)+c_\downarrow(x,t))}{\sqrt{2}}\,|x+1,\uparrow\rangle + \frac{\left(c_\uparrow(x,t)-c_\downarrow(x,t)\right)}{\sqrt{2}}\,|x-1,\downarrow\rangle \\ &= \sum_x c_\uparrow(x+1,t+1)\,|x+1,\uparrow\rangle + c_\downarrow(x-1,t+1)\,|x-1,\downarrow\rangle\ , \end{aligned} \tag{3.35}$$

[iii] A different approach can be found on the same reference articles[15,32] and in the reviews.[9,14]

Taking $x \to x-1$ for the up state coefficients and $x \to x+1$ for the down ones, we derive a recursive map for the walker state coefficients

$$c_{\uparrow}^{x}(t+1) = \frac{(c_{\downarrow}^{x-1}(t) + c_{\uparrow}^{x-1}(t))}{\sqrt{2}} \tag{3.36}$$

$$c_{\downarrow}^{x}(t+1) = \frac{(c_{\uparrow}^{x+1}(t) - c_{\downarrow}^{x+1}(t))}{\sqrt{2}} \ , \tag{3.37}$$

where $c_{\uparrow,\downarrow}^{x}(t)$ is an abbreviated form of $c_{\uparrow,\downarrow}(x,t)$. In matrix form, or simply considering the coin state at x

$$|\psi_c^x(t+1)\rangle = M_+ \left|\psi_c^{x-1}(t)\right\rangle + M_- \left|\psi_c^{x+1}(t)\right\rangle \ , \tag{3.38}$$

where

$$M_+ = \begin{pmatrix} 1/\sqrt{2} & 1/\sqrt{2} \\ 0 & 0 \end{pmatrix}; \ \ M_- = \begin{pmatrix} 0 & 0 \\ 1/\sqrt{2} & -1/\sqrt{2} \end{pmatrix} \ . \tag{3.39}$$

Definition 3.2.1. (*Discrete time Fourier transform*): The discrete time Fourier transform (DTFT) on the position state is defined as[9,14,15]

$$|k\rangle = \sum_{x=-\infty}^{\infty} e^{ikx} |x\rangle \ , \tag{3.40}$$

with $k \in [-\pi, \pi]$. The inverse transformation is given by

$$|x\rangle = \frac{1}{2\pi} \int_{-\pi}^{\pi} e^{-ikx} |k\rangle \ . \tag{3.41}$$

Describing the position ket as an inverse DTFT, the quantum walker state becomes

$$|\psi(t)\rangle = \sum_x \frac{1}{2\pi} \int_{-\pi}^{\pi} dk \ e^{-ikx} |k, \psi_c^x(t)\rangle \ . \tag{3.42}$$

Using Eq. (3.38) in the above equation, we get

$$\begin{aligned} |\psi(t)\rangle &= \sum_x \frac{1}{2\pi} \int_{-\pi}^{\pi} dk \ e^{-ikx} |k\rangle \left(M_+ \left|\psi_c^{x-1}(t-1)\right\rangle + M_- \left|\psi_c^{x+1}(t-1)\right\rangle\right) \\ &= \sum_x \frac{1}{2\pi} \int_{-\pi}^{\pi} dk \ \ |k\rangle \left(e^{-ik} M_+ e^{-ik(x-1)} \left|\psi_c^{x-1}(t-1)\right\rangle + e^{ik} M_- e^{-ik(x+1)} \left|\psi_c^{x+1}(t-1)\right\rangle\right) . \end{aligned}$$

Defining the coin state with momentum k as

$$\left|\psi_c^k(t)\right\rangle = \sum_{x=-\infty}^{\infty} e^{-ikx} |\psi_c^x(t)\rangle \ , \tag{3.43}$$

we obtain

$$|\psi(t)\rangle = \frac{1}{2\pi}\int_{-\pi}^{\pi} dk\ |k\rangle \otimes M_k \left|\psi_c^k(t-1)\right\rangle, \tag{3.44}$$

or in terms of the initial coin state

$$|\psi(t)\rangle = \frac{1}{2\pi}\int_{-\pi}^{\pi} dk\ |k\rangle \otimes M_k^t \left|\psi_c^k(0)\right\rangle, \tag{3.45}$$

with

$$M_k = \frac{1}{\sqrt{2}}\begin{pmatrix} e^{-ik} & e^{-ik} \\ e^{ik} & -e^{ik} \end{pmatrix}. \tag{3.46}$$

The usefulness of this representation resides in the fact that the evolution of the walker state is now governed by only one matrix. Therefore, we only need to diagonalize M_k to find the walker state in some time step.

The eigenvectors of M_k are

$$|\lambda_\pm\rangle = \frac{1}{\sqrt{2(1+\cos^2 k \mp \cos k\sqrt{1+\cos^2 k})}}\begin{pmatrix} 1 \\ \pm\sqrt{2}e^{ik\mp\omega_k} - 1 \end{pmatrix} \tag{3.47}$$

with eigenvalues

$$\lambda_\pm = \pm e^{\mp i\omega_k}, \text{ where } \sin\omega_k = \frac{\sin k}{\sqrt{2}} \tag{3.48}$$

Applying the t-th power of M_k on the initial coin state in momenta space results in

$$M_k^t \left|\psi_c^k(0)\right\rangle = e^{i\omega_k t}\left\langle\lambda_+\middle|\psi_c^k(0)\right\rangle|\lambda_+\rangle + e^{-i\omega_k t}\left\langle\lambda_-\middle|\psi_c^k(0)\right\rangle|\lambda_-\rangle \tag{3.49}$$

Taking an initially localized walker with up chirality, i.e. $|\psi(0)\rangle = |0\rangle|\uparrow\rangle$, the coin state in momenta space becomes

$$\begin{aligned}\left|\psi_c^k(t)\right\rangle = &\frac{1}{2}\left[\frac{e^{-i\omega_k t}}{1+\cos^2 k - \cos k\sqrt{1+\cos^2 k}} + \frac{(-1)^t e^{i\omega_k t}}{1+\cos^2 k + \cos k\sqrt{1+\cos^2 k}}\right]|\uparrow\rangle \\ &+ \frac{1}{2}\left[\frac{e^{-i\omega_k t}(\sqrt{2}e^{i(k-\omega_k)} - 1)}{1+\cos^2 k - \cos k\sqrt{1+\cos^2 k}} + \frac{(-1)^{t+1} e^{i\omega_k t}(\sqrt{2}e^{i(k+\omega_k)} + 1)}{1+\cos^2 k + \cos k\sqrt{1+\cos^2 k}}\right]|\downarrow\rangle.\end{aligned} \tag{3.50}$$

Now we have to find the coin state in the position basis in order to get the probabilities. Taking the inner product of Eq. (3.45) with $|x\rangle$ in the momentum basis, we find that

$$\langle x|\psi(t)\rangle = \frac{1}{(2\pi)^2}\int_{-\pi}^{\pi}\int_{-\pi}^{\pi} dk\, dk'\, \langle k'|k\rangle \otimes e^{ik'x}\left|\psi_c^k(t)\right\rangle$$
$$\leftrightarrow |\psi_c^x(t)\rangle = \frac{1}{2\pi}\int_{-\pi}^{\pi} dk\, e^{ikx}\left|\psi_c^k(t)\right\rangle \ . \tag{3.51}$$

The coefficients of the coin state at position x at time t are given by the following integrals

$$c_\uparrow^x(t) = \frac{1}{2\pi}\int_{-\pi}^{\pi} dk \left(\frac{1}{2} + \frac{\cos k}{2\sqrt{1+\cos^2 k}}\right) e^{i(kx-\omega_k t)} + \\ + \frac{1}{2\pi}\int_{-\pi}^{\pi} dk \left(\frac{1}{2} - \frac{\cos k}{2\sqrt{1+\cos^2 k}}\right)(-1)^t e^{i(kx+\omega_k t)} \tag{3.52}$$

$$c_\downarrow^x(t) = \frac{1}{2\pi}\int_{-\pi}^{\pi} dk(\sqrt{2}e^{i(k-\omega_k)} - 1)\left(\frac{1}{2} + \frac{\cos k}{2\sqrt{1+\cos^2 k}}\right) e^{i(kx-\omega_k t)} + \\ - \frac{1}{2\pi}\int_{-\pi}^{\pi} dk(\sqrt{2}e^{i(k+\omega_k)} + 1)\left(\frac{1}{2} - \frac{\cos k}{2\sqrt{1+\cos^2 k}}\right)(-1)^t e^{i(kx+\omega_k t)} \tag{3.53}$$

To solve these integrals we are going to use the *stationary phase method* (see Appendix A.1), that will give us the time-asymptotic regime of the probability distribution. First, we note that the integrals that have the $(-1)^t$ factor are the ones that accounts for the modularity property of the probability distribution,[9,15] therefore we can only calculate the first integrals and after it add the following factor

$$\frac{1+(-1)^{t-x}}{2}. \tag{3.54}$$

Following the stationary phase method, with $\alpha = x/t$ we have to consider three cases, where $\alpha = \pm 1/\sqrt{2}$, $-1\sqrt{2} < \alpha < 1/\sqrt{2}$ and $-1 < \alpha < -1/\sqrt{2} \cup 1/\sqrt{2} < \alpha < 1$. [iv].

- $\alpha = \pm 1/\sqrt{2}$

  With $\alpha = \pm 1/\sqrt{2}$ the integrals in Eqs. (3.52) and (3.53) take the form

  $$I(\alpha) \approx \left(\frac{f(0)e^{it\phi_\alpha(0)}}{|\phi_\alpha^{(3)}(0)|^{1/3}} + \frac{f(\pi)e^{it\phi_\alpha(\pi)}}{|\phi_\alpha^{(3)}(\pi)|^{1/3}}\right) e^{-i\pi/6}\frac{\Gamma(1/3)}{3}\left(\frac{6}{t}\right)^{1/3} . \tag{3.55}$$

  This means that for the points where $x = \pm t/\sqrt{2}$, the probability distribution decays with $t^{-2/3}$.

- $1/\sqrt{2} < \alpha < 1 \cup -1 < \alpha < -1/\sqrt{2}$

  In this two intervals we do not have any stationary points, therefore, the stationary method tell us that the probability distribution decays faster than any power of t, with $I(\alpha) \in O(1/t)$ and $\Pr(\alpha, t) \in O(1/t^2)$.

[iv] For more details of the calculation see Appendix A.2

- $-1\sqrt{2} < \alpha < 1/\sqrt{2}$

$$c^x_{\uparrow}(t) \approx \frac{1}{\sqrt{2\pi}} \frac{(1+\alpha)}{\sqrt{t(1-\alpha^2)\sqrt{1-2\alpha^2}}} \cos(\phi_\alpha t + \pi/4) \tag{3.56}$$

$$c^x_{\downarrow}(t) \approx \frac{1}{\sqrt{2\pi}} \left(\cos(\phi_\alpha t + \pi/4)\alpha - \sqrt{1-2\alpha^2}\sin(\phi_\alpha t + \pi/4)\right) \frac{1}{\sqrt{t(1-\alpha^2)\sqrt{1-2\alpha^2}}}, \tag{3.57}$$

where $\phi_\alpha = \phi(k_\alpha, \alpha) = k_\alpha \alpha - \omega_{k_\alpha}$ with k_α being the stationary points of ϕ considering the interval for α.

Finally, the time-asymptotic probability distribution is obtained through the coin states coefficients using Eq.(3.34)

$$\begin{aligned} \Pr(\alpha, t) \approx \frac{1}{2\pi}\Big[&(1-\alpha^2)\cos^2(\phi_\alpha t + \pi/4 + k_\alpha) + \\ &+ (1+\alpha)^2 \cos^2(\phi_\alpha + \pi/4)\Big] \frac{1}{t(1-\alpha^2)\sqrt{1-2\alpha^2}}, \end{aligned} \tag{3.58}$$

or in terms of the position

$$\begin{aligned} \Pr(x, t) \approx \frac{1}{2\pi}\Big[&(t^2-x^2)\cos^2(\phi_{x,t} t + \pi/4 + k_{x,t}) + \\ &+ (t+x)^2 \cos^2(\phi_{x,t} + \pi/4)\Big] \frac{1}{(t^2-x^2)\sqrt{t^2-2x^2}} \ . \end{aligned} \tag{3.59}$$

3.2.2 Properties of the Hadamard Walk

In calculating the moments of the asymptotic distribution of the Hadamard walk we can make further approximations. The first one tell us that we only have to consider the points where $-1/\sqrt{2} + e < \alpha < 1/\sqrt{2} - e$, with e being an arbitrary small positive constant, as the net probability in this interval is $1 - 2e/\pi + O(1)/t$.[32] This means that the contribution of points off this interval decreases with $1/t$. The second approximation is made by separating Eq.(3.59) in to two parts

$$\Pr(x, t) \approx \Pr_{fast}(x, t) + \Pr_{slow}(x, t) \ , \tag{3.60}$$

with

$$\Pr_{slow}(x, t) = \frac{t}{\pi(t-x)\sqrt{t^2-2x^2}} \ , \tag{3.61}$$

and taking only the slow varying function. This approximation is justified when we look at the error introduced when we take only the slow part, that also decays with $1/t$.[15,32]

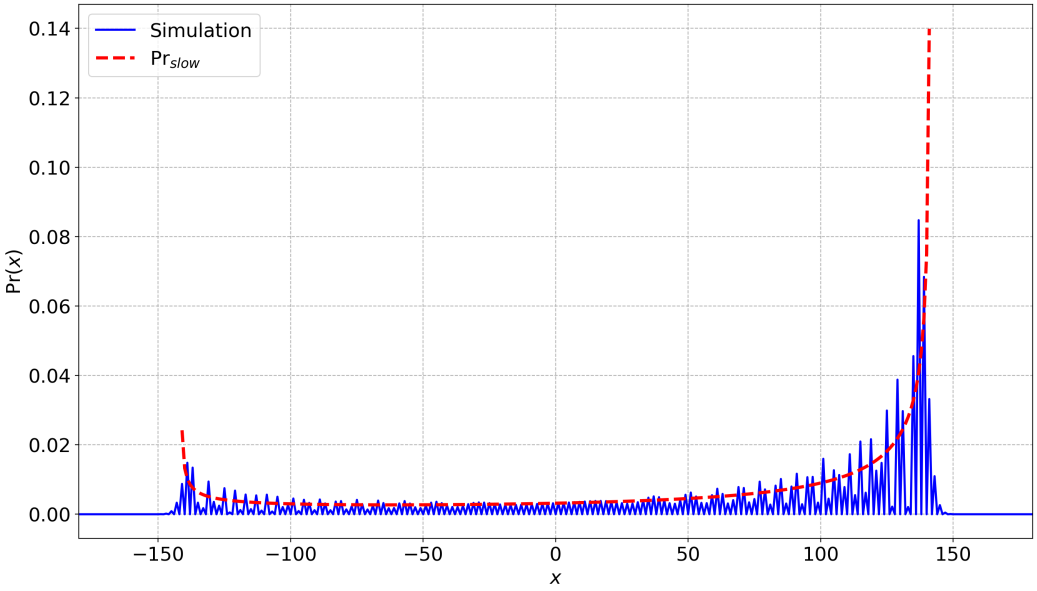

Figure 7 – Comparison between the Hadamard walk with initial state $|0,\uparrow\rangle$ position probability distribution, obtained through a simulation, and the $\Pr_{slow}$ function Eq.(3.61) at time step $t = 200$. The $\Pr_{slow}$ function was multiplied by two because it has support on odd values too.

Source: By the author.

Looking at Fig. 7 wee see that Eq. (3.61) approximates very nicely the total distribution in the corresponding interval.

We can check that these approximations are consistent by looking at the normalization condition

$$\int_{-t/\sqrt{2}}^{t/\sqrt{2}} \frac{t}{\pi(t-x)\sqrt{t^2-2x^2}} = 1 \ , \tag{3.62}$$

that we see that is satisfied. The mean position and squared position give us

$$\langle x \rangle \approx \frac{\sqrt{2}-1}{\sqrt{2}} t \tag{3.63}$$

$$\langle x^2 \rangle \approx t^2 \frac{\sqrt{2}-1}{\sqrt{2}} \ , \tag{3.64}$$

so that the Hadamard walk asymptotic variance goes with

$$\mathrm{Var}(t) \approx t^2 \left(\frac{4\sqrt{2}-5}{2\sqrt{2}} \right) \ . \tag{3.65}$$

This result tells us that the Hadamard walk dispersion rate has a quadratic gain over the classical random walk (Eq. (2.45)), that goes with $\sqrt{t}$.

Now that we have the time-asymptotic probability distribution of the Hadamard walk, we can ask what is the average time that the quantum walker needs to go from one position to another and, if it exists, the minimum time required for the probability to get closer to the stationary distribution. One might just use the earlier definitions of hitting time and mixing time Eqs. (2.53) and (2.54), yet a careful consideration must be taken as we are now dealing with a quantum evolution.

The first remark that we make is about the stationary distribution, closely related with the mixing time. A stationary distribution cannot be defined, in general, for unitary quantum evolutions. The reason behind this comes from the property of unitary matrices of preserving the inner-product between any two states. Given that the initial state is $|\psi(0)\rangle$, and we supposedly have a stationary state $|\pi\rangle$, then $\lim_{t\to\infty} \langle\pi| U^t |\psi(0)\rangle = \langle\pi|\psi(0)\rangle \neq 1$. As the probability distribution is determined through the state $|\psi(t)\rangle$, we do not have a stationary distribution either.

One way to circumvent this problem is by defining an average probability distribution

$$\bar{\Pr}(x,T) = \frac{1}{T}\sum_{t=0}^{T-1} \Pr(x,t) \ , \tag{3.66}$$

in which the following limit always exists

$$\lim_{T\to\infty} \bar{\Pr}(x,T) = \pi(x|\psi(0)) = \sum_{i,j,k} = \alpha_i \alpha_j^* \langle x,k|\phi_i\rangle \langle\phi_j|x,k\rangle \ , \tag{3.67}$$

where $|\psi(0)\rangle = \sum_{i,k} \alpha_i |x,k\rangle$, with $k = \{\uparrow,\downarrow\}$ and $|\phi_j\rangle$ are the eigenvectors of U. The notation $\pi(x|\psi(0))$ is introduced with the intention to reiterate that the stationary distribution is, in general, initial state dependent. [v] We can understand the average probability distribution Eq. (3.66) as the distribution one obtains when considering an evolution in which the quantum walker is led to evolve until a time step T randomly picked from an uniform distribution.

With the definition of the stationary distribution is possible to define a suitable mixing time for a quantum evolution[33]

Definition 3.2.2. (***Quantum mixing time***): The mixing time of a quantum markov chain is defined as the minimum time in which the average probability distribution is e-close to the stationary distribution

$$\mathcal{M}_e^q = \min\{T \mid \forall t \geq T : |\pi(.|\psi(0)) - \bar{\Pr}(x,t)|_{tvd} \leq e\} \ , \tag{3.68}$$

[v] The proof of the above statement, and above definitions in a more general context, is provided in the work on quantum walks on general graphs from Aharonov *et al.*[33]

where $\pi(.|\psi(0))$ is the stationary distribution of the process conditioned on the initial state $|\psi(0)\rangle$.

Another one, less restrictive than the above and used in,[15] is the instantaneous mixing time

Definition 3.2.3. (*Instantaneous mixing time*): Given that the initial state of a quantum markov chain is $|u\rangle$, then the instantaneous mixing time is defined as

$$\mathcal{M}_e^i = \max_u \min_t \{t \mid |\pi(.|u) - \Pr(.|u)|_{tvd} \leq e\} \ . \tag{3.69}$$

One can determine the Hadamard walk's mixing time by remembering that in the interval $[-t/\sqrt{2}, t/\sqrt{2}]$ Eq. (3.61) is a very good approximation and that it is almost equal to the uniform distribution. Therefore, the Hadamard walk, taking the asymptotic limit $\Pr_{slow}$ with stationary distribution, in the corresponding interval where it is valid, being equal to the uniform distribution, mixes linear in time, i.e. $\mathcal{M}_e^i \in O(t)$, in contrast to classical random walks where the mixing time is $O(t^2)$.[15]

If we want to devise a similar measure to the hitting time we have to take into account the fact that measurements destroy the superposition, altering the evolution of the quantum state. In this way, the earlier definition would not be appropriate. In place, we can construct an evolution in which we query if the walker is in the desired position at every time step, and if we find so then we stop the evolution. Let $\Pi_j = |j\rangle\langle j| \otimes \mathbb{I}_c$ be the projector on the position basis state on $|j\rangle$, independent of the coin state, and $\Pi_j^\perp = \mathbb{I} - \Pi_j$ the complementary projector. Then, by evolution of the walker density matrix following Eq. (3.20) and the probability of measuring the walker in the position j is given by

$$\Pr^t(j) = \mathrm{tr}(\mathcal{E}_1 \mathcal{E}_0^{t-1}(\rho(0))) \ , \tag{3.70}$$

where $\mathcal{E}_1 = \Pi_j(.)\Pi_j^\dagger$ and $\mathcal{E}_0 = \Pi_j^\perp U(.)U^\dagger(\Pi_j^\perp)^\dagger$. With this probability we define the notion of *concurrent hitting time*[52]

Definition 3.2.4. (*Concurrent hitting time*): A quantum walk has concurrent hitting time (T, p) between two vertices i, the starting position, and j if the process of obtaining $\Pr^t(j)$ stops at time $t \leq T$ when the total probability is equal or greater than p

$$h_c^q(i,j) = \left\{(T,p) : \Pr^{t \leq T}(j) \geq p\right\} \ . \tag{3.71}$$

This definition of hitting time for quantum walks is suitable when we do not have information on the structure of the underlying graph, so that we do not know when we have to measure if the walker is in the desired position. If we know the structure of the graph maybe the *one-shot hitting time*[52] is more appropriate

Definition 3.2.5. (***One-shot hitting time***): The one-shot hitting time between two vertices is defined as the time step T and probability p in which the quantum walk with initial state $|i\rangle$ and unitary evolution operator U has probability greater than p after T time steps

$$h_o^q(i,j) = \left\{ (T,p) \ : \ |\langle j| U^T |i\rangle|^2 \geq p \right\} . \tag{3.72}$$

Computational problems in which the hitting time is an essential quantity are the ones related to finding a given vertex in a graph structure. For instance, we have the problem of traversing a n-dimensional hypercube, where the classical random walk takes an exponential on n number of time steps to hit the opposite vertex of the hypercube, whereas by using quantum the algorithm can be exponentially faster.[52] In the case of the binary glued tree, where one desires to reach the root of one tree from the other, quantum walks has showed to prevail over its classical counterpart when one introduce random cycles in the graph, giving also an exponential gain.[53–55] Considering the quantum walk on a line, in[54] is also shown that the hitting time of the quantum walk is linear in time.

Another striking feature of quantum walks that appears only on the quantum realm is the emergence of entanglement between the coin and the position of the walker. In Sec. 3.1 we have shown that when considering composite quantum systems it is possible that the subsystems become entangled, meaning that it is not possible to describe the subsystems individually. For quantum walks, this means that the coin becomes correlated with the position state of the walker, something that does not occur in the classical case. Let us see this in more detail.

The quantum walker density matrix is given by, usign Eq. (3.32)

$$\rho(t) = \sum_{x,x'} |x\rangle\langle x'| \otimes \begin{pmatrix} c_\uparrow(x,t)c_\uparrow^*(x',t) & c_\uparrow(x,t)c_\downarrow^*(x',t) \\ \\ c_\downarrow(x,t)c_\uparrow^*(x',t) & c_\downarrow(x,t)c_\downarrow^*(x',t) \end{pmatrix} , \tag{3.73}$$

where $c_{\uparrow,\downarrow}^*$ denotes the complex conjugate of $c_{\uparrow,\downarrow}$. Taking the partial trace over the position degree of freedom we get the coin density matrix

$$\rho_c(t) = \begin{pmatrix} A(t) & B(t) \\ B^*(t) & C(t) \end{pmatrix} \tag{3.74}$$

with $A(t) = \sum_x |c_\uparrow^x(t)|^2$, $B(t) = \sum_x c_\uparrow^x(t)c_\downarrow^x(t)^*$, $C(t) = \sum_x |c_\downarrow^x(t)|^2$ and $c_{\uparrow,\downarrow}^x(t)$ as an abbreviation of $c_{\uparrow,\downarrow}(x,t)$.

Accordingly, the von Neumann entropy Eq. (3.17) of the coin state will be

$$S_E = -\lambda_+ \log \lambda_+ - \lambda_- \log \lambda_- \ , \text{with} \tag{3.75}$$

$$\lambda_\pm = \frac{1}{2}\left(1 \pm \sqrt{(1 - 4(AC - |B|^2)}\right) \ , \tag{3.76}$$

where we utilized the fact that $\mathrm{tr}(\rho_c(t)) = 1 \leftrightarrow A + C = 1 \ \forall \ t$.

To find the entanglement entropy of the coin, we are going to use the time asymptotic limit walker state coefficients equations Eqs. (3.52) and (3.53) of the Hadamard walk with initial state $|0, \uparrow\rangle$, numerically determined by,[56] following.[57] $A(t)$ and $B(t)$ are given by, after some algebra

$$A(t) = \int_{-\pi}^{\pi} \frac{dk}{4\pi}\left[\left(1 + \frac{\cos^2 k}{1 + \cos^2 k}\right) + (-1)^t \left(1 - \frac{\cos^2 k}{1 + cos^2 k}\right)\cos(2\omega_k t)\right] \tag{3.77}$$

$$\begin{aligned} B(t) = \int_{-\pi}^{\pi} \frac{dk}{4\pi}\Bigg[&\left(1 + \frac{\cos^2 k}{1 + \cos^2 k}\right)\sqrt{2}e^{-ik}\sqrt{1 - \frac{\sin^2 k}{2}} + \frac{\cos k}{\sqrt{1 + \cos^2 k}}(2e^{-ik} i \sin k - 1) \\ &+ \left(1 - \frac{\cos^2 k}{1 + \cos^2 k}\right)(-1)^t \left(\sqrt{2}e^{-ik}\cos((2t+1)\omega_k) - \cos(2\omega_k t)\right)\Bigg] \ . \end{aligned} \tag{3.78}$$

In $A(t)$ integrals we can ignore the ones with the time-dependent term. In the case of $B(t)$'s integral, the first and second term are zero, therefore we have to take into account the time dependent factors. To do so, we use the stationary phase method (Appendix A.1) again, taking only the zero-order of the phase expansion, that is, setting the integral equal to the integrands at the stationary points of the phase functions. By doing that, we find

$$\lim_{t\to\infty} A(t) = \bar{A} \approx 0.64645 \tag{3.79}$$

$$\lim_{t\to\infty} B(t) = \bar{B} \approx -0.15915 \ . \tag{3.80}$$

Using these two results in the equation for the eigenvalues Eq. (3.76) we encounter the approximate entanglement entropy of the coin Eq. (3.75) in the Hadamard walk with the initial state $|0, \uparrow\rangle$, $\bar{S}_E \approx 0.8604$. This value tells us that the quantum coin is in a highly entangled state, having correlations with the position of the walker that does not exist in the classical domain.

3.2.3 Reduced dynamics of the coin in the discrete time quantum walk

As we saw in Sec. 2.3, we can think of the classical random walk position random variable as a sum of modified Bernoulli random variables. These random variables are like the result of a coin toss, where they do not depend on its previous values. Looking at the reduced evolution for the quantum coin it is possible to see that this does not

happen in the discrete-time quantum walk.[vi] The non-Markovian behavior of the coin dynamics in quantum walks was studied by M. Hinarejos *et al.*[58] and more deeply by N. Kumar,[59] where they distinguished the different sources of noise in the quantum walk evolution considering other non-Markovian sources of noise like the random telegraph and the Ornstein-Uhlenbeck noises. Here we will follow the article of J. Naikoo et. al[60] to derive a quantum channel in the form of Kraus operators for the reduced dynamics of the quantum coin and show that the reduced evolution of the quantum coin is non-Markovian.

First we want to derive an equation for the Kraus operators of the quantum coin evolution. The coin density matrix at time step t is given by, using Eq. (3.19) and the partial trace operation over the position degree of freedom

$$\rho_c(t) = \mathrm{tr}_x(U^t\rho(0)(U^\dagger)^t) = \sum_x \langle x|\,(U^t\rho(0)(U^\dagger)^t\,|x\rangle \ , \tag{3.81}$$

with U being the unitary evolution operator given by Eq. (3.30). Following with the calculations, we suppose that the quantum walker initial density matrix is a separable one, i.e. $\rho(0) = \rho_p \otimes \rho_c$, with the position density matrix being equal to $|\psi_p\rangle\langle\psi_p|$. In this way we can find an equation for the Kraus operators Eq. (3.22)

$$\rho_c(t) = \mathcal{E}_t(\rho_c(0)) = \sum_x E_x^t \rho_c(0) E_x^{t^\dagger} \ , \tag{3.82}$$

where

$$E_x^t = \langle x|\,U^t\,|\psi_p\rangle \ . \tag{3.83}$$

Now that we have a formula for the Kraus operators, it is useful to take a closer look in U^t and simplify it. We can rewrite the evolution operator as

$$\begin{aligned} U = S \otimes (I_p \otimes C) &= \left(\sum_x \sum_\sigma |x+\sigma\rangle\langle x| \otimes |\sigma\rangle\langle\sigma|\right)\left(\sum_{\sigma',\sigma''} C_{\sigma'}^{\sigma''}\,|\sigma'\rangle\langle\sigma''|\right) \\ &= \sum_x \sum_{\sigma,\sigma''} C_\sigma^{\sigma''}\,|x+\sigma\rangle\langle x| \otimes |\sigma\rangle\langle\sigma''| \ , \end{aligned}$$

where $\sigma = \pm 1$ and the coin basis states were relabeled as $|+1\rangle$ and $|-1\rangle$ for ease of notation. Defining

[vi] One must bear in mind that the comparison between classical Markovian and quantum Markovian processes is subtle and in general the various definitions in the quantum domain do not coincide with the classical one.

$$C_{+1} = \sum_{\sigma''} C_{+1}^{\sigma''} |+1\rangle\langle\sigma''| \,, \; C_{-1} = \sum_{\sigma''} C_{-1}^{\sigma''} |-1\rangle\langle\sigma''| \tag{3.84}$$

$$S_{+1} = \sum_{x} |x+1\rangle\langle x| \,, \; S_{-1} = \sum_{x} |x-1\rangle\langle x| \;\; , \tag{3.85}$$

the one-step unitary operator can be rewritten as

$$U = S_{+1} \otimes C_{+1} + S_{-1} \otimes C_{-1} = P + Q \;\; , \tag{3.86}$$

where $P = S_{+1} \otimes C_{+1}$ and $Q = S_{-1} \otimes C_{-1}$. In this form, U^t can be written as a binomial expansion of $(P+Q)^t$ by using a relation related to the commutator of P and Q

$$(P+Q)^t = \sum_{k=0}^{t} \binom{t}{k} P^k Q^{t-k} + \sum_{k=0}^{t} \binom{t}{k} \hat{D}_k(Q,P) Q^{t-k} \;\; , \tag{3.87}$$

with

$$\hat{D}_k(Q,P) = [Q, P^k] + P\hat{D}_{k-1}(Q,P) + [Q, \hat{D}_{k-1}(Q,P)] \;\; . \tag{3.88}$$

The term associated with $\hat{D}_k(Q,P)$ comes from the fact that P and Q do not commute. [vii] Consequently, the Kraus operators are given by the following final formula

$$E_x^t = \sum_{k=0}^{t} \binom{t}{k} \langle x| \, (P^k + \hat{D}_k(Q,P)) Q^{t-k} \, |\psi_p\rangle \;\; . \tag{3.89}$$

To check if the reduced coin evolution is Markovian we are going to use the Breuer-Laine-Piilo (BLP) definition[61,62] of Markovian process[viii], that states, essentially, that a Markovian process is one in which the degree of distinctness between any two states does not increase, indicating that we do not have an information backflow.

Let us calculate the one-step Kraus operators, i.e. with $t = 1$. Taking the walker initial position state as the origin and considering the Kempe coin Eq. (3.28) we find that

$$E_{-1}^1 = \begin{pmatrix} 0 & 0 \\ i\sin\theta & \cos\theta \end{pmatrix} \,, \; E_1^1 = \begin{pmatrix} \cos\theta & i\sin\theta \\ 0 & 0 \end{pmatrix} \;\; . \tag{3.90}$$

Fixing the coin initial state to $|\psi_c(0)\rangle = (1/\sqrt{2})(|\uparrow\rangle + |\downarrow\rangle)$, the application of the one-step quantum channel to the coin initial density matrix leads us to

[vii] For a proof of Eq. (3.87) check Appendix B.

[viii] For more details on the BLP definition of non-Markovian processes check Appendix C

$$\mathcal{E}_1(\rho_c(0)) = E_{-1}\rho_c E_{-1}^\dagger + E_1\rho_c E_1^\dagger$$
$$= \frac{1}{2}\begin{pmatrix} 0 & 0 \\ 0 & 1 \end{pmatrix} + \frac{1}{2}\begin{pmatrix} 1 & 0 \\ 0 & 0 \end{pmatrix} = \frac{\mathbb{I}}{2} \, .$$

Calculating for the orthogonal state to ρ_c, $\rho_c^\perp$, give us the same result, i.e. $\mathcal{E}_1(\rho_c^\perp) = \mathbb{I}/2$. By applying the same one-step quantum channel n times we will get the same result, as the channel is unital

$$\mathcal{E}_1\left(\frac{I}{2}\right) = \frac{E_1 E_1^\dagger}{2} + \frac{E_{-1}E_{-1}^\dagger}{2} = \frac{\mathbb{I}}{2} \, . \tag{3.91}$$

The consequence of this result is that the trace-distance

$$D(\rho, \sigma) = \frac{1}{2}\|\rho - \sigma\|_1 \, , \tag{3.92}$$

where $\|A\|_1 = \mathrm{tr}(\sqrt{AA^\dagger})$, between ρ_c and $\rho_c^\perp$ - that is a measure of the similarity between two quantum states (Appendix C) – when both are subjected to the same quantum channel $(\mathcal{E}_1)^n$ will be given by

$$D((\mathcal{E}_1)^n(\rho_c), (\mathcal{E}_1)^n(\rho_c^\perp)) = \begin{cases} 1, \text{ if } n = 0 \\ 0, \text{ if } n \neq 0 \end{cases} \, , \tag{3.93}$$

therefore the process would be Markovian as the trace-distance derivative, that is the degree of distinctness between the states, does not increases in the whole evolution, indicating that we do not have an information backflow. But numerically we can see that this does not happen, as we note in Fig. 8. This proves that the reduced coin dynamics is not Markovian for all coin operators, according to the BLP definition, and therefore the process is not divisible $\mathcal{E}_n \neq (\mathcal{E}_1)^n$.

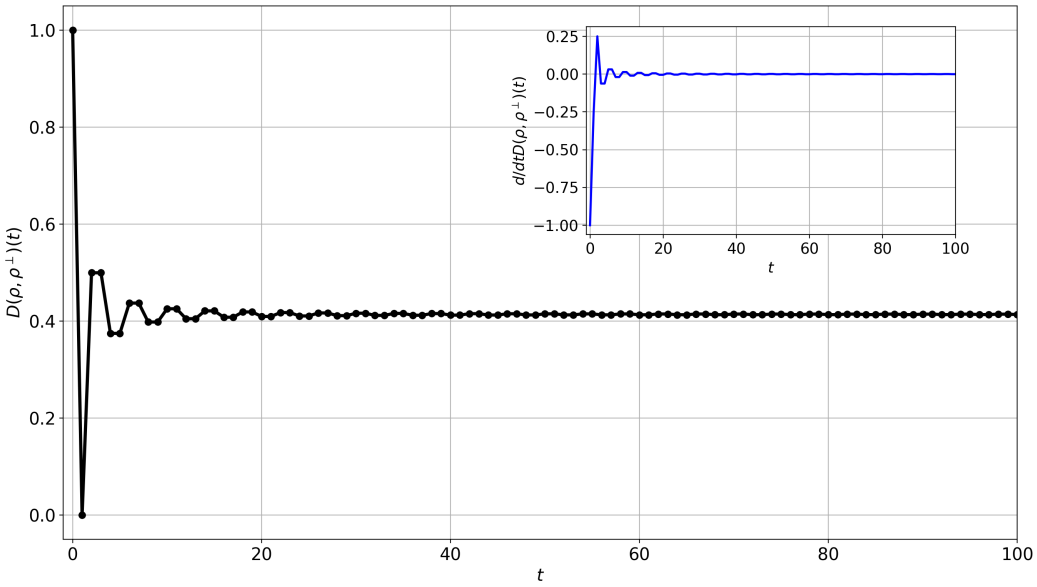

Figure 8 – Trace distance between two orthogonal coin states as a function of time. The quantum walker initial state is $|\psi(0)\rangle = |0\rangle \otimes |\psi_c(0)\rangle = |0\rangle \otimes \frac{|\uparrow\rangle+|\downarrow\rangle}{\sqrt{2}}$ such that $\rho_c(0) = |\psi_c(0)\rangle\langle\psi_c(0)|$ and $\rho_c^{\perp}(0) = \left|\psi_c^{\perp}(0)\right\rangle\left\langle\psi_c^{\perp}(0)\right|$. In the inset we have the time evolution of the first time derivative of the trace distance for the same initial states.

Source: By the author.

3.3 The generalized Elephant Quantum Walk

The quantum walk model that we considered in this work is dubbed the generalized Elephant Quantum Walk (gEQW). It consists in a discrete time quantum walk on a lattice where the steps sizes are chosen randomly accordingly with a probability distribution, a model devised by G. D. Molfetta *et al.*[2,3] The name *elephant quantum walk* was chosen in reference to the classical elephant random walk,[11] a non-Markovian random walk where the probability of the walker moving in a given direction depends on its previous steps. In a given setting of the memory of the elephant walk, the walker have greater probability of moving to the edges of the graph. In the quantum version, this feature is explored and generalized by using different step distributions in the generalized elephant quantum walk.

Unitary random quantum walks were previously introduced in a variety of settings. For example, C. M. Chandrashekar[63] introduced a type of discrete-time quantum walk that has randomness built on the quantum coin operation and found that the disorder leads to Anderson localization[64] and in certain cases to maximally entangled coin states. After this work, R. Vieira *et al.*[65,66] analyzed the coin entanglement entropy of this same type of quantum walk in the discrete time setting for various initial parameters. Moreover, quantum walks with randomness in the hopping sizes were also previously proposed and experimentally studied in the discrete time[67,68] and continuous-time setting.[69,70] Nonetheless, none of these aforementioned works described a quantum walk with a variety

of scaling behaviors and interesting features that the generalized elephant quantum walk shows. The motivations to study these types of quantum walks comes from the fact that we can use quantum walks as a framework to study dissipative quantum computation[71] and quantum computation with decoherence, where,[72] for example, found that in certain cases the introduction of decoherence can actually be better for the development of quantum walk based quantum algorithms. These types of randomness mimics a non-perfect physical implementation of a quantum walk or its behavior over a random media and it is also another motivation for the gEQW.

Now, let us have a closer look at the generalized elephant quantum walk. In order to have random step sizes at each time step, the shift operator in one dimension is changed to[3]

$$S_t = \sum_{x=-\infty}^{\infty} \left[|x+\Delta_t\rangle\langle x| \otimes |\uparrow\rangle\langle\uparrow| + |x-\Delta_t\rangle\langle x| \otimes |\downarrow\rangle\langle\downarrow| \right] , \tag{3.94}$$

where S_t is the shift operator at time step t and Δ_t is the step size chosen at the same time instant. Thus, for every instant we are going to have a random unitary operator of the form Eq. (3.30), with S_t in place of S, using the coin operators as Eq. (3.27) and Eq. (3.28) in the same manner as the DTQW.

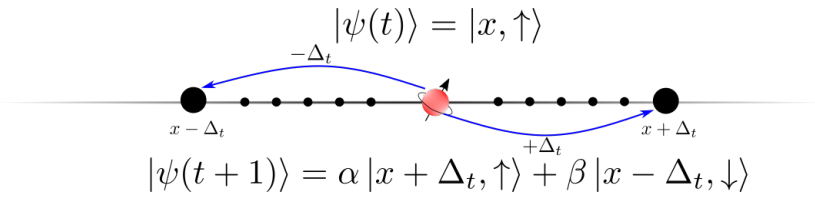

Figure 9 – Representation of one time step of the one-dimensional generalized elephant quantum walk.

Source: By the author.

The probability distribution used for choosing the steps sizes is a discretized version of the q-Exponential distribution, devised by C. Tsallis in the context of nonextensive statistical mechanics[73]

$$\Pr(\Delta_t) = e_q(\Delta_t) = \tau_t[1-(1-q)\Delta_t]^{1/1-q} , \tag{3.95}$$

with $\Delta_t \in [1,2,\ldots,t]$ and τ_t being a time-dependent normalization factor. The support of this probability distribution is

$$\text{supp}(e_q(x)) = \begin{cases} [0, \frac{1}{1-q}),\ q \leq 1 \\ [0,\infty),\ q > 1\ . \end{cases} \tag{3.96}$$

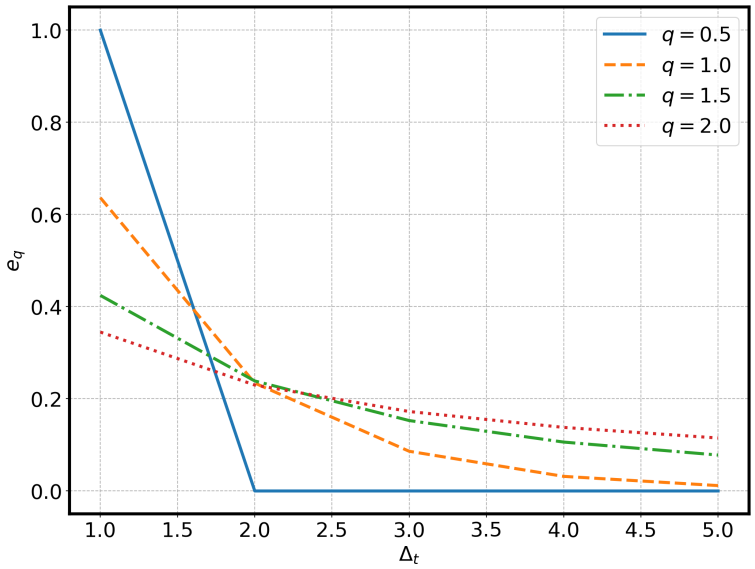

Figure 10 – q-Exponential probability distribution as a function of the step sizes for different values of q.

Source: By the author.

It is worth noting some limiting q-exponential probability distributions. The first one we get when we set $q = 1/2$, resulting in

$$e_{1/2}(\Delta_t) = \tau_t \left(1 - \frac{\Delta_t}{2}\right)^2 . \tag{3.97}$$

$e_{1/2}$ has support only on the interval $[0, 2)$, therefore, we see that in this case only unit step sizes are possible, matching with the standard DTQW. Lastly, taking the limit of q going to infinity we get the uniform distribution

$$\lim_{q\to\infty} e_q(\Delta_t) = \frac{\tau_t}{t} , \tag{3.98}$$

characterizing the elephant quantum walk.

Fig. 11 shows us the position probability distributions for some values of q at the same time instant. The first panel at the top left shows us the probability distribution of the standard quantum walk, being more localized than the ones for $q = 2$ or $q = \infty$, but more dispersed than the probability distribution for $q = 1$. This means that by varying the q parameter we could vary not only the shape of the probability distribution, but also the degree of spreading of the quantum walk.

In order to compare the degree of dispersion of the quantum walks, M. A. Pires et al[3] considered the asymptotic limit of the position variance. It is expected that its limiting

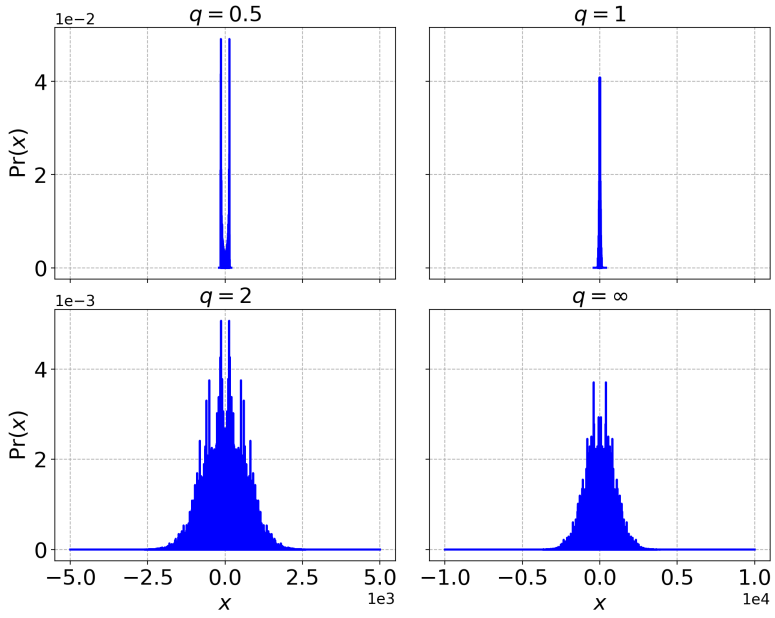

Figure 11 – Probability distributions of the generalized elephant quantum walk for different q's at time step $t = 148$. The initial walker state used was $|\psi\rangle = |0\rangle \otimes \frac{|\uparrow\rangle+|\downarrow\rangle}{\sqrt{2}}$ and Eq. (3.28) with $\theta = \pi/4$ as a coin operator.

Source: By the author.

behavior obeys

$$\mathrm{Var}_X(t) = \sigma_X^2 \approx t^\alpha, \;\; t \gg 1, \tag{3.99}$$

where α is called *diffusion exponent*. By taking the logarithm of the position variance graph, it is possible to estimate the diffusion exponent and compare the quantum walks dispersion for different values of q. It is worth remembering that the evolution of this type of DTQW is random, in the sense that for a given time instant the unitary operator can be different for different runs of the quantum walk. Consequently, the most appropriate is to consider an average diffusion exponent.

In Fig. 12 we have the graph of the mean diffusion exponent as a function of q in the range $[0.5, 1.9]$. It is also included the value of the mean diffusion exponent for $q = \infty$. The behavior of the curve formed by the data points is similar to the one obtained in,[3] and show us that after $q = 0.5$, the average diffusion exponent decreases until reaches its minimum value on $q = 1$. Then, for values of q greater than a critical point, $q_c \approx 1.3$, the mean diffusion exponent starts to increase and reaches an asymptotic limit of $\bar{\alpha} \approx 3$ with $q = \infty$, corresponding to the elephant quantum walk case. This interesting feature tell us that the q-exponential distribution allow us to control the scaling behavior of the quantum walk, with a strong randomness in the step sizes leading the quantum walk to a hyper-ballistic regime, while a weak randomness can lead it to similar classical random walk diffusive regimes.

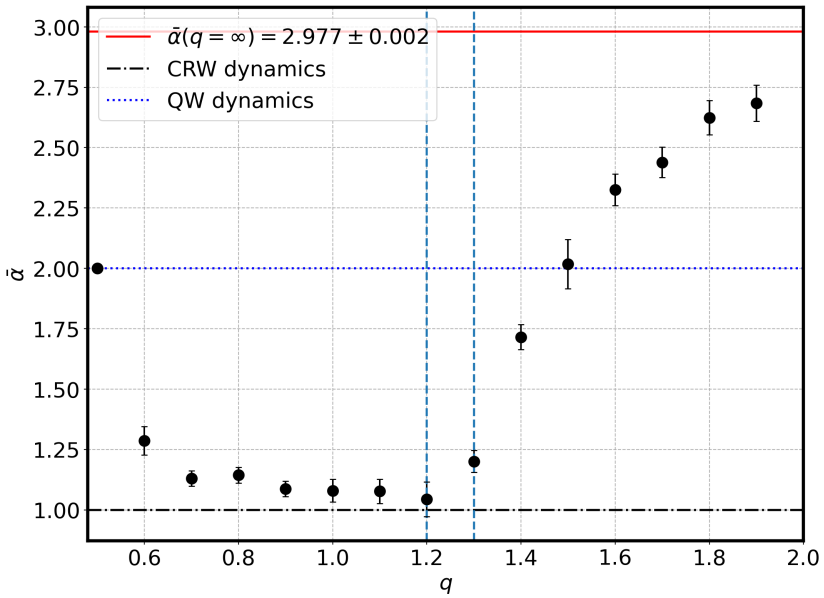

Figure 12 – Mean diffusion exponent as a function of the q parameter considering the quasi-stationary part of the evolution. The dashed vertical lines indicates the interval of q in which the diffusion exponent starts to monotonically increase. The same quantum walker initial state, $|0\rangle \otimes \frac{|\uparrow\rangle+|\downarrow\rangle}{\sqrt{2}}$, was considered for all values of q, and the same coin operator, that is $C_k(\pi/4)$.

Source: By the author.

Another aspect of the one-dimensional DTQW with random step sizes that was analyzed is the coin entanglement entropy. Fig. 13 show us the coin entanglement entropy as a function of time in the gEQW for different q considering the same initial state. We can conclude that for all q, but $q = 0.5$, the entanglement entropy of the coin reaches its maximum value on the long run. Some of the evolutions get to it slower than the others, but essentially all of them appear to get an average maximum entanglement entropy.

Summarizing, the generalized elephant quantum walk provide us a way to obtain different diffusive behaviors through the use of the q-exponential distribution. This distribution assigns to the gEQW the property of varying between the classical random walk spreading and the hyper-ballistic of the highly random evolution of the elephant quantum walk. Remarkably, while having this property, the gEQW appears that can produce maximally entangled coin states for all q parameters different than half, considering the initial state and the coin operator used in,[3] something that does not appears in other works where the increase on the entanglement is only followed by a limited ballistic spreading.[63,74–76] Taking into account the works that uses random coin operators,[63,65,66] this is an indicative that the production of highly entangled coin states is a feature of unitary random quantum walks. Therefore, we address the following questions, is this production coin initial state and coin operator dependent in the gEQW? How much randomness one must introduce in order to have highly entangled coin states? How does the entanglement entropy between

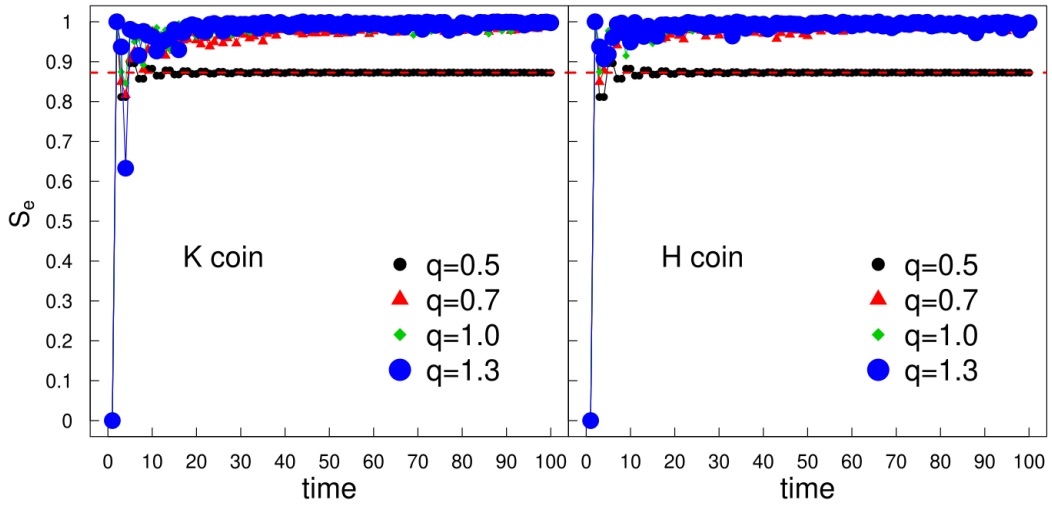

Figure 13 – Entanglement entropy as a function of time in the gEQW for different q parameter of the q-exponential distribution. All curves considered an initially localized walker state with the equal superposition of coin basis states and the Kempe coin with $\theta = \pi/4$ (left panel) and the Hadamard operator (right panel).

Source: Adapted from PIRES *et al.*[3]

the internal and external degrees of freedom varies as one utilizes delocalized walker initial states?

In the next chapter we consider an analysis of the coin entanglement entropy, published also as an article,[77] as a function of the coin initial state and of the coin operators for an initially localized and Gaussian-distributed walker in the gEQW. We also check how the q-exponential distribution used, i.e. the amount of randomness, affects the time average entanglement entropy. Finally, we also check the quasi-stationary regime for different generalized elephant quantum walks considering both initially localized and delocalized walker states.

4 RESULTS

4.1 Coin entanglement entropy in the generalized elephant quantum walk

In Sec. 3.3 we introduced the generalized elephant quantum walk, a DTQW model with random step sizes drawn from the q-exponential distribution Eq. (3.95). There, we saw that this type of quantum walk leads the coin to a maximally entangled state for some q parameters, considering the initial state $|\psi(0)\rangle = |0\rangle \otimes \frac{|\uparrow\rangle+|\downarrow\rangle}{\sqrt{2}}$, the Kempe coin (Eq.(3.28)) $C_k(\pi/4)$ and the Hadamard operator. In this section, we present our work in the analysis of the entanglement entropy as a function of the walker initial state and the coin operator used – as these are important factors in determining the asymptotic properties of the quantum walk – and also how the amount of disorder introduced affects the entanglement generation.

Following the equation for the coin density matrix Eq. (3.74) given before, in order to find its entanglement entropy Eq. (3.17) in a given time step we need to find its eigenvalues, prescribed by Eq. (3.76). The eigenvalues are determined through the coin state coefficients, where $A(t) = \sum_x |c_\uparrow^x(t)|^2$, $C(t) = 1 - A(t)$ and $B = \sum_x c_\uparrow^x(t) c_\downarrow^x(t)^*$. Given that the gEQW evolution is random, we find the coin state coefficients in a general evolution through numerical simulations using a modified version of the recurrence relations Eq. (3.37),

$$c_\uparrow(x,t) = \cos\theta c_\uparrow^{x-\Delta_t}(t-1) + \sin\theta e^{i\beta} c_\downarrow^{x-\Delta_t}(t-1) \tag{4.1}$$

$$c_\downarrow(x,t) = \sin\theta e^{i\gamma} c_\uparrow^{x+\Delta_t}(t-1) - \cos\theta e^{i(\beta+\gamma)} c_\downarrow^{x+\Delta_t}(t-1)\ , \tag{4.2}$$

where we used the general coin operator Eq. (3.26).

As computers have finite memory, the numerical simulation is set to run until it reaches the edges of the lattice, i.e. the maximum time step is set to be equal to half of the lattice size, in this way stopping the simulation when the walker reaches the edge of the graph. In order to we have a symmetric lattice, we always choose an odd number of vertices, that is $|V| = 2N + 1$, given a maximum time step of $t_{\max} = N$. For Gaussian initial states the same can be done, but care must be taken as if one chooses a small lattice size the borders conditions starts to affect the evolution.

4.1.1 Localized initial states

We begin considering the following initially localized states

$$|\psi(0)\rangle = |0\rangle \otimes \left(\cos\frac{\Omega}{2}|\uparrow\rangle + e^{i\phi/2}\sin\frac{\Omega}{2}|\downarrow\rangle\right)\ , \tag{4.3}$$

where $\Omega \in [0, \pi]$ and $\phi \in [0, 2\pi]$ are the polar and azimuth angles of the coin Bloch sphere.[43]

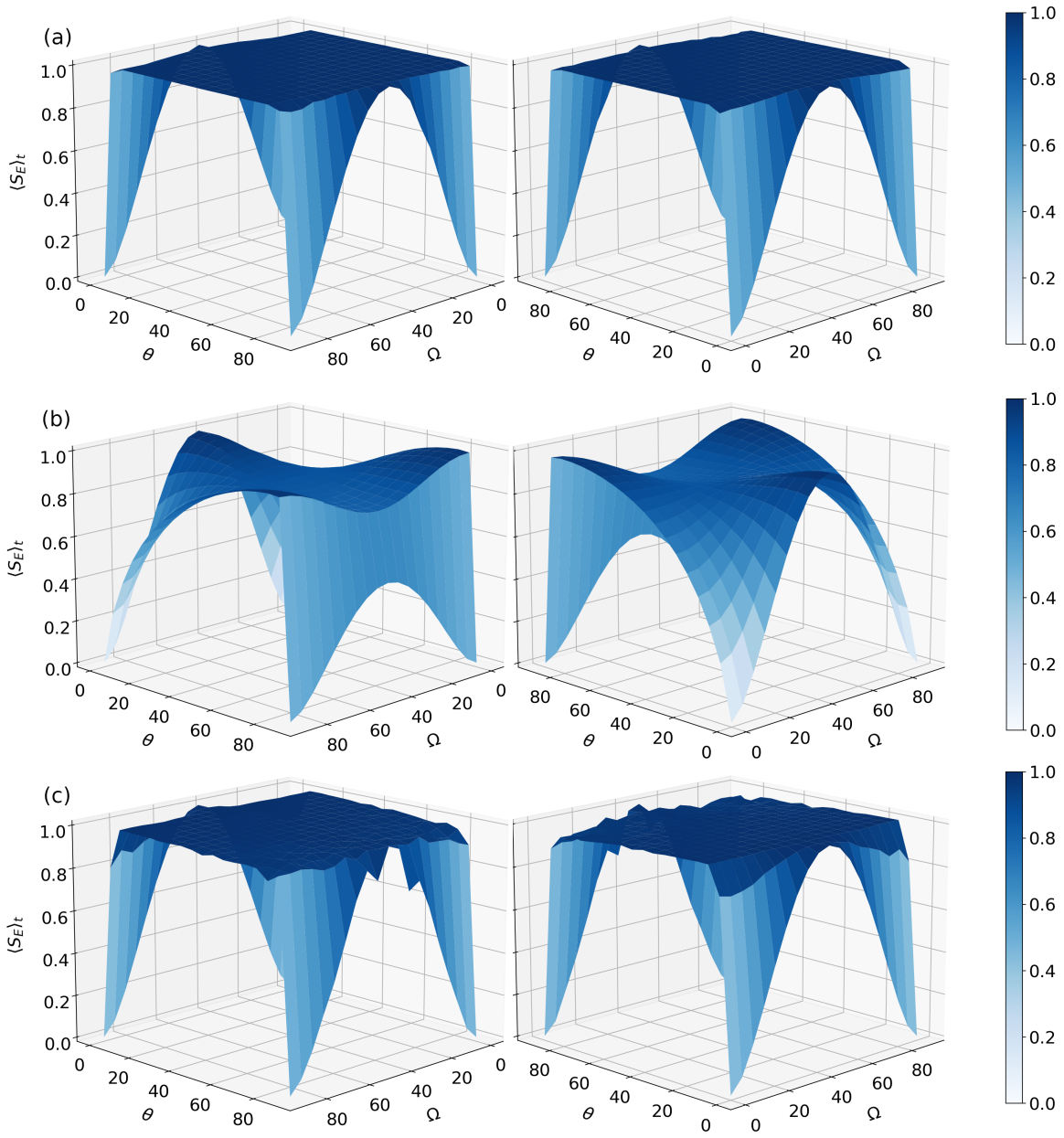

Figure 14 – Time average coin entanglement entropy for the gEQW as a function of the Kempe coin parameter θ and the Bloch polar angle Ω with $q = \infty$ (a), $q = 0.5$ (b) and $q = 1$ (c) using $|\psi_p(0)\rangle = |0\rangle$ and the phase angle $\phi = 0$.

Source: By the author.

As a way to study the entanglement generation as a function of the initial parameters, throughout this work we have considered the time average entanglement entropy taking only the quasi-stationary part of the entanglement evolution. It is expected that, after an initial increase, the entanglement entropy reaches, at least, an average constant value,[65,66] hence the use of the term "quasi-stationary". Given that the quasi-stationary regime varies with the type of quantum walk, initial state and coin operator, it was

determined individually for each evolution analyzed here by looking at the whole von Neumann entropy time evolution.

In Fig. 14(b) we have a 3D plot of the mean entanglement entropy as a function of θ in the Kempe coin and Ω in the standard DTQW, i.e. $q = 0.5$, where the average was taken with respect to time in the quasi-stationary part of the evolution and the phase angle ϕ set to zero. It is possible to note that only for some values of θ and Ω the walker coin state is led to the maximally entangled state, represented by the dark blue color. Also, there are some values of these two parameters that give us a separable state, with θ and Ω in the set $\{0°, 90°\}$.

Taking different values of q, such as $q = \infty$ and $q = 1$ Fig. 14(a) and (c), respectively, give us a dark blue plateau that indicates that for almost all values of the space parameter considered $\{\theta, \Omega\}$, we have an average time asymptotic maximally entangled coin state. There are intervals in the θ and Ω axis that does not give us a maximally average entanglement entropy, for instance, considering $\theta = 0$, i.e. the identity operator, we only get a maximally entangled state with $\Omega = \pi/4$. Nonetheless, these results are a strong indicative that the generalized elephant quantum walk can generate maximally entangled coin states for almost all coin initial states and Kempe coin operators when $q \neq 1/2$.

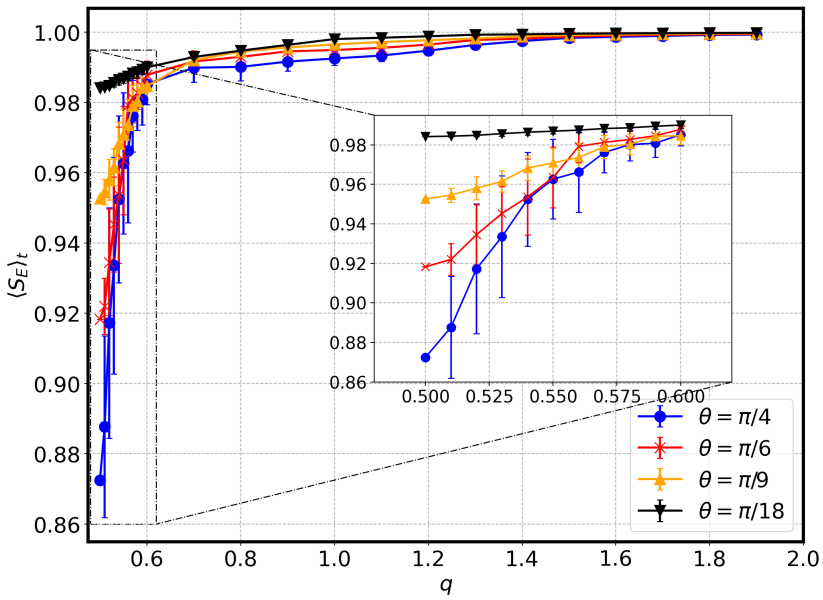

Figure 15 – (Color online)Time average entanglement entropy as a function of q in the q- exponential distribution Eq. (3.95) in the gEQW for different values of θ in the Kempe coin operator Eq. (3.28). The data points were obtained through the average of 50 simulations each and the error bars indicate the standard deviation of the points. In all simulations the initial state was $|0\rangle \otimes (|\uparrow\rangle + |\downarrow\rangle)/\sqrt{2}$, i.e. $\Omega = \pi/2$ and $\phi = 0$.

Source: By the author.

In Fig. 15, we analyze the time-averaged entanglement entropy of the coin system as

a function of the q parameter, i.e. the amount of disorder introduced in the shift operator, for some values of θ in the Kempe coin operator. From it, we observe that the entanglement entropy increases very fast in the interval $[0.5, 0.6]$ and goes asymptotically to $\langle S_E \rangle_t = 1$ as $q \to \infty$. Going back to the q-exponential function, we understand that changing from $q = 0.5$ to $q = 0.6$ we only soar the probability of having steps of size equal to 2 from 0 to approximately 6%; still, we have a substantial increase in the average entanglement, going from 0.8724 to 0.9852 for $\theta = \pi/4$, and a moderate increase for $\theta = \pi/6$, from 0.9183 to 0.9878. With $\theta = \pi/18$, as the average entanglement with $q = 0.5$ is already significant (look at Fig. 14(b)), the increase is also small. Changing the parameter q to one, in the long time limit the probability of unit step sizes is approximately 63%, of step sizes equal to two approximately 23%, while of steps of sizes equal to three 9%, but for all θ we already have an almost fully entangled state of $\langle S_E \rangle_t \approx 0.99$. Therefore, considering an initially localized walker and the Kempe coin, we say that by allowing steps $\Delta_t = 2$ with a small probability we enhance the generation of entanglement between the coin and position subsystems – not being necessary a strong randomness in the step sizes – and with a probability of approximately 9% of $\Delta_t = 3$ the time-averaged coin von Neumann entropy almost reaches its maximum value.

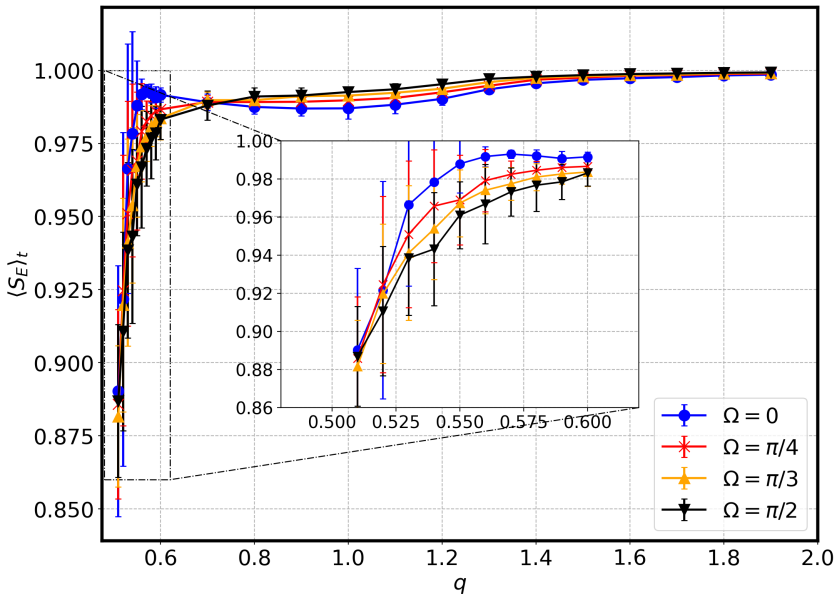

Figure 16 – (Color online) Time average entanglement entropy as a function of q in the q-exponential distribution Eq. (3.95) in the gEQW with the Kempe coin operator Eq. (3.28) with $\theta = \pi/4$ for different coin states Bloch polar angles Ω using $\phi = 0$ for all of them. The data points were obtained through the average of 50 simulations each and the error bars indicate the standard deviation of the points. In all simulations the localized walker initial state was used.

Source: By the author.

We have also studied how the time average entanglement entropy of the gEQW with $\theta = \pi/4$ in Eq. (3.28) behaves as we change the coin initial state Bloch polar angle

Ω. In Fig. 16, we confirm that by varying Ω we are able to control the increase of the entanglement entropy for q in the interval $[0.5, 0.6]$, with $\Omega = 0$ giving the greater rate. For $q > 0.6$, the entanglement entropy decreases thus swapping the proportionality relation between Ω and the entanglement entropy by increasing parameter q, which only converges with the other curves at $q = 1.6$, approximately.

Following, we investigate the time-averaged entanglement entropy in more general coin operators by modifying one of the phase angles of the coin operator in Eq. (3.26), namely β, as depicted in the 3D plots of the mean entanglement entropy as a function of θ and β for $q = 1/2$ Fig. 17(a) and $q = \infty$ Fig. 17(b).

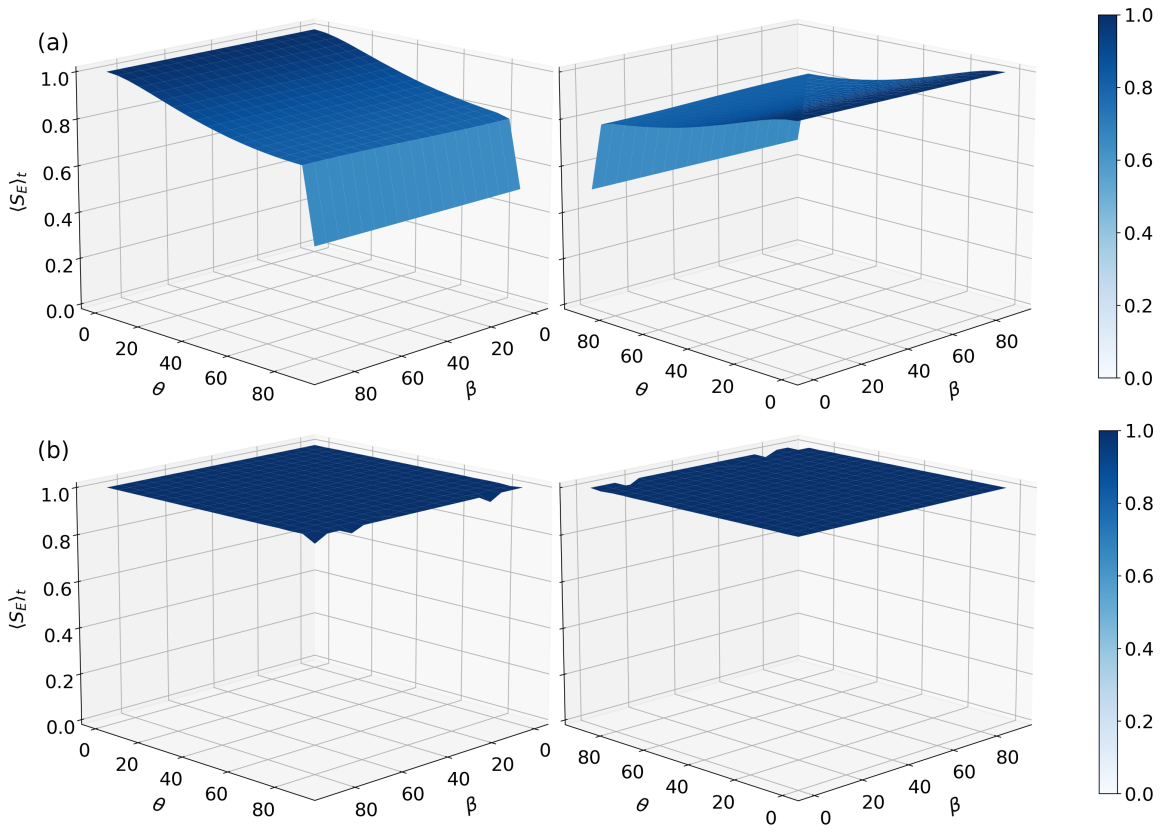

Figure 17 – Time average entanglement entropy of the coin state in the generalized elephant quantum walk as a function of θ and β in the coin operator Eq. (3.26). In (a) we have $q = 0.5$ and in (b) $q = \infty$. All simulations were done considering an initially localized walker state and $\Omega = \pi/2$ and $\phi = 0$ in Eq. (4.3).

Source: By the author.

Using $\Omega = \pi/2$ with $\phi = 0$, we have understood that by varying the phase angle β in the standard quantum walk the time average entanglement entropy of the coin state does not changes for a given value of θ, as $\langle S_E \rangle_t \times \beta$ remains virtually constant. The same conclusion is drawn for the elephant quantum walk in Fig. 17(b). In addition, it does not matter whether we vary θ for a given value of β, because $\langle S_E \rangle_t \times \theta$ remains constant. That is a strong indicative that the generalized elephant quantum walk, for $q \neq 1/2$, produces

highly entangled coin states, $S_E > 0.87$ for $q \in (0.5, 0.6]$, and maximally entangled coin states for $q \to \infty$, for all coin operators and coin initial states, considering an initially localized walker state.

In order for us to get a physical intuition on why the generalized elephant quantum walk yields highly coin entangled states it is worth introducing another perspective about its evolution. We can think of the gEQW random unitary evolution as an open evolution that the walker goes through where we observe at each time step which unitary operator was selected by the environment. Let $\mathcal{H}_E$ be the Hilbert space of the environment surrounding the walker spanned by the set $\{|\Delta_j\rangle, j = 1, \ldots, t\}$, so that the total Hilbert space is $\mathcal{H}_S \otimes \mathcal{H}_E$ and the total density matrix is $\rho_{S,E}$. Considering that together both systems constitute a closed system, it evolves according to a unitary evolution following Eq. (3.20). The unitary evolution must be one that associates to each random unitary operator of the gEQW a state of the environment, hence

$$U = \sum_{j=1}^{t} U_j \otimes |\Delta_j\rangle\langle\Delta_j| \ , \tag{4.4}$$

where $U_j = S_j(\mathbb{I}_p \otimes C_2)$. Let the total state be of the form $\rho_S \otimes |\psi_E(t)\rangle\langle\psi_E(t)|$ with the environment state $|\psi_E(t)\rangle = \sum_{j=1}^{t} \sqrt{e_q(\Delta_j)}\,|\Delta_j\rangle$, then following Eq. (3.20), the total state at time t is obtained from

$$\rho_{S,E}(t+1) = \sum_{j,j'} \sqrt{p(\Delta_j)}\sqrt{p(\Delta_{j'})} U_j \rho_S(t) U_{j'}^{\dagger} \otimes |\Delta_j\rangle\langle\Delta_{j'}| \ . \tag{4.5}$$

Therefore, by applying a projective measurement $P_t = |\Delta_t\rangle\langle\Delta_t|$ on the environment state and eliminating its degree of freedom through the partial trace we obtain the following unnormalized walker state

$$\rho_S(t+1) = e_q(\Delta_t) U_t \rho_S(t) U_t^{\dagger} \ , \tag{4.6}$$

with $e_q(\Delta_t)$ being the probability of $U_t \rho_S(t) U_t^{\dagger}$ be selected from the ensemble $\sum_j e_q(\Delta_j) U_j \rho_S(t) U_j^{\dagger}$.

Bearing in mind this interpretation, by looking at the norm of the coin density matrix coherence time evolution $|B(t)|$ Eq. (3.76), Fig. 18, we see that in the DTQW, the coherence absolute value has a decaying oscillating behavior, stabilizing into a value of approximately 0.2. By increasing the amount of randomness, the coin goes progressively into a stronger decoherent evolution induced by the surrounding environment, going to zero for the maximally random case, i.e. the EQW. This behavior is in agreement with the observed behavior of the average entanglement entropy as a function of q Figs. 15 and 16.

Next we survey the time-averaged coin von Neumann entropy for delocalized Gaussian walker initial states.

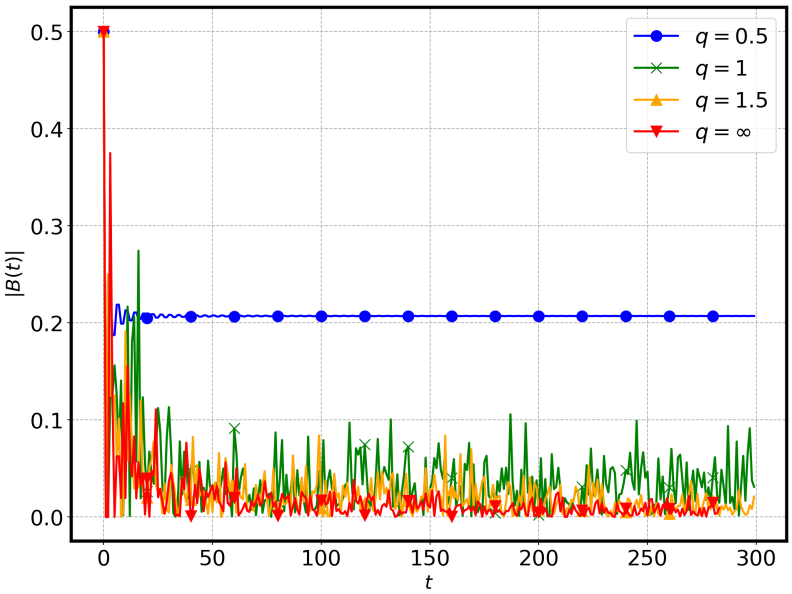

Figure 18 – (Color online) Time evolution of the coin density matrix coherence absolute value for different generalized elephant quantum walks using $C_k(\pi/4)$. The initial state used in all simulation was the one localized at the origin and with the parameters $\phi = 0$ and $\Omega = \pi/2$ for the coin.

Source: By the author.

4.1.2 Delocalized initial states

The form of the delocalized position initial states that we considered is Gaussian

$$|\psi_p(0)\rangle = \sum_{x=-\infty}^{\infty} N e^{\frac{-x^2}{4\sigma^2}} |x\rangle \ , \tag{4.7}$$

where N is a normalization factor and σ the standard deviation of the distribution. In the standard DTQW, by using delocalized initial states the position variance only gets a polynomial form in the short time period, like $a_0 + a_1\ t + a_2\ t^2$. Regarding the coin entanglement entropy, A. C. Orthey and E. P. Amorim[78] studied the asymptotic coin state when one considers a Gaussian for the position initial state as well, but in the Hadamard walk Eq. (3.27) instead, and they found a relation between the coin initial state angles on the Bloch sphere that gives a maximally entangled coin state, following our notation

$$\cos\phi = -\cot\Omega \ , \tag{4.8}$$

when the initial position variance $\sigma \gg 1$.

Aiming at capture the effect on the entanglement entropy of introducing randomness in the step sizes, we have computed the time evolution of the entanglement entropy for an initial coin state with $\Omega = \pi/3$ and $\phi \approx 0.696\pi$, following Eq. (4.8) in Fig. 19. In Fig. 19(a), we see that the quantum walk with random step sizes leads the entanglement entropy

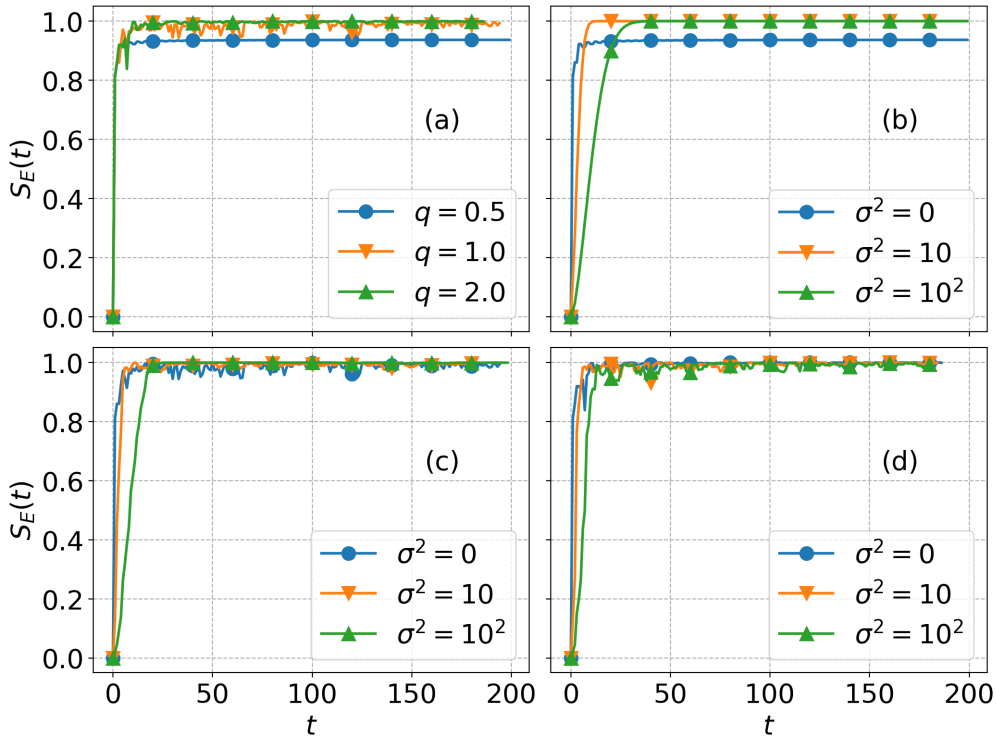

Figure 19 – Time evolution of the coin entanglement entropy for different values of q and $\sigma^2 = 0$ (a), $q = 0.5$ (b), (left bottom panel) $q = 1$ (c), $q = 2$ (d) and different values of σ in the Hadamard Walk. The coin initial state used was the one following Eq. (4.8) with $\Omega = \pi/3$.

Source: By the author.

to the maximum value while the same does not happen for the standard DTQW where an initially localized state is considered. This is in agreement with our previous results. However, as we change the variance of initial position Fig. 19(b), the coin entanglement entropy gets to the maximal, reproducing the previous results of Orthey and Amorim.[78] The only significant difference between the initially localized and delocalized states in the cases where we use the gEQW Fig. 19(c,d) are in the increase rate of the entanglement entropy as a function of time, where as we increase σ we get a slower $S_E(t)$ initial increase.

The below 3D plot shows the time-averaged entanglement entropy as a function of the Kempe coin operator parameter and the coin initial Bloch polar angle in the standard DTQW Fig. 20(a), where we have considered a Gaussian initial state with $\sigma^2 = 10^3$. It is visible that the average coin entanglement entropy has lowered for all $\{\theta, \Omega\}$ pairs, with the maximum value obtained when we set $\theta = 0°$ and $\Omega = 90°$. For almost all pairs with $\theta > 20°$ the coin entanglement entropy reaches its minimal value; in other words, the coin-position system is a separable one, something that happens only for a few points in the localized initial state case (see Fig. 14(b)). Hence, in the standard DTQW the introduction of highly delocalized walker initial states drastically affects the asymptotic entanglement.

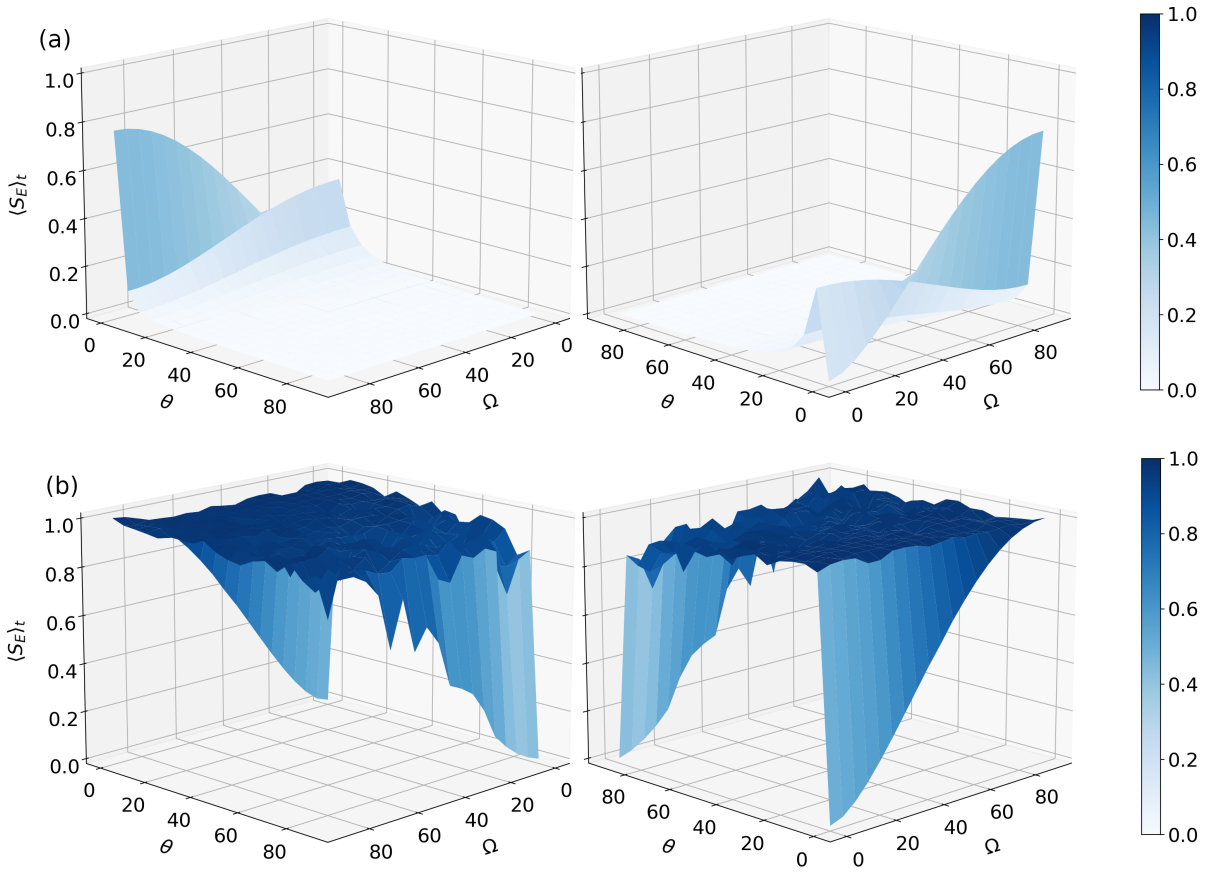

Figure 20 – Time average entanglement entropy as a function of θ in Eq. (3.28) and Ω in Eq. (4.3) for the gEQW with $q = 1/2$ (a) and $q = \infty$ (b). The position initial state used was a Gaussian distribution Eq. (4.7) with $\sigma^2 = 10^3$ for both plots.

Source: By the author.

Figure 20(b) shows us the 3D plot of the elephant quantum walk case. Therein, we note that for almost all pairs the average entanglement entropy is still close to its supreme, but with more oscillations around it. Furthermore, the behavior of the surface on the regions where $\theta \approx 0°$ or $\theta \approx 90°$ has significantly changed, with a decrease of $\langle S_E \rangle_t$ to 0.8 as θ goes to $90°$ and Ω goes to $0°$. This scenario indicates us that the coin entanglement entropy in the elephant quantum walk using the Kempe coin operator is robust against the use of highly delocalized walker initial states for a significant part of the set of possible $\{\theta, \Omega\}$ pairs, while this does not happen in the standard quantum walk.

Next, we investigate how the mean entanglement entropy varies as we change q in the q-exponential distribution with delocalized initial states. Fig. 21 depicts the time average entanglement entropy in the generalized elephant quantum walk as a function of q for different position initial variances in (a) with $\Omega = \pi/2$ and $\phi = 0$ and (b) with $\Omega = \pi/3$ and ϕ given by Eq. (4.8), in the coin initial state. Taking $q = 0.5$, we can see that the time average entanglement indeed decreases as we increase the initial position variance, at least in the case where we use the Kempe coin operator with $\theta = \pi/4$ and $\Omega = \pi/2$

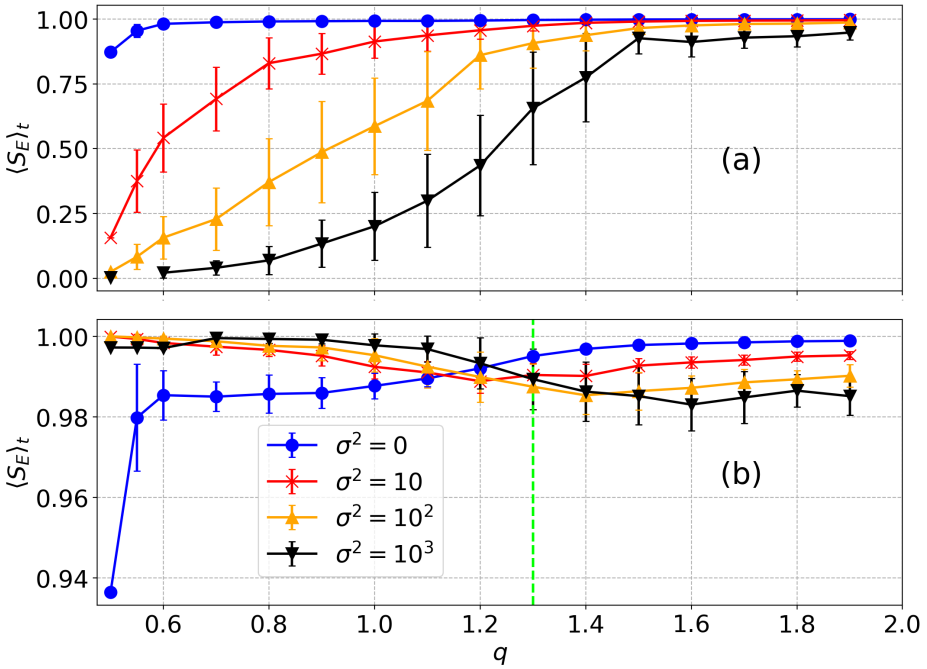

Figure 21 – (Color online) Time average coin entanglement entropy as a function of the q parameter in Eq.(3.95) for the gEQW with $\sigma^2 = 0$ (blue circle), $\sigma^2 = 10$ (red star), $\sigma^2 = 10^2$ (orange up triangle) and $\sigma^2 = 10^3$ (black down triangle). The coin operator used in (a) was Eq. (3.28) with $\theta = \pi/4$ and with $\Omega = \pi/2$ and $\phi = 0$, and in (b) the Hadamard operator with $\Omega = \pi/3$ and $\phi \approx 0.696\pi$. Each data point was obtained through 50 simulations.

Source: By the author.

(a). We note that for $q \in (0.5, 1.5]$ the entanglement entropy decreases in comparison with the initially localized case as well; however, there is concomitantly an increase in the uncertainty of the data points. That can be assigned to the fact that the time evolution of the entanglement in the gEQW with q in this region presents very large oscillations, which in our interpretation indicates that with the use of initially delocalized states the walker takes more time to reach the quasi-stationary regime. Nonetheless, comparing with the deterministic DTQW we have an increase on the coin entropy and by inferring the asymptotic behavior of $\langle S_E \rangle_t \times q$ we can say that this diminishing goes to zero as $q \to \infty$.

Considering the lower panel (b), we see that the average entropy also decreases – but in a smaller degree due to the use of an initial state that leads to a maximally entangled state in the deterministic walk – as we increase q from 0.5 in the delocalized cases, being surpassed by the localized ones when $q = 1.3$. As in Fig. 21(a) panel, that can be attributed to a delay in reaching the quasi-stationary regime by the use of delocalized initial states. Bridging those observations with the results obtained in Fig. 20(b), it is possible to assert this decrease goes to zero as $q \to \infty$.

Finally, we look at the time-averaged coin entanglement entropy as a function of q for different values of θ in Eq. (3.28) and considering a Gaussian position initial state with

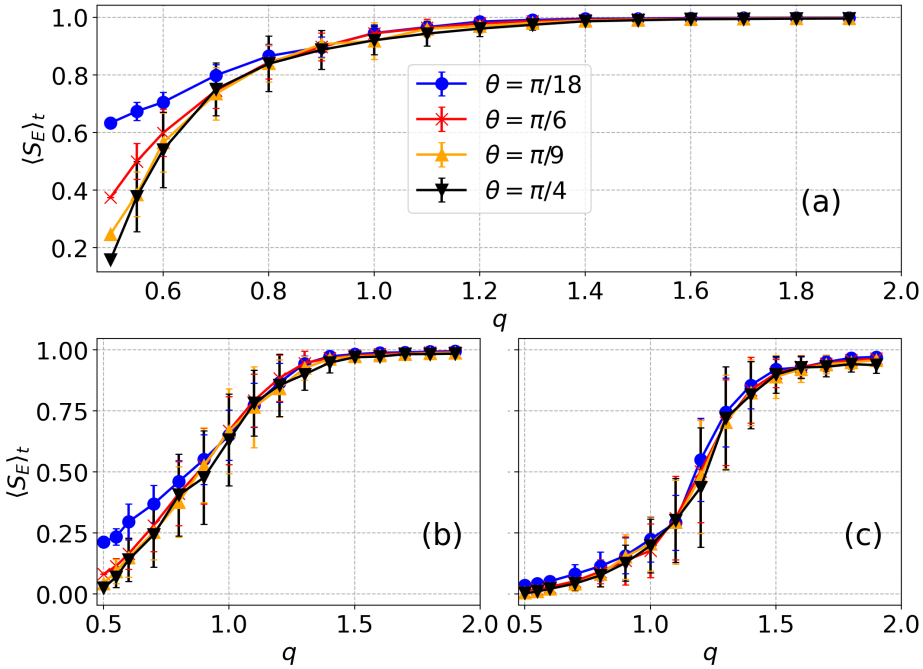

Figure 22 – (Color online)Time average entanglement entropy as a function of q in Eq. (3.95) considering different values of θ of the Kempe coin operator in the initially delocalized gEQW using $\sigma = 10$ (a), $\sigma = 10^2$ (b) and $\sigma = 10^3$ (c). In all simulations a coin initial state was used with $\Omega = \pi/2$ and $\phi = 0$ in Eq. (4.3). Each data point was obtained through 50 simulations.

Source: By the author.

$\sigma^2 = 10$ Fig. 22(a), $\sigma^2 = 10^2$ (b) and $\sigma^2 = 10^3$ (c). We see that by varying the θ parameter the mean entanglement curve changes significantly only as the initial position variance is low, indicating that with regard to the Kempe coin operator the initial position variance plays a major role in the time average coin entanglement entropy for greater values of σ.

As it was previously mentioned, random quantum walks with the disorder embedded in the coin operator were previously studied showing also to enhance the entanglement between the coin and position of the walker.[65,66] In the case of a time-dependent randomness, taking into account our results, we find the interesting result that the generation of maximally entangled states is a feature of dynamically random quantum walks, with the randomness either in the coin operator or in the shift operator. Here we have also shown that the entanglement enhancement in the gEQW is robust with respect to the initial conditions of the walker – in both initially localized and delocalized walker states – and the use of different coin operators.

It is worthwhile also to mention that for some algorithmic applications it is desired to control the propagation of the walker while also controlling the way in which the quantum coin participates in the full state.[72,79] The generalized elephant quantum walk can be interesting for this purpose since, with the q-exponential distribution, we can control

its propagation and the participation of the coin as we can see in Fig. 23 through the *Inverse Participation Ratio*, $\text{IPR} = (\sum_x (P_t(x))^2)^{-1}$. The IPR of a probability distribution measures how its spread over its domain having two extremes, (i) fully localized states where $P_t(x) = \delta_{x,x_0}$ with $\text{IPR} = 1$ and (ii) completely delocalized states where $P_t(x) = 1/N$ with $\text{IPR} = N$ and N being the lattice size. Fig. 23 shows us that in the gEQW it is possible to control the spreading behavior of the walker while also controlling how the walker is localized through the lattice without reducing the coin-position entanglement.

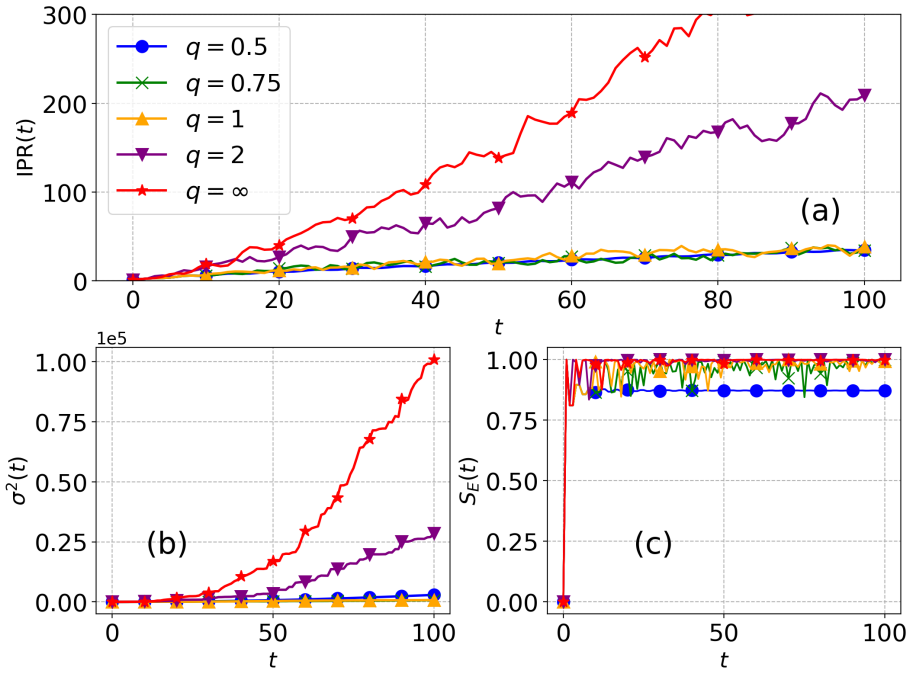

Figure 23 – (Color online) IPR time series for different generalized elephant quantum walks (a), variance (b) and von Neumann entropy (c) time evolution for the same gEQWs. The coin operator used was $C_k(\pi/4)$ Eq. (3.28) and the initial state considered in all curves was the one localized in the origin with $\phi = 0$ and $\Omega = \pi/2$ in Eq. (4.3) as coin initial state.

Source: By the author.

4.1.3 Quasi-stationary regime

To analyze the long-time behavior of the quantum coin evolution with regard to its state changes we are going to use the trace distance as a measure of distinctness between quantum states Eq.(3.92). We can employ it by noting that if a quantum state reaches a quasi-stationary regime, the trace distance between any two time successive states will be constant on average, being zero in the case of a true stationary regime where $\rho_c(t+1) = \rho_c(t)$. Hence, by calculating the trace distance between two successive states, $D(\rho_c(t+1), \rho_c(t))$, we can find how, if so, the generalized elephant quantum walk goes to the quasi-stationary regime.

We begin by looking at the trace distance evolution for different generalized elephant quantum walks, with the standard DTQW included, using initially localized walker states. For $q \neq 0.5$, given that the evolution is stochastic, the trace distance considered is an ensemble average. From Fig. 24 we can see that the trace distance decays following a power law in time, $\bar{D} \propto t^{-\beta}$. Also, by increasing the amount of randomness the quantum walk goes to the stationary regime slower than in the deterministic case, with the decay law exponent β – given by the log-log inset fittings – equal to approximately 1.5 for the standard DTQW, $\beta \approx 0.03$ for $q = 0.6$, $\beta \approx 0.24$ for $q = 1$ and $\beta \approx 0.66$ for the elephant quantum walk. Moreover, it is possible to affirm that the decay exponent does not follow a simple inverse relationship with the amount of randomness, since the decay exponent for the completely random case is greater than for $q = 0.6$ and $q = 1$.

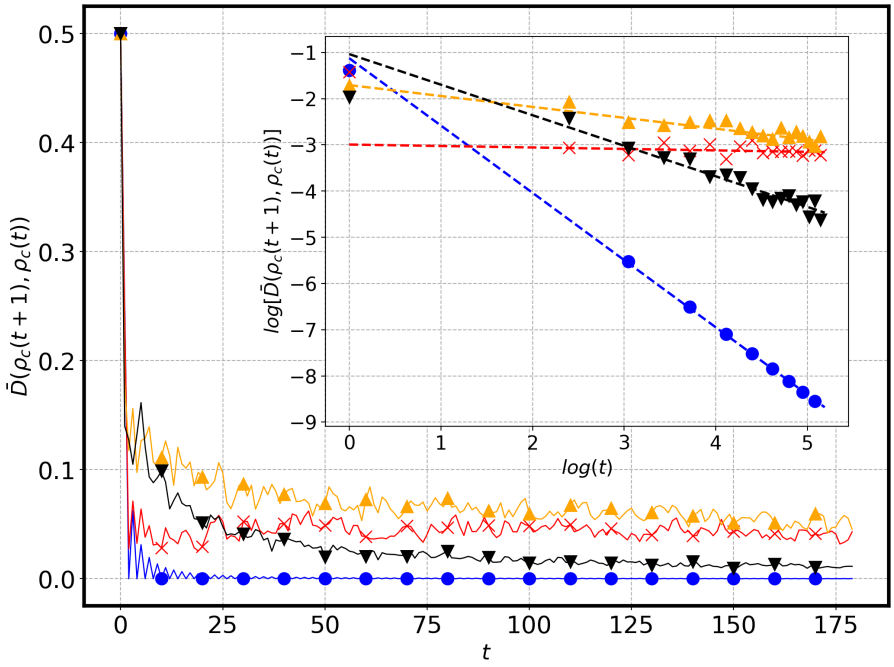

Figure 24 – (Color online) Time evolution of the trace distance between two successive coin states for the initially localized gEQW with $q = 0.5$ (blue circle), $q = 0.6$ (red cross), $q = 1$ (orange up triangle) and $q = \infty$ (black down triangle). The coin initial state used was the one following Eq. (4.3) with $\Omega = \pi/2$ and $\phi = 0$, using $C_k(\pi/4)$ as coin operator through the evolution. The size of the simulation sample considered for all curves, except $q = 0.5$, was 50. The inset shows the log-log graph of the same curves, with corresponding decay exponents $-\beta$, (-1.456 ± 0.004) for $q = 0.5$, (-0.03 ± 0.02) for $q = 0.6$, (-0.236 ± 0.008) for $q = 1$ and (-0.66 ± 0.01) for $q = \infty$.

Source: By the author.

Now we move to see what are the effects of using an initially delocalized state. As a means of comparison, first we look at the standard DTQW trace distance Fig. 25(a). It is possible to note that the use of initially delocalized states introduces oscillations and a transient regime in evolution that is made longer when we increase the initial variance.

Moreover, by fitting the data points for $t \gg 1$ into a power law and calculating the decay exponents (TAB. 1) we see that by increasing the initial delocalization the quantum walk reaches the quasi-stationary regime faster than in the localized case when $\sigma^2 = 10$ (red cross curve) but slower when $\sigma^2 = 10^2$ (orange up triangle curve). Besides the fact that a true stationary regime does not exist, for the quantum walks with random step sizes, $q = 0.6$ Fig. 25(b), $q = 1$ Fig. 25(c) and $q = \infty$ Fig. 25(d) the same features are observed. With $q = 0.6$, when we use $\sigma^2 = 10$ the quasi-stationary regime is achieved faster than in the localized case, but with $\sigma^2 = 10^2$ it is achieved much more slower, with a longer initial transient increasing. As we increase the amount of randomness this transient takes much more time, as we can note from Fig. 25(c-d) and we do not observe a faster decay for $\sigma^2 = 10$ (see TAB. 1).

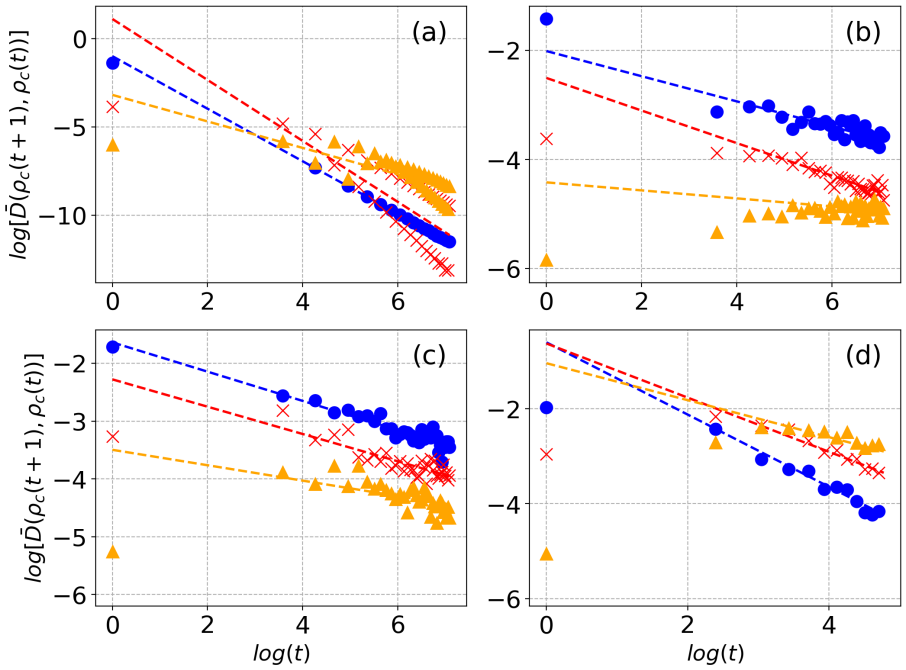

Figure 25 – (Color online) Log-log graphs of the average trace distance between two successive coin states time evolution in the generalized elephant quantum walk using $C_k(\pi/4)$ as coin operator with $\phi = 0$ and $\Omega = \pi/2$ determining the coin initial state with different initial variances. The initial variances are $\sigma^2 = 0$ (blue circle), $\sigma^2 = 10$ (red star) and $\sigma^2 = 10^2$ (orange up triangle). In (a) panel we have the standard DTQW, (b) $q = 0.6$, (c) with $q = 1.0$ and (d) corresponding to $q = \infty$. The average was calculated through 50 simulations for each curve.

Source: By the author.

This property of retarding the quasi-stationary regime as one increases the initial delocalization explains the greater uncertainty and lower values of the average entanglement of Fig. 21 when one also increases the amount of randomness. It is also remarkable that the feature of extending the transient regime was previously observed in quantum walks with

Table 1 – Table of the decay exponent β of the trace distance between two time successive states considering the different values of q and initial variance σ^2 obtained through the fittings of the curves for $t \gg 1$ in Fig. 25.

q \ σ^2	0	10	10^2
0.5	1.487 ± 0.001	1.73 ± 0.04	0.75 ± 0.02
0.6	0.23 ± 0.01	0.30 ± 0.01	0.07 ± 0.01
1	0.253 ± 0.003	0.236 ± 0.005	0.133 ± 0.006
∞	0.76 ± 0.02	0.57 ± 0.02	0.37 ± 0.03

Source: By the author.

dynamically random coin operators[i], where the decaying trace distance follows a power law with an exponent equal to $-1/4$. This tells us that this property is indeed a feature of dynamically random quantum walks, now including the use of random shift operators. We highlight that the figures 24-25 can also be used as evidence that in average the quantum walk with random steps sizes indeed have a quasi-stationary regime, with some of them taking more time than others to reach it depending on the initial delocalization and degree of randomness of the step sizes.

[i] Please look at the supplement material of Vieira *et al.*[65]

5 CONCLUSION AND PERSPECTIVES

In this work we further analyzed the coin entanglement generation in the generalized elephant quantum walk, following the previous results of Pires *et al.*[3] By looking at the initially localized walker state, we saw that the time average coin entanglement reaches its maximum value for almost all parameters in the Kempe coin operator and polar angles in the coin initial state Bloch sphere when $q = \infty$ and $q = 1$, something that does not happen in the standard discrete time quantum walk considering the same parameters. When we use a more general type of coin operator, Eq. (3.26), our results tell us that the elephant quantum walk entanglement does not change, considering the same initial walker state, while in the DTQW the time average entanglement entropy can vary from its value given when we use $\theta = \pi/4$ in the Kempe coin up to almost the maximum value. Looking at the time-averaged entanglement entropy as a function of the amount of disorder introduced in the shift operator, we saw that it only takes a small amount of disorder in order to greatly improve the time average entanglement, going from $\langle S_E \rangle_t \approx 0.8724$ with only unit step sizes to 0.9852 with probability of approximately 6% of having steps of sizes equal to 2 ($q = 0.6$), for $\theta = \pi/4$. By changing the θ Kempe coin parameter, one only increases the initial entanglement average as a function of q increase rate and the same goes for the Bloch polar angle of the coin initial state.

Taking Gaussian delocalized initial states, the use of random steps sizes also improved the time average coin entanglement when one uses the Kempe coin operator and $\Omega = \pi/2$ and $\phi = 0$ in the coin initial state, yet with an increasing uncertainty in the data and still lower than the values of the initially localized cases. The same thing goes when we consider the Hadamard walk and we use an initial coin state that goes to the maximally entangled one in the DTQW according to Ref.[78] Nonetheless, we assert that for almost all initial coin states and coin operators, the generalized elephant quantum walk enhances the coin entanglement entropy for delocalized initial states taking it to the supreme as $q \to \infty$.

With an analysis of the quasi-stationary regime through the trace distance between two time successive states, we showed that by using random step sizes the quantum walk goes to the quasi-stationary regime slower than in the deterministic case, with a power law decay exponent β equal to approximately -1.5 for the DTQW, -0.236 for $q = 1$ and -0.66 for the EQW, while a clear relationship between the amount of randomness and the trace distance decay rate was not determined. When we considered increasingly delocalized initial states we observed a decrease in the decay rate, summarized in TAB. 1, and an increase in the time length of the transient regime, common features with coin operator disordered quantum walks. This behavior of the quantum walk's quasi-stationary

regime explained the aforementioned observed properties of the time average entanglement entropy.

The above results are in a striking contrast with the idea that disorder in quantum processes acts as a weakening factor to generation of entanglement. A similar feature was already described mathematically,[63] numerically[65,66] and experimentally[80,81] in previous works that uses random quantum walks where the disorder is dynamically embedded in the coin operator. Despite that, a significant difference arises between the gEQW model and the above-mentioned types of quantum walks. While in the first case we have an enhancement of the entanglement generation maintaining the controllability of the spreading behavior, in the quantum walks with random coin operators the diffusion is weakened to a sub-ballistic behavior, showing the richness of the gEQW. Summing up the aforementioned results, we highlight that as in our model the disorder is introduced in the shift operator, we can conclude that the production of maximally entangled coin states for almost all coin initial states and coin operators is a feature of dynamically disordered quantum walks, with disorder in either coin or shift operator – taking an initially localized and delocalized walker for $q \to \infty$.

A natural question one can make about the generalized elephant quantum walk is if it is an efficient way to generate entanglement between its degrees of freedom and how its efficiency compares with other types of random quantum walks, since, from an experimental point of view, this can be a major factor. Moreover, no extensive analysis of the role of quantum memory effects on the coin evolution, that might provide insightful results, was made for this type of quantum walk. Therefore, we look forward to address these problems in a future work.

Interesting features can be obtained when one consider higher dimensional quantum walks, such as in the introduction of decoherence through the use of broken-link noise type[36] and the previously mentioned work of Chandrashekar,[63] where he observed the walker's localization when using unitary noise through the coin operator. Consequently, we also expect to address the problem of a two-dimensional version of the generalized elephant quantum walk introducing correlations between the degrees of freedom and investigating the effects on the diffusive behavior of the quantum walk.

REFERENCES

1 AHARONOV, Y.; DAVIDOVICH, L.; ZAGURY, N. Quantum random walks. **Physical Review A**, v. 48, n. 2, p. 1687–1690, 1993. ISSN 10502947.

2 MOLFETTA, G. D.; SOARES-PINTO, D. O.; QUEIRÓS, S. M. Elephant quantum walk. **Physical Review A**, v. 97, n. 6, p. 1–6, 2018. ISSN 24699934.

3 PIRES, M. A.; MOLFETTA, G. D.; QUEIRÓS, S. M. Multiple transitions between normal and hyperballistic diffusion in quantum walks with time-dependent jumps. **Scientific Reports**, v. 9, n. 1, p. 1–8, 2019. ISSN 20452322.

4 PEARSON, K. The problem of the random walk. **Nature**, v. 72, n. 1867, p. 342–342, 1905. ISSN 0028-0836.

5 BROWN, R. A brief account of microscopical observations made... on the particles contained in the pollen of plants, and on the general existence of active molecules in organic and inorganic bodies. **Philosophical Magazine**, v. 4, n. 21, p. 161–173, 1828.

6 EINSTEIN, A. Über die von der molekularkinetischen theorie der wärme geforderte bewegung von in ruhenden flüssigkeiten suspendierten teilchen. **Annalen der physik**, v. 322, n. 8, p. 549–560, 1905.

7 COURTAULT, J.-M. *et al.* Louis bachelier on the centenary of théorie de la spéculation. *In*: COURTAULT, J.-M.; EKELAND, I.; KABANOV, Y. (ed.). **Louis Bachelier: aux origines de la finance mathématique**. Paris: Presses Universitaires Franc-Comtoises Besançon, 2002. p. 5–86.

8 XIA, F. *et al.* Random walks: a review of algorithms and applications. **IEEE Transactions on Emerging Topics in Computational Intelligence**, v. 4, n. 2, p. 95–107, 2020.

9 REITZNER, D.; NAGAJ, D.; BUŽEK, V. Quantum walks. **Acta Physica Slovaca**, v. 61, n. 6, 2011. DOI: 10.2478/v10155-011-0006-6.

10 BREUER, H. P.; PETRUCCIONE, F. **The theory of open quantum systems**. Oxford: Oxford University Press, 2002.

11 SCHÜTZ, G. M.; TRIMPER, S. Elephants can always remember: exact long-range memory effects in a non-markovian random walk. **Physical Review E**, v. 70, p. 045101, 2004. DOI: 10.1103/PhysRevE.70.045101.

12 MONTEIRO, V. M. **Passeios aleatórios do elefante:** efeitos de memória no caso multidimensional. 2019. Tese (Doutorado em Ciências) — Instituto de Física de São Carlos, Universidade de São Paulo, São Carlos, SP, 2019.

13 REIF, F. **Fundamentals of statistical and thermal physics**. Tokyo: McGraw Hill, 1965.

14 VENEGAS-ANDRACA, S. E. Quantum walks: a comprehensive review. **Quantum Information Processing**, v. 11, n. 5, p. 1015–1106, 2012. ISSN 15700755.

15 AMBAINIS, A. *et al.* One-dimensional quantum walks. *In*: STOC'os: 33rd ACM SYMPOSIUM ON THEORY OF COMPUTING, 2001. **Proceedings** [...] New York: Association for Computing Machinery, 2001. p. 37–49.

16 RILEY, K. F.; HOBSON, M. P.; BENCE, S. J. **Mathematical methods for physics and engineering:** a comprehensive guide. 2nd. ed. Cambridge, UK: Cambridge University Press, 2002.

17 BENIOFF, P. **Space searches with a quantum robot**. 2001. Available from: https://arxiv.org/abs/quant-ph/0003006. Accessible at: 23 Jan. 2022.

18 SHENVI, N.; KEMPE, J.; WHALEY, K. B. Quantum Random-walk search algorithm. **Physical Review A -** atomic, molecular, and optical physics, v. 67, n. 5, p. 523071–5230711, 2003. ISSN 10502947.

19 AMBAINIS, A.; KEMPE, J.; RIVOSH, A. **Coins make quantum walks faster**. 2004. Available from: https://arxiv.org/abs/quant-ph/0402107. Accessible at: 23 Jan. 2022.

20 LOVETT, N. B. *et al.* Spatial search using the discrete time quantum walk. **Natural Computing**, v. 11, n. 1, p. 23–35, 2012. ISSN 15677818.

21 CHILDS, A. M.; GOLDSTONE, J. Spatial search by quantum walk. **Physical Review A -** atomic, molecular, and optical physics, v. 70, n. 2, p. 1–11, 2004. ISSN 10502947.

22 CHILDS, A. M. Universal computation by quantum walk. **Physical Review Letters**, v. 102, n. 18, p. 1–4, 2009. ISSN 00319007.

23 LOVETT, N. B. *et al.* Universal quantum computation using the discrete-time quantum walk. **Physical Review A -** atomic, molecular, and optical physics, v. 81, n. 4, p. 042330, 2010. ISSN 10502947.

24 SINGH, S. *et al.* **Computational power of single qubit discrete-time quantum walk**. 2019. Available from: http://arxiv.org/abs/1907.04084. Accessible at: 23 Jan. 2022.

25 FELDMAN, N.; GOLDSTEIN, M. **Noisy quantum computation modeled by quantum walk**. 2021. Available from: http://arxiv.org/abs/2104.12096. Accessible at: 23 Jan. 2022.

26 ROMANELLI, A. Thermodynamic behavior of the quantum walk. **Physical Review A -** atomic, molecular, and optical physics, v. 85, n. 1, p. 1–8, 2012. ISSN 10502947.

27 ROMANELLI, A. *et al.* Thermodynamics of N -dimensional quantum walks. **Physical Review A -** atomic, molecular, and optical physics, v. 90, n. 2, p. 1–9, 2014. ISSN 10941622.

28 VALLEJO, A.; ROMANELLI, A.; DONANGELO, R. Initial-state-dependent thermalization in open qubits. **Physical Review A**, v. 98, n. 3, p. 1–7, 2018. ISSN 24699934.

29 HATIFI, M. *et al.* Quantum walk hydrodynamics. **Scientific Reports**, v. 9, n. 1, p. 1–7, 2019.

30 MOHSENI, M. *et al.* Environment-assisted quantum walks in photosynthetic energy transfer. **Journal of Chemical Physics**, v. 129, n. 17, p. 174106, 2008. DOI: 10.1063/1.3002335.

31 MOLFETTA, G. D.; PÉREZ, A. Quantum walks as simulators of neutrino oscillations in a vacuum and matter. **New Journal of Physics**, v. 18, n. 10, p. 103038, 2016.

32 NAYAK, A.; VISHWANATH, A. **Quantum walk on the line**. 2000. Available from: http://arxiv.org/abs/quant-ph/0010117. Accessible at: 30 Oct. 2021.

33 AHARONOV, D. *et al.* Quantum walks on graphs. *In*: STOC'os: 33rd ACM SYMPOSIUM ON THEORY OF COMPUTING, 2001. **Proceedings** [...] New York: Association for Computing Machinery, 2001. p. 50–59.

34 BRUN, T. A.; CARTERET, H. A.; AMBAINIS, A. Quantum to classical transition for random walks. **Physical Review Letters**, v. 91, n. 13, p. 1–4, 2003. ISSN 10797114.

35 ANNABESTANI, M.; AKHTARSHENAS, S. J.; ABOLHASSANI, M. R. Decoherence in a one-dimensional quantum walk. **Physical Review A -** atomic, molecular, and optical Physics, v. 81, n. 3, p. 1–9, 2010. ISSN 10502947.

36 OLIVEIRA, A. C.; PORTUGAL, R.; DONANGELO, R. Decoherence in two-dimensional quantum walks. **Physical Review A -** atomic, molecular, and optical Physics, v. 74, n. 1, p. 1–8, 2006. ISSN 10502947.

37 SCHREIBER, A. *et al.* Decoherence and disorder in quantum walks: from ballistic spread to localization. **Physical Review Letters**, v. 106, n. 18, p. 1–4, 2011. ISSN 00319007.

38 VENEGAS-ANDRACA, S. E. Quantum walks for computer scientists. **Synthesis Lectures on Quantum Computing**, v. 1, n. 1, p. 1–119, 2008.

39 ZHOU, W. Review on quantum walk algorithm. **Journal of Physics:** conference series, v. 1748, n. 3, p. 032022, 2021. ISSN 17426596.

40 PORTUGAL, R. **Quantum walks and search algorithms**. New York: Springer, 2013.

41 KENDON, V. Decoherence in quantum walks - a review. **Mathematical Structures in Computer Science**, v. 17, n. 6, p. 1169–1220, 2007. ISSN 09601295.

42 KADIAN, K.; GARHWAL, S.; KUMAR, A. Quantum walk and its application domains: a systematic review. **Computer Science Review**, Elsevier, v. 41, p. 100419, 2021. DOI: 10.1016/j.cosrev.2021.100419.

43 NIELSEN, M. A.; CHUANG, I. L. **Quantum computation and quantum information**. Cambridge: Cambridge University Press, 2000.

44 WILDE, M. M. **Quantum information theory**. USA: Cambridge University Press, 2013. ISBN 1107034256.

45 HORODECKI, R. *et al.* Quantum entanglement. **Review of Modern Physics**, v. 81, p. 865–942, 2009. DOI: 10.1103/RevModPhys.81.865.

46 SCHMIDT, E. Zur theorie der linearen und nichtlinearen integralgleichungen. *In*: PIETSCH, A. (ed.). **Integralgleichungen und Gleichungen mit unendlich vielen Unbekannten**. Wiesbaden: Springer, 1989. p. 190–233. ISBN 978-3-322-84410-1. DOI: 10.1007/978-3-322-84410-1_3.

47 SHANNON, C. E. A mathematical theory of communication. **Bell System Technical Journal**, v. 27, n. 3, p. 379–423, 1948.

48 UMEGAKI, H. Conditional expectation in an operator algebra, IV (entropy and information). **Kodai Mathematical Seminar Reports**, v. 14, n. 2, p. 59–85, 1962.

49 RUSKAI, M. B. Inequalities for quantum entropy: a review with conditions for equality. **Journal of Mathematical Physics**, v. 43, n. 9, p. 4358–4375, 2002.

50 LINDBLAD, G. On the generators of quantum dynamical semigroups. **Communications in Mathematical Physics**, v. 48, n. 2, p. 119–130, 1976.

51 KRAUS, K. *et al.* **States, effects, and operations:** fundamental notions of quantum theory: lectures in mathematical physics at the University of Texas at Austin. Berlin: Springer, 1983.

52 KEMPE, J. **Quantum random walks hit exponentially faster**. 2002. Available from: http://arxiv.org/abs/quant-ph/0205083. Accessible at: 30 Apr. 2021.

53 KEMPE, J. Quantum random walks: an introductory overview. **Contemporary Physics**, v. 44, n. 4, p. 307–327, 2003. ISSN 00107514.

54 CHILDS, A. M. *et al.* Exponential algorithmic speedup by a quantum walk. *In*: STOC 'os: 33rd ACM SYMPOSIUM ON THEORY OF COMPUTING, 2003. **Proceedings** [...] New York: Association for Computing Machinery, 2001. p. 59–68.

55 FARHI, E.; GUTMANN, S. Quantum computation and decision trees. **Physical Review A**, v. 58, p. 915–928, 1998. DOI: 10.1103/PhysRevA.58.915.

56 CARNEIRO, I. *et al.* Entanglement in coined quantum walks on regular graphs. **New Journal of Physics**, v. 7, 2005. ISSN 13672630. DOI: 10.1088/1367-2630/7/1/156.

57 ABAL, G. *et al.* Quantum walk on the line: entanglement and nonlocal initial conditions. **Physical Review A -** atomic, molecular, and optical physics, v. 73, n. 4, p. 1–9, 2006. ISSN 10502947.

58 HINAREJOS, M. *et al.* Chirality asymptotic behavior and non-Markovianity in quantum walks on a line. **Physical Review A -** atomic, molecular, and optical physics, v. 89, n. 5, p. 1–7, 2014. ISSN 10941622.

59 KUMAR, N. P. *et al.* Non-Markovian evolution: a quantum walk perspective. **Open Systems and Information Dynamics**, v. 25, n. 3, 2018. ISSN 12301612. DOI: 10.1142/S1230161218500142.

60 NAIKOO, J.; BANERJEE, S.; CHANDRASHEKAR, C. M. Non-Markovian channel from the reduced dynamics of a coin in a quantum walk. **Physical Review A**, v. 102, n. 6, p. 1–9, 2020. ISSN 24699934.

61 LAINE, E.-M.; PIILO, J.; BREUER, H.-P. Measure for the non-markovianity of quantum processes. **Physical Review A**, v. 81, n. 6, p. 062115, 2010. DOI: 10.1103/PhysRevA.81.062115.

62 BREUER, H.-P.; LAINE, E.-M.; PIILO, J. Measure for the degree of non-markovian behavior of quantum processes in open systems. **Physical Review Letters**, v. 103, n. 21, p. 210401, 2009. DOI: 10.1103/PhysRevLett.103.210401.

63 CHANDRASHEKAR, C. M. **Disorder induced localization and enhancement of entanglement in one- and two-dimensional quantum walks**. p. 1–13, 2012. Available from: http://arxiv.org/abs/1212.5984. Accessible at: 30 Apr. 2022.

64 ANDERSON, P. W. Absence of diffusion in certain random lattices. **Physical Review**, v. 109, p. 1492–1505, 1958.

65 VIEIRA, R.; AMORIM, E. P.; RIGOLIN, G. Dynamically disordered quantum walk as a maximal entanglement generator. **Physical Review Letters**, v. 111, n. 18, p. 1–5, 2013. ISSN 00319007.

66 VIEIRA, R.; AMORIM, E. P.; RIGOLIN, G. Entangling power of disordered quantum walks. **Physical Review A -** atomic, molecular, and optical physics, v. 89, n. 4, p. 1–11, 2014. ISSN 10941622.

67 LAVIČKA, H. *et al.* Quantum walk with jumps. **European Physical Journal D**, v. 64, n. 1, p. 119, 2011.

68 SEN, P. Scaling and crossover behaviour in a truncated long range quantum walk. **Physica A:** statistical mechanics and its applications, v. 545, n. 12, p. 123529, 2020.

69 MÜLKEN, O.; PERNICE, V.; BLUMEN, A. Universal behavior of quantum walks with long-range steps. **Physical Review E**, v. 77, n. 2, p. 021117, Feb. 2008.

70 CHATTARAJ, T.; KREMS, R. V. Effects of long-range hopping and interactions on quantum walks in ordered and disordered lattices. **Physical Review A**, v. 94, n. 2, p. 023601, Aug. 2016.

71 SINAYSKIY, I.; PETRUCCIONE, F. Efficiency of open quantum walk implementation of dissipative quantum computing algorithms. **Quantum Information Processing**, v. 11, n. 5, p. 1301–1309, 2012. ISSN 15700755.

72 KENDON, V.; TREGENNA, B. Decoherence can be useful in quantum walks. **Physical Review A -** atomic, molecular, and optical physics, v. 67, n. 4, p. 6, 2003. ISSN 10941622.

73 TSALLIS, C. Nonadditive entropy and nonextensive statistical mechanics-an overview after 20 years. **Brazilian Journal of Physics**, v. 39, n. 2A, p. 337–356, 2009.

74 ORTHEY, A. C.; AMORIM, E. P. Weak disorder enhancing the production of entanglement in quantum walks. **Brazilian Journal of Physics**, v. 49, n. 5, p. 595–604, 2019. ISSN 16784448.

75 KUMAR, N. P.; BANERJEE, S.; CHANDRASHEKAR, C. M. Enhanced non-Markovian behavior in quantum walks with Markovian disorder. **Scientific Reports**, v. 8, n. 1, p. 1–7, 2018. ISSN 20452322. DOI: 10.1038/s41598-018-27132-7.

76 PIRES, M. A.; QUEIRÓS, S. M. Quantum walks with sequential aperiodic jumps. **Physical Review E**, v. 102, n. 1, p. 12104, 2020. ISSN 24700053. DOI: 10.1103/PhysRevE.102.012104.

77 NAVES, C. B. *et al.* Enhancing entanglement with the generalized elephant quantum walk from localized and delocalized states. **Physical Review A**, v. 106, n. 4, p. 042408, 2022.

78 ORTHEY, A. C.; AMORIM, E. P. Asymptotic entanglement in quantum walks from delocalized initial states. **Quantum Information Processing**, v. 16, n. 9, 2017. ISSN 15700755. DOI: 10.1007/s11128-017-1672-1.

79 MARTÍN-VÁZQUEZ, G.; RODRÍGUEZ-LAGUNA, J. Optimizing the spatial spread of a quantum walk. **Physical Review A**, v. 102, n. 2, p. 022223, 2020.

80 WANG, Q.-Q. *et al.* Dynamic-disorder-induced enhancement of entanglement in photonic quantum walks. **Optica**, v. 5, n. 9, p. 1136–1140, 2018.

81 TAO, S.-J. *et al.* Experimental optimal generation of hybrid entangled states in photonic quantum walks. **Optics Letters**, v. 46, n. 8, p. 1868–1871, 2021.

82 BENDER, C.; ORSZAG, S. **Advanced mathematical methods for scientists and engineers I**. New York, NY: Springer, 1999. v. 1.

83 RIVAS, A.; HUELGA, S. F.; PLENIO, M. B. Entanglement and non-markovianity of quantum evolutions. **Physical Review Letters**, v. 105, p. 050403, 2010. DOI: 10.1103/PhysRevLett.105.050403.

84 CHRUSCINSKI, D.; MANISCALCO, S. Degree of non-markovianity of quantum evolution. **Physical Review Letters**, v. 112, p. 120404, 2014. DOI: 10.1103/PhysRevLett.112.120404.

APPENDIX

APPENDIX A – TIME-ASYMPTOTIC EVOLUTION OF THE ONE-DIMENSIONAL HADAMARD WALK

A.1 The stationary phase method

The stationary phase method[16,82] is a method that give us the leading behavior of an integral of the form

$$I(\chi) = \int_a^b f(t) e^{i\chi\phi(t)}\, dt \ , \tag{A.1}$$

that is called a generalized Fourier integral, when $\phi'(t) = 0$ in the interval $[a, b]$. The reasoning behind the approximations is that in the limit $\chi \to \infty$, the integrating function becomes a rapid oscillating function, owing to the phase factor. Consequently, the largest contributions will come from the intervals where the $\phi(t)$ does not vary too much, i.e. in the vicinity of its stationary points.

If the function $\phi(t)$ has stationary points on the interval $[a, b]$, we divide the integration interval around these points and for each division we rewrite $\phi(t)$ as a Taylor expansion around the corresponding stationary point. Considering that we have only one stationary point in the interval $[a, b]$ that is t', we have

$$I(\chi) = \int_a^b f(t) e^{i\chi(\phi(t') + \phi'(t')(t-t') + \frac{\phi''(t')}{2!}(t-t')^2 + \dots)} \ . \tag{A.2}$$

Supposing that f is a smooth function of t, we can take it out of the integral by setting it to the value of the stationary point. We approximate the expansion of $\phi(t)$ only to the first non-zero term of the expansion and integrate over the entire real axis. This means that in general we have to solve integrals of the form

$$I(p) = \int_0^\infty e^{\pm i\lambda u^p} \ .$$

The solution of the above integral is found by using complex calculus and the Cauchy theorem,[16] and it is given by

$$I(p) = e^{\pm i(\pi/2p)} \lambda^{-1/p} \frac{\Gamma(1/p)}{p} \ , \tag{A.3}$$

so that the approximate solution to the generalized Fourier integral is given by

$$I(\chi) \approx f(t') \ \exp\left\{ i\chi\phi(t') + \mathrm{sgn}(\phi^{(p)}(t')) i \frac{\pi}{2p} \right\} \left(\frac{p!}{\chi |\phi^{(p)}(t')|} \right)^{1/p} \frac{\Gamma(1/p)}{p} \ . \tag{A.4}$$

It is possible that $\phi(t)$ does not have any stationary point in the integration interval. If that is so, we perform an integration by parts finding that

$$I(\chi) = \frac{1}{i\chi}\frac{f(t)}{\phi'(t)}e^{i\chi\phi(t)}\Big|_b^a - \frac{1}{i\chi\phi'(t)}\int_a^b dt\left(\frac{f'(t)}{\phi'(t)}\right)e^{i\chi\phi(t)}\ , \tag{A.5}$$

which means that the integral decays as $O(1/\chi)$.

A.2 Calculation of the time-asymptotic coin coefficient integrals in the Hadamard Walk

The integrals that we have to calculate are given by Eqs. (3.52) and (3.53). Taking only the integrals that do not have the $(-1)^t$ factor and considering Eq. (A.1), we can make the following associations

$$f_\uparrow(k) = \left(\frac{1}{2} + \frac{\cos k}{2\sqrt{1+\cos^2 k}}\right)$$
$$f_\downarrow(k) = (\sqrt{2}e^{i(k-\omega_k)} - 1)\left(\frac{1}{2} + \frac{\cos k}{2\sqrt{1+\cos^2 k}}\right)\ .$$

The phase function ϕ will be a function of two parameters, the integrating variable k and $\alpha = x/t$, a change of variables in order to us get the right form of the phase

$$\phi(k,\alpha) = k\alpha - \omega_k\ . \tag{A.6}$$

Calculating the first derivative of ϕ we find its stationary points

$$\frac{\partial\phi}{\partial k} = \alpha - \frac{d\omega_k}{dk} = \alpha - \frac{\cos k}{\sqrt{1+\cos^2 k}} = 0$$
$$\leftrightarrow \frac{\cos k_\alpha}{\sqrt{1+\cos^2 k_\alpha}} = \alpha\ . \tag{A.7}$$

The above result tell us that the interval where we have stationary points is, since the cosine function is bounded to $[-1,1]$

$$\frac{-1}{\sqrt{2}} \le \alpha \le \frac{1}{\sqrt{2}}\ . \tag{A.8}$$

Taking the second derivative with respect to k of ϕ, we get

$$\frac{\partial^2\phi}{\partial k^2} = \frac{\sin k_\alpha}{(1+\cos^2 k_\alpha)^{3/2}}\ . \tag{A.9}$$

To find the asymptotic regime of the coin coefficient integrals we are going consider the cases where $\alpha = \pm 1/\sqrt{2}$, $-1/\sqrt{2} < \alpha < +1/\sqrt{2}$ and $\alpha > 1/\sqrt{2} \cup \alpha < -1/\sqrt{2}$.

- $\alpha = \pm\frac{1}{\sqrt{2}}$

  In this case $k_\alpha = 0, \pi$ and the second derivative of ϕ is zero, therefore we have to look at the third derivative, that is

$$\frac{\partial^3 \phi}{\partial k^3} = \frac{(3 - \cos(2k_\alpha))\cos k_\alpha}{(1 + \cos^2 k\alpha)^{5/6}} \neq 0 \text{ for } k_\alpha = 0, \pi \ . \tag{A.10}$$

  Consequently, the integral results considering $\alpha = \pm 1/\sqrt{2}$ will have the form, by using Eq. (A.4) as we stated in Eq. (3.55),

$$I(\alpha) \approx \left(\frac{f(0)e^{it\phi_\alpha(0)}}{|\phi_\alpha^{(3)}(0)|^{1/3}} + \frac{f(\pi)e^{it\phi_\alpha(\pi)}}{|\phi_\alpha^{(3)}(\pi)|^{1/3}} \right) e^{-i\pi/6} \frac{\Gamma(1/3)}{3} \left(\frac{6}{t}\right)^{1/3} \ . \tag{A.11}$$

- $-1/\sqrt{2} < \alpha < 1/\sqrt{2}$

  Here the second derivative is not zero and we have two stationary points $\pm k_\alpha$. Therefore the integrals will have the form, with $p = 2$

$$\exp\left\{ it\phi_\alpha(k_\alpha) + \text{sgn}(\phi_\alpha^{(2)}(k_\alpha)) i\frac{\pi}{4} \right\} \left(\frac{2!}{t|\phi_\alpha^{(p)}(k_\alpha)|} \right)^{1/2} \frac{\Gamma(1/2)}{2} \ . \tag{A.12}$$

  Rewriting the second derivative as a function of α, noting that $\cos k_\alpha = \alpha/\sqrt{1-\alpha^2}$,

$$\frac{\partial^2 \phi}{\partial k^2} = (1 - \alpha^2)\sqrt{1 - 2\alpha^2} \ , \tag{A.13}$$

  and using that $\Gamma(1/2) = \sqrt{\pi}$, after a little of algebra we get the results as stated in Eqs. (3.56) and (3.57).

- $1/\sqrt{2} < \alpha < 1 \cup -1 < \alpha < -1/\sqrt{2}$

  Finally, when α is greater than $1/\sqrt{2}$ or less than $-1/\sqrt{2}$, we have no stationary points. Consequently, we use Eq. (A.5) and find that the integral decays faster than any power of t, given that $1/t$ is its superior limit.

APPENDIX B – BINOMIAL EXPANSION FOR NON-COMMUTING MATRICES

Let A and B be two non-commuting matrices of the same dimension and $n \in \mathbb{N}$. The binomial expansion of $(A+B)^n$ can be written as

$$(A+B)^n = \sum_{k=0}^{n} A^k B^{n-k} + \sum_{k=1}^{n-1} AB^k A^{n-1-k} + \sum_{k=1}^{n-1} BA^k B^{n-1-k} + \dots \tag{B.1}$$

We can try to find a recurrence relation by induction. If $n = 2$, then we get

$$\begin{aligned}(A+B)^2 &= A^2 + AB + B^2 + BA = A^2 + AB + B^2 + [B,A] + AB \\ &= A^2 + 2AB + B^2 + [B,A].\end{aligned}$$

For $n = 3$, and using the above expansion

$$(A+B)^3 = A^3 + 2A^2B + AB^2 + A[B,A] + BA^2 + 2BAB + B^3 + B[B,A].$$

The sum of the following elements can be rewritten as

$$\begin{aligned}BA^2 + 2BAB &= [B,A^2] + A^2B + 2([B,A] + AB)B \\ &= [B,A^2] + A^2B + 2[B,A]B + 2AB^2,\end{aligned}$$

and using the following equality

$$[B,[B,A]] = B[B,A] - [B,A]B,$$

we find that

$$(A+B)^3 = A^3 + 3A^2B + 3AB^2 + B^3 + A[B,A] + [B,A^2] + 3[B,A]B + [B,[B,A]]. \tag{B.2}$$

Therefore, in general, by induction we will have

$$(A+B)^n = \sum_{k=0}^{n} \binom{n}{k} A^k B^{n-k} + \sum_{k=0}^{n-1} \binom{n}{k} D_k(B,A) B^{n-k}, \tag{B.3}$$

with

$$D_{k+1}(B,A) = AD_k(B,A) + [B,A^k] + [B,D_k(B,A)] \tag{B.4}$$

$$D_0(B,A) = 0 \tag{B.5}$$

APPENDIX C – BREUER-LAINE-PIILO NON-MARKOVIAN PROCESSES

In classical stochastic processes, Markovianity is defined in a precise way. Sec. (2.2) tells us that a stochastic process is Markovian if, and only if, the conditional probability of a random variable assuming a result in a given time step depends only on the immediate past result Eq. (2.16). Considering quantum dynamics, defining Markovianity can be tricky. The reason is that, as we discussed in Sec. (3.1), measurements destroy the coherence of quantum processes and the evolution of quantum systems often involves non-classical correlations. Consequently, many definitions of Markovianity have surged.

One aspect that one might look at in quantum evolutions is the one of information flow. When a quantum system evolves randomly, that is interacting with another quantum system, many times it tends to go to a stationary state, sometimes not depending on the initial state. This means that quantum states evolving through open system dynamics become less and less distinguishable. If any two quantum states going through the same evolution become more distinguished for some time instant we have an information flow going from the environment to the system, making the evolution depend on past states, therefore giving us a way to define Markovianity in quantum dynamics. Let us see this in more detail.

A common measure of distinguishability between quantum states is the *trace distance*[43] between two quantum states

$$D(\rho,\sigma) = \frac{1}{2}\|\rho-\sigma\|_1 \ , \tag{C.1}$$

where $\|A\|_1 = \mathrm{tr}(\sqrt{AA^\dagger})$ is the 1-norm of A. To see that it is a measure of distinguishability between quantum states consider the following Bloch sphere representation of two qubits, $\rho = (1/2)(\mathbb{I} + \vec{r}\cdot\vec{\sigma})$, $\gamma = (1/2)(\mathbb{I} + \vec{g}\cdot\vec{\sigma})$,[43] where $\vec{\sigma} = (\sigma_1,\sigma_2,\sigma_3)$ is the vector of Pauli matrices. Then, the difference between ρ and γ is given by $\rho-\gamma = (1/2)(\vec{r}-\vec{g})\cdot\vec{\sigma}$. Putting in the trace distance definition, we find that

$$D(\rho,\gamma) = \frac{1}{4}\|(\vec{r}-\vec{g})\cdot\vec{\sigma}\|_1 = \frac{1}{2}|\vec{r}-\vec{g}| \ , \tag{C.2}$$

as the eigenvalues of $(\vec{r}-\vec{g})\cdot\vec{\sigma}$ are given by $\pm|\vec{r}-\vec{g}|$, therefore the trace distance between two qubit quantum states resumes to half the distance between its two Bloch sphere vectors. If two quantum states are equal they have the same Bloch vector, therefore the trace distance between them is zero. If they are orthogonal, their Bloch vectors also are and the trace distance is maximum.

There is an important theorem[43] that states that the trace distance is contractive under complete positive trace-preserving quantum operations Eq. (3.19), that is

Theorem C.0.1. ***(Trace distance contraction under TP operations)****: Let ρ and σ be any two quantum states in $\mathcal{B}(\mathcal{H}^2)$. Let $\mathcal{E}$ be a complete positive and trace-preserving quantum operation. Then, the trace distance between ρ and σ is always greater or equal than the trace distance between the evolved states*

$$D(\mathcal{E}(\rho), \mathcal{E}(\sigma)) \leq D(\rho, \sigma) \ . \tag{C.3}$$

The above theorem tells us that any two quantum states undergoing the same complete positive and trace preserving evolution cannot become more distinguishable as time passes.

The *Breuer-Laine-Piilo* (BLP) definition of quantum Markov process[61,62] states that a quantum dynamical process is Markovian if, and only if, no information backflow occur between the environment and the system, in such a way that any pair of states cannot become more distinct for any time interval. If we have an information backflow, this means that the states can become momentarily distintic, increasing the trace distance and making the process non-Markovian. Therefore, a BLP non-Markovian process is defined as

Definition C.0.1. (***BLP non-Markovian process***): A quantum process characterized by the dynamical map $\mathcal{E}(t, t_0)$ is non-Markovian if, and only if, for any two quantum states ρ, σ evolving through $\mathcal{E}(t, t_0)$ and some time $t_0 \leq t' \leq t$

$$\frac{d}{dt} D(\rho(t'), \sigma(t')) > 0 \ . \tag{C.4}$$

One consequence of Markovianity in classical stochastic processes is that the stochastic matrix between two time instants, $T^{(t,t_0)}$, can be divided into the application of $t - t_0$ transition matrices. Therefore, the divisibility of the transition matrix is a signature of Markovianity. With this idea in mind, some definitions of Markovianity in quantum dynamics consider the divisibility property of quantum maps, like the Rivas-Huelga-Plenio definition.[83] Nonetheless, unlike classical maps, quantum maps must maintain another property, that is the one of complete positivity (see Sec. 3.1).

A quantum dynamical map $\mathcal{E}(t, t_0)$ is said to be k-divisible if for any intermediate time t', we can write $\mathcal{E}(t, t_0) = \mathcal{E}(t, t')\mathcal{E}(t', t_0)$ and the intermediate map $\mathcal{E}(t, t')$ is k-positive, that is $(\mathcal{I}_k \otimes \mathcal{E}(t, t'))$ maps positive operators to positive operators. A P-divisible map is a quantum map in which the intermediate map is only 1-divisible, while a CP-divisible map is one that is d-divisible, with d being the dimension of the system. Note that for $\mathcal{E}(t, t')$ be well defined we have that $\mathcal{E}(t, t_0)$ must be invertible, so that we can set $\mathcal{E}(t, t') = \mathcal{E}(t, t_0)\mathcal{E}^{-1}(t', t_0)$.

It is possible to connect the BLP definition of Markov processes with the divisibility of a quantum map if we take into account the following theorem[84]

Theorem C.0.2. ***(k-divisibility and trace-distance)****: An invertible quantum dynamical map $\mathcal{E}(t,t_0)$ is k-divisible if, and only if, the trace distance is monotonically decreasing*

$$\frac{d}{dt}\| \left((\mathbb{I}_k \otimes \mathcal{E}(t,t_0))(\rho-\sigma)\right) \|_1 \leq 0 \ . \tag{C.5}$$

for any ρ, σ two density operators.

Setting $k = 1$, we see that a BLP Markovian quantum process is a P-divisible process and vice-versa.